

AD723532

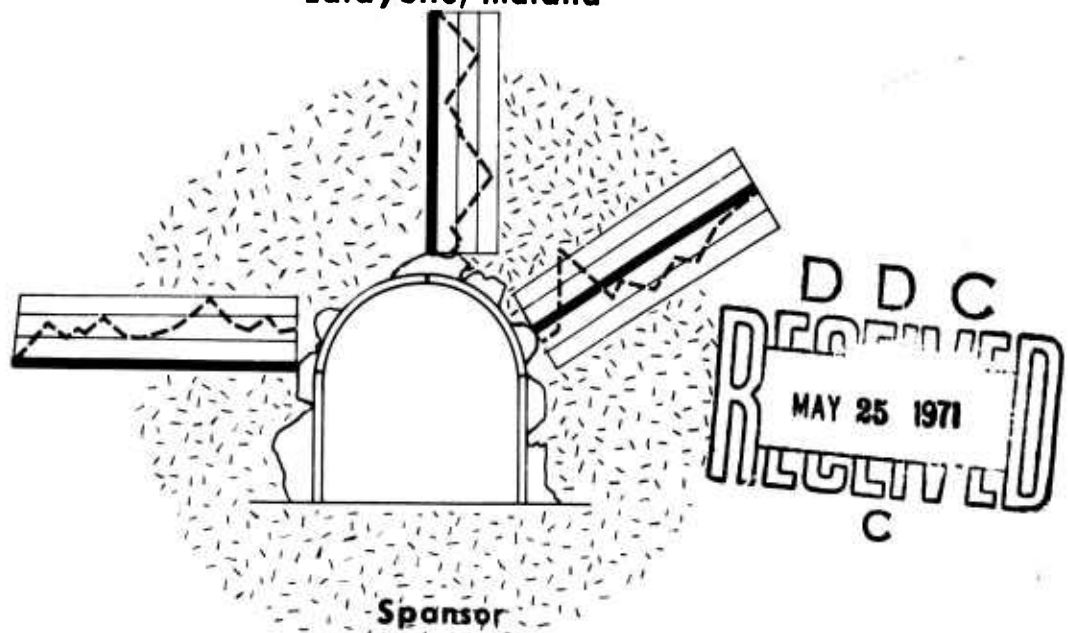
# Strain Distribution Around Underground Openings

Technical Report No. 5

## COMPARISON BETWEEN PREDICTED AND MEASURED DISPLACEMENTS

William R. Judd and William H. Perloff

Soil and Rock Mechanics Area  
School of Civil Engineering  
Purdue University  
Lafayette, Indiana



ADVANCED RESEARCH PROJECTS AGENCY  
DEPARTMENT OF DEFENSE

March 1971

Prepared For  
OFFICE OF THE CHIEF OF ENGINEERS  
DEPARTMENT OF THE ARMY  
WASHINGTON, D.C.

Reproduced by  
NATIONAL TECHNICAL  
INFORMATION SERVICE  
Springfield, Va. 22151

DISTRIBUTION STATEMENT A  
Approved for public release;  
Distribution Unlimited

Strain Distribution Around Underground Openings

Technical Report No. 5

COMPARISON BETWEEN  
PREDICTED AND MEASURED DISPLACEMENTS

Wm. R. Judd & Wm. H. Perloff

Soil & Rock Mechanics Area  
School of Civil Engineering  
Purdue University  
Lafayette, Indiana

Contract No. DACA 73-68-C-0002

Sponsor

ADVANCED RESEARCH PROJECTS AGENCY  
DEPARTMENT OF DEFENSE

March 1971

Prepared For

OFFICE OF THE CHIEF OF ENGINEERS  
DEPARTMENT OF THE ARMY  
WASHINGTON, D.C.

Distribution of this document is unlimited

## TABLE OF CONTENTS

	Page
Abstract	1
Foreword and Acknowledgments	11
1. INTRODUCTION	1
2. INSTRUMENTATION	4
3. ANALYTICAL METHOD	8
Input Information	8
General Comments	8
Formulation	9
4. COMPARISON BETWEEN ANALYTICAL AND MEASURED DISPLACEMENTS	11
Straight Creek Pilot Bore	11
The "Tension Arch"	17
Pacheco Tunnel	19
Navajo Tunnel No. 1	21
Green River Tunnels	23
Morrow Point Underground Powerplant	25
5. CONCLUSIONS	29
References	31
Appendix A	
Appendix B	
Appendix C	

### Abstract

The objective of this research was to establish whether existing theoretical methods could be used to predict the amount of displacement that would occur around an underground opening during or soon after the excavation process. The first step of the study selected a finite element method of analysis based upon an elastic continuum as the most promising theoretical method. The accuracy of the predictions was analyzed by comparison with in-situ measurements of strain around as-built openings. For three of the five openings analyzed, three appeared to present no useful correlation between the magnitudes of the predicted and measured displacements; for two of the openings (Morrow Point and Green River), 75% of the cases where the displacements were in the same direction had less than an order of magnitude difference in the amount of the displacement. In general, a finite element method based upon an elastic continuum does not appear to provide an acceptable predictive method except where the rock-system behavior approximates that of an elastic continuum.

### Foreword and Acknowledgments

This report presents the results of one stage of a research project that was initiated in September 1967. Previous reports published on this project are as follows:

Brown, L. A., Data Bank: Underground Openings-Rock Deformation Measurements - Abstracts, Tech. Rept. No. 3, Soil and Rock Mechanics Area, School of Civil Engineering, Purdue University, Lafayette, Indiana, Jan. 1970

Judd, W. R., Statistical Methods to Compute and Correlate Rock Properties and Preliminary Results, Tech. Rept. No. 2, *ibid*, December 1969.

Nahas, P., Statistical Methods to Compute and Correlate Rock Properties - Computer Techniques, Tech. Rept. No. 4, *ibid*, May 1970.

Perloff, W. H., Finite Element Analysis of Underground Openings, Tech. Rept. No. 1, *ibid*, June 1969.

The project will be completed with the publication of one additional report on the finite element analysis and one on the statistical analyses.

### Acknowledgments

The project was sponsored by the Advanced Research Projects Agency of the Department of Defense and technical progress was supervised by the Office of the Chief of Engineers, Corps of Engineers.

A number of graduate students at Purdue University participated in this portion of the project, but special recognition is given to the efforts of Mr. C. Marshall, L. S. Melzer, A. Mohan and U. Saltzman. Mrs. P. Nahas developed the computer and CALCOMP programs for displaying the time-displacement plots.

The study was made possible by the cooperation of the following who provided the field and most of the laboratory data required for the analyses:

Colorado State Highway Department  
Dr. John Abel (University of Arizona)  
Teledyne Terrametrics, Inc., Golden, Colo.  
U.S. Bureau of Reclamation  
Wyoming State Highway Department

STRAIN DISTRIBUTION AROUND UNDERGROUND OPENINGS -  
COMPARISON BETWEEN PREDICTED AND MEASURED DISPLACEMENTS

1. INTRODUCTION

1.1 This report summarizes a portion of the work accomplished on Project No. DACA-73-68-C-0002. This work was accomplished between 8 September 1967 and 1 January 1971.

1.2 The primary objective of this research was to determine if any existing methods of analysis would predict the actual behavior of underground openings. A study of the existing analytical methods indicated that the finite element method of analysis probably would provide the closest approximation of prototype behavior. Therefore, the first step was to develop a computerized finite element method that could use an elastic continuum as a model. If the elastic continuum model did not provide reasonable predictions, then the research would consider modifications that would provide a closer simulation of the actual rock system.

1.3 To evaluate the prediction accuracy of the finite element method, it is necessary to compare the predicted results with actual measurements of displacements that occurred around actual underground openings. To obtain the most valid such comparison and where the variables might be susceptible to analysis, we decided to study those openings where

- a. Displacement measurements in the rock had been obtained by instrumentation methods similar for all openings;
- b. The more common geometries of a circle and a horseshoe were used;
- c. The effects of different geological environments could be evaluated; and
- d. An appreciable range in the spans of the openings was represented.

1.4 Using these criteria, the following openings were selected for study:

Straight Creek Pilot Bore

Horseshoe (13 ft span), Colorado State Highway Dept.

Pacheco Water Tunnel

Horseshoe (17 ft span), U.S. Bureau of Reclamation

Navajo Water Tunnel

Circle (20 ft 10 in span), U.S. Bureau of Reclamation

Green River Twin Highway Tunnels

Semi-circular Horseshoe (34 ft span), Wyoming State Highway Department

Morrow Point Underground Powerplant

Horseshoe (57 ft 4 in span), U.S. Bureau of Reclamation

1.5 The initial stages of the research also had intended to study one or more of the chambers in the North American Air Defense Command (NORAD) headquarters in Colorado and the Veytaux Underground Powerplant (Switzerland). However, examination of the NORAD data indicated that any comparative analysis for this opening would have to be subject of later research because a three-dimensional finite element method of analysis would have to be formulated; this new method would be required if we were to obtain a reasonably accurate simulation of the prototype. As of the date of the present report, such a 3-D method of analysis has not been formulated (by us or other researchers) to the degree where it could be used for the intended purpose. The comparative analysis for the Veytaux openings had to be abandoned because the designers and constructors of this chamber were unable to comply with their original promise to provide us with the necessary measurement data. The latter development was regrettable because the Veytaux opening has a span of some 100 feet, and it is believed that a partial failure occurred during construction. And, since the opening was instrumented throughout the excavation period, the resulting data might have been useful in developing failure criteria for underground openings.

1.6 In regard to the latter situation, the prediction of safe spans for underground openings still is hampered by the lack of failure criteria for underground openings. To our knowledge, there has been only one tunnel that was properly instrumented at the time of a significant failure; unfortunately these failure data have been held confidential

and thus cannot be used for reporting purposes. In any case, such data from only one tunnel would have been insufficient to develop acceptable criteria for safe spans. Because of this lack of adequate field data, our research has been directed primarily at determining if the finite element method of analysis will give a useful prediction of the displacements that will occur around underground openings.

1.7 After selection of the tunnel for analysis, the next step was to prepare all data in a format that would permit comparisons between the analytical and the measurement plots. For this purpose a computer program was developed to reduce the measurement data from the raw strain measurements to a plot of measurement time versus displacements in micro-inches. A major and time-consuming effort was required to convert the strain measurements to a format suitable for computer operation: although all measuring instruments were of the same manufacture and type, the agencies doing the measuring used different recording and collation methods. Thus many months were required to assemble into a common format, the thousands of data points that were made available to us on tape, punch cards, computer printout sheets and field notebooks. During this assembly of the field data, finite element meshes were generated with node points located that permitted rapid extrapolation of the displacements expected at the points where actual measurements were made around the underground openings.



## 2. THE INSTRUMENTATION

2.1 In the tunnels selected for study the multiple-position-borehole-extensometer (MPBX) was used to measure the displacements in the rock around each opening . It measures axial displacement components within a borehole, and is illustrated in Figure 1. The instruments used in the tunnels studied had a sensitivity of 0.0005 in. and an accuracy of 0.001 in.; each instrument has 5 principal components:

1. The instrument head;
2. The collar-anchor assembly;
3. The downhole anchor system;
4. The signal cable;
5. The readout apparatus.

2.2 The MPBX is designed for installation in a 2-1/4 inch diameter drill hole but can be modified for use in holes of larger diameter. Generally, the number of anchors used in any one hole will depend upon the measurement detail that is desired; a frequently used system contains eight downhole anchors. Each anchor is spring loaded against the side of the hole and connected by a 0.41 inch diameter wire to a spring-type cantilever in the instrument head. Any movement of the anchor relative to the head causes a comparable increase or decrease in the wire length between the anchor and the instrument head; the resultant motion in the cantilever is reflected by changes in resistance in the electrical strain gage fixed to the cantilever. These changes are read on a conventional readout bridge that is attached to the instrument head only during the time that the reading is being made.

2.3 After installation, each instrument is corrected for ambient temperature conditions. The cantilevers are encased in a steel instrument head to minimize possible damage from construction operations. Readings can be taken periodically, or a continuous recording system can be affixed to each instrument head.

2.4 The data we have studied suggest that significant movements within the rock system may occur within a relatively short time after installation of the instrument; however, these movements may not all be recorded when a periodic method of readout is used. This latter situation introduces the possibility that a maximum strain may occur between recordings. Therefore, a continuous recording system is highly preferred during the first week or so after installation; particularly during the time period when excavation of the working face still has a significant influence on the strain at the instrument station.

2.5 Each MPBX system should be of sufficient length for the last anchor to be affixed in a rock zone that has not, nor will be influenced by the excavation of the opening\*. The borehole should be so oriented that its axis is parallel to the anticipated direction of the movements most significant to the problem being studied. For this latter reason, when the geologic structure of the rock mass is such that its behavior can be expected to approximate a homogeneous body, the most desirable orientation for the instruments is to provide one vertical MPBX at the crown of the opening and a horizontal MPBX at each spring line of the opening. In addition, for some geological environments it may be desirable to install an MPBX vertically downward to determine the strain adjacent to the invert. A major difficulty with this orientation would be protecting the instrument against damage by construction operations. If information is required on adjacent fault zones, the instrument should be oriented so its longitudinal axis is transverse to the principal planes of movement; this permits measurement of separation. Or it should be installed at a small angle to these planes of movement so it will measure the components of translatory displacement. In a similar manner, the orientation of major joints should be considered when locating the MPBX's.

2.6 In our project, 52 MPBX's installed in 28 tunnel sections were analyzed. The raw measurement data obtained were reduced by computer methods to anchor displacements relative to the anchor furthest from the opening face; these displacements then were depicted graphically by use of a CALCOMP plotter. The resultant plots for the instruments studied are shown on the figures in Appendix A. A description of the program used to compute and prepare these plots is presented in Appendix B. Preparing the data in this

\*In the absence of specific data on the influence of the excavation, present practice is for the final anchor to be embedded at a distance equal to 1.5 to 2 times the opening diameter. The present study indicates the preferred distance is 2 to 2.5 times the opening diameter.

manner permits the quick recognition of what may be anomalous readings caused by instrument faults rather than actual movement in the rock. For example, on Figure A-19 (2201) the large spike in the center of the plot for anchor 5 probably indicates anchor slippage or an accidental jarring of the instrument and therefore should be disregarded in analyses. The time-displacement plots permitted visual identification of:

- a. the maximum amount of movement that occurred at each instrument (which is designated by the letter "M" on the comparison plots), and
- b. the magnitude of permanent displacement after the instrument had been positioned for a relatively long time period (which is designated by the letter "S" on the comparison plots).

2.7 It is believed that the "M" values will be of use in the design of temporary supports for openings; the "S" values probably are indicative of permanent displacement and thus would assist in the design of permanent supports and linings for tunnels. The "M" values also could be used to estimate the amount of strain (or displacement) a rock system can accept without immediate collapse of the opening.

2.8 As may be apparent in the time-displacement plots, it frequently was difficult to establish the M and S displacement values. However, if continuous recordings had been used, the peak and the horizontal asymptote for each curve might have been identified more readily and accurately. We assumed that the "M" and "S" values we selected would be significant representations of actual displacement that occurred in each opening. For some instruments, a stable condition never appears to have been reached, and frequently it could not be determined if this was attributable to instrument faults or because the opening actually did not reach equilibrium during the period of measurement. For example, the plots shown on Figure A-7 indicate that the displacements did not stabilize during the period of measurement.

Generally, we found that the maximum recorded displacement occurred relatively soon after installation of the instrument and that all later displacements were a considerably lesser amount. Here it is important to

recognize that because an instrument cannot be installed immediately after the excavation of the rock within an opening, a significant amount of displacement may occur that never is recorded by this type of instrumentation\*. Thus, where the depth of cover permits, it would be very desirable to install such instruments in a hole bored from the ground surface and have the bottom anchor in the hole in close proximity to the proposed excavated perimeter of the opening; if such instruments then were attached to continuous recorders it would be possible to measure the amount of displacement that occurred during and immediately after the excavating process. Part of this latter procedure was followed at the Pacheco Tunnel where the MPBX's were installed from the ground surface prior to excavation. Continuous records were not made, but the records clearly show that as the excavation approaches and passes the instrument, there is a corresponding change in the displacement readings<sup>1/</sup>.

---

\*Therefore, the values shown on the plots in many cases might be moderately to considerably increased if the absolute displacement had been recorded.

### 3. THE ANALYTICAL METHOD

#### Input Information

3.1 Concurrent with the reduction of the measured data, the finite element analyses were conducted. The results of these studies were predicted displacements at each of the instrument stations for each geometry and geology selected. To avoid biasing the results, the field information made available for the finite element study was limited to

1. Young's Modulus and Poisson's Ratio of the rock as determined by laboratory tests on intact specimens;
2. the opening geometry; and
3. the depth of cover above the opening.

3.2 In this stage of the project, other geological factors such as joint systems and faults were not introduced with the exception of two of the instrument stations at the Morrow Point Underground Powerplant. In the latter case, the chamber was intersected by two shear zones. The manner in which these zones were considered in the finite element analysis is discussed below.

#### General Comments

3.3 Analytical solutions to boundary value problems in which gravity stresses are important, opening geometry is complex, and various strata may occur (even if the material is assumed to be continuous) are difficult to generate. Such problems recommend the use of numerical solutions such as the finite element method<sup>2,3/</sup>. The finite element computer program used for the analyses discussed herein is a modification of that described by Wilson<sup>4/</sup>. A detailed description of the method we used is presented in Reference 5.

### Formulation of the Problem

3.4 Each of the underground openings and the surrounding material are depicted as shown schematically in Figure 2. The region surrounding the opening is subdivided into a mesh of finite elements. Meshes used herein are square with a height approximately 12 times a characteristic dimension of the opening. Thus the top surface of the mesh does not always correspond to the ground surface. Boundary conditions applied to the exterior of the mesh are:

- a. The horizontal top surface is subjected to a normal stress  $q$  of magnitude

$$q = \gamma H_1 \quad (1)$$

in which  $\gamma$  is the unit weight of the rock above the zone considered and  $H_1$  is the top of the mesh below the ground surface.

- b. The vertical boundaries are subjected to a horizontal normal stress, increasing linearly with depth of magnitude

$$\sigma_x = K(q + \gamma x) \quad (2)$$

in which  $\sigma_x$  is the horizontal normal stress,  $q$  is the vertical normal stress at the top of the finite element mesh as defined in Equation 1,  $z$  is the depth below the top of the finite element mesh,  $\gamma$  is the unit weight of the rock within the mesh and  $K$  is a coefficient related to the nature of the prestress inherent in the rock mass.

- c. The horizontal bottom surface is restrained from vertical movement, but horizontal movement of all node points but one, is permitted. This boundary condition is depicted schematically by the roller-supports shown in Figure 2. The one restrained node point, usually in the middle (as shown on Figure 2), prevents rigid body displacement of the entire mesh.

- d. The material was assumed to exhibit a unit weight,  $\gamma$ , which was applied to all of the elements within the continuum.

3.3 Generally, a zero-horizontal displacement boundary condition is used for an outer vertical boundary rather than the stress boundary condition description under b. above. Such an approach is useful if the coefficient  $K$  is equal to that for an isotropic linear elastic material under plane strain conditions,  $K_0$ .

$$K_0 = \frac{\nu}{1-\nu} \quad (3)$$

in which  $\nu$  is Poisson's ratio. For the more usual circumstances where the rock has been prestressed,  $K$  is likely to be larger than that indicated by Equation 3<sup>6/</sup>. Results of elastic analyses for the openings investigated were obtained for values of  $K$  ranging from  $K_0$  to  $K = 1$ .

3.4 In calculating stresses due to the various applied and gravity loadings, when an elastic analysis is being performed, it was necessary to apply all the loads simultaneously. However, in order to calculate the displacements within the medium due only to the construction of the underground opening it was necessary to carry out two analyses. The displacements resulting from the excavation were considered to be the difference between these two cases (See paragraph 4.55).

#### 4. COMPARISON BETWEEN ANALYTICAL AND MEASURED DISPLACEMENTS

4.1 The points on the comparative displacement plots for the five tunnels were computed by the methods described in the preceding sections of this report and in Appendix B. In studying the plots, particular attention must be paid to the displacement scales: in several cases the differences were so great that it was necessary to plot the measured displacements and the calculated displacements on different scales. In these illustrations, the curves referred to as "C" or "K" are the displacement plots derived from the finite element analyses; the "M" and the "S" plots are those based on the measured maximum and the measured "stable" or permanent displacements, respectively. The latter points were selected as representative of what appeared to be the ultimate and final displacement of the instrument; i.e., there appeared to be little or no additional significant movement of the anchors.

4.2 When the displacement is along the axis of the MPBX toward the tunnel it is plotted as "Axis Extension (+)", and when the anchor moves away from the tunnel along the MPBX axis, the displacement is plotted as "Axis Contraction (-)". On each illustration there is a schematic presentation of the orientation of the joints around that particular section. This latter information will assist in interpreting anomalies that appear in the displacement plots.

4.2 The illustrations are ordered according to the span of the tunnel sections being discussed. In the initial discussion of the objectives of this research, it was indicated that we had hoped to determine the influence of the span width and the opening shape on the displacements. However, we found there were too many anomalies and too few instrument points to allow a reasonable analysis to be made of the influence of opening span and shape.

##### Straight Creek Pilot Bore

4.4 This tunnel was constructed by the Colorado State Highway Department; it is about 55 miles west of Denver, Colorado on proposed Highway I-70. Its purpose was to obtain information on the geologic and rock



mechanics conditions that would assist in the design and construction of twin-bore highway tunnels; the latter are to be located parallel to and within a few hundred feet of the longitudinal axis of the pilot bore.

4.5 The geometry of the pilot bore is that of a horseshoe approximately 13 feet in height and width. The tunnel is about 8300 feet long. The maximum depth of cover is about 1500 feet at a point some 2,000 feet from the west portal of the tunnel. The actual amount of cover at each instrument station discussed in this report will be noted in the respective descriptions for these sections.

#### Geology

4.6 The bedrock at the surface and in the pilot bore consists of the Pre-Cambrian Silver Plume granite with inclusions of older Pre-Cambrian metamorphic rocks (Idaho Springs formation) formed from sedimentary rocks (Figure 3). About 75% of the rock is granite, fine-to-medium-grained and consists chiefly of plagioclase feldspar, microcline, quartz and biotite with accessory muscovite. The foliation in the rock is derived from the microcline grains which usually have a subparallel orientation. The metasedimentary rocks include a wide variety of biotite-rich gneisses, schists, and locally, quartzite. All rock is locally cut by diorite dikes that probably are Tertiary age. The tunnel is transected by the Loveland Pass fault zone. This zone consists of numerous faults and shear zones of diverse orientation and these are separated by relatively competent ribs of granitic or metamorphic rock. The faulted rock ranges from claylike gouge to highly fragmented metamorphic and igneous rocks. The average attitude of the faults and shear zones greater than 1 foot wide is about  $N45^{\circ}E$  with dips of  $50^{\circ}$  to  $70^{\circ}SE$ . The average attitude of the foliation, particularly in the metasedimentary rocks is about  $N40^{\circ}E$  with a dip of  $30^{\circ}SE$ .

4.7 The joint and fracture surfaces commonly are coated and show slickensides. Typically, the joint is coated with chlorite and the rock for .01 to 0.1 of a foot to either side of the joint is partially altered. The average dip of the joints is about  $50^{\circ}$  but they tend to have a random strike and dip.

### Rock Properties

4.8 Results of physico-mechanical tests reported by Robinson & Lee<sup>7/</sup> probably represent maximum values measured on the more competent rock and are not considered truly representative of the elastic properties of the rock system. Table 1 presents average values for the granite and metamorphic rock types.

### Instrumentation

4.9 A total of 44 rock-mechanics instrument stations were installed in this tunnel. Of these, 21 representing 9 tunnel sections were selected for study; the balance of the MPBX-type instruments were not considered because of difficulty in interpreting the measured displacements. In the latter regard, this tunnel was one of the more difficult ones to analyze because of apparent problems with the instrumentation. This was one of the first tunnels where extensive use was made of the MPBX system, and thus debugging difficulties apparently occurred. However, we believe that sufficient accurate displacement measurements were obtained to provide a reasonable basis for comparison with the elastic analysis. In addition to MPBX and single-position extensometers, the loads on several of the steel supports were measured by electronic load cells placed between the legs of the sets and the footblocks, and in a few cases in horizontal positions in the crown of the sets and between leg and invert struts. The data from the load cells were not considered in this research, but they are described in some detail by Abel<sup>2/</sup>.

### Analytical Model

4.10 The geologic information and rock property data suggested the use of a homogeneous\* section for the finite-element analysis. The section used for this purpose is shown on Figure 4. The elastic properties used in the analysis were an E of 8,980,000 psi and a  $\nu$  of 0.243. This value of E compares favorably with the laboratory results and an average E derived from the field sonic measurements.

\*Homogeneous" in the sense that the majority of the rock was granite; in this report, consideration was not given to the jointing and faults. The influence of such discontinuities in structure is the subject of a later report.

Table 1.<sup>8/</sup>

<u>Rock Property (Laboratory)</u>	<u>Granite</u>	<u>Metamorphic</u>
Porosity, percent	1.13	1.62
Grain density, gm/cc	2.66	2.75
Dry bulk density, gm/cc	2.63	2.71
Saturated bulk density, gm/cc	2.64	2.72
Powder-grain density, gm/cc	2.6702	2.7679
Longitudinal velocity, fps	16,976	15,490
Transverse velocity, fps	9,699	8,267
Young's modulus, dynamic, psi	$8.45 \times 10^6$	$7.12 \times 10^6$
Modulus of rigidity, dynamic, psi	$3.38 \times 10^6$	$2.76 \times 10^6$
Poisson's ratio, dynamic	0.243	0.283
Unconfined compression tests:		
Strength, psi	25,600	15,800
Secant Young's modulus, psi	$7.57 \times 10^6$	$7.33 \times 10^6$
Poisson's ratio	0.22	0.22
Tensile strength, psi	1,290	770
Triaxial compression tests,		
confining pressure	1500 psi	
Strength, psi	40,600	24,900
Secant Young's modulus, psi	$9.40 \times 10^6$	$6.75 \times 10^6$
Poisson's ratio	0.19	0.17
Triaxial compression tests,		
confining pressure	4000 psi	
Strength, psi	55,800	
Secant Young's modulus, psi	$8.66 \times 10^6$	
Poisson's ratio	0.21	
Final swell pressure of fault gouge and altered rock samples from pilot		
bore, psf	625 - 3,270	230 - 9,000

Field measurements made in the pilot bore yielded a sonic velocity of 13,750 to 20,150 fps and an electrical resistivity of 36 to 2,200 ohm-m in the undisturbed rock.

### Comparative Analysis

4.11 Station 43 + 85 (Figures 5A and B), (250' cover): The shear zone appears to control the displacements, therefore, it was not reasonable to correlate the results of an analysis based upon a homogeneous system with the measured data. The two figures show the large discrepancies that occurred.

4.12 Station 49 + 27 (Figure 6), (680' cover): With the exception of MPBX 2027 the directions of the predicted movement generally agree with those actually measured. However, the analytical results suggest that the springline MPBX orientation of  $45^{\circ}$  is an undesirable orientation because most of the movement is normal to the instrument axis. Also, there would be considerable influence by the effective anisotropy caused by jointing. On this basis, calculations for MPBX 2027 show very small movement but the measured values approximate 0.2 in. However, it should be noted that the MPBX is parallel to the important joints. Also, it should be noted that the maximum displacement generally is away from the tunnel wall. This direction of movement may have been caused by blast damage; if so, it would not be predicted by the analytical methods. In general, to obtain agreement between the calculated and measured values, we would require a K value greater than 1, that is, approximately 2. For the vertical MPBX, the equivalent modulus then would have to be 1/10 of the intact modulus but for the nearly horizontal MPBX's the equivalent modulus needs to be approximately 1/100 of the intact modulus.

4.13 Station 59 + 35 (Figure 7), (1300' cover): Note should be made of the major perturbation in the time-displacement curves that occurred about one month after the MPBX was installed (Figure A-7); this may be the result of instrument or human error. The best K values, that is those which have the best agreement with the measured values, would be 1.0 for MPBX 2015 and 2021 and 0.321 for MPBX 2020. The very small movements on the measured plots suggest that the instrument was installed too late to record the majority of the movement; the displacement shown for MPBX 2020 may reflect movement along a joint set, possibly due to blasting.

4.14 Station 65 + 94 (Figure 8), (1300' cover): The extreme irregularity in the measured movements makes it difficult to obtain a fair comparison with the analytical plots. However, it would appear that the closest approximation is for a K value of 0.321. One point of interest on

the measured plot of this station is the apparent occurrence of a so-called "tension" zone approximately 1/2 diameter away from the crown of the tunnel. (The latter is discussed in paragraph 4.22.)

4.15 Station 69 + 81 (Figure 9), (1300' cover): The most reasonable value for K at this section appears to be 0.321 with an equivalent modulus of 1/4 of the actual modulus. Although the major joint sets are approximately vertical, they probably have a limited influence because of the large amount of cover.

4.16 Station 73 + 57 (Figure 10), (1300' cover): A K value of 0.321 appears to give the best approximation to the measured data. The equivalent modulus would have to be about 1/10th of the actual modulus to achieve a good comparison between the measured and calculated data.

4.17 Station 78 + 17 (Figure 11), (1100' cover): For K = 1.0 there appears to be general agreement between measured and predicted displacement insofar as direction of movement is concerned. However, the prediction based on a K of 1.0 predicts a displacement some 50 times less than what actually occurred. It is possible that the large actual displacement may have been caused by slippage of joint blocks in this severely fractured rock system. The equivalent modulus would have to be approximately one-third of the actual modulus.

4.18 Station 81 + 41 (Figure 12), (1100' cover): This section was in a severely sheared area. The latter may account for an actual displacement that was some two orders of magnitude greater than what was predicted for a K value of 0.321. Also, the orientation of the gouge zone on the right side of the tunnel would cause it to intersect the MPBX; thus there could have been mass movement of a large block of rock over seven of the eight anchors.

4.19 Station 83 + 93 (Figure 13), (1100' cover): The large discrepancy between the measured and actual displacements probably can be explained by the existence of the clay gouge zone that intersects the upper part of the tunnel; this would strongly influence all three of the MPBX's at this station.

4.20 Station 104 + 83 (Figure 14), (680' cover): The K = 1 value appears to be the most reasonable for MPBX's 2004 and 2005; and a K of

0.321 is best for MPBX 2006. The equivalent modulus could vary as much as 1/100th of the measured modulus.

4.21 Station 114 + 53 (Figure 15), (250' cover): The considerable discrepancies between the measured and actual displacements at this section are not readily explainable but may be due to a strong influence of joints and their subsequent movement.

#### The "Tension Arch"

4.22 On several of the instruments there is a zone of maximum displacement that may represent a "tension arch" that has been described by some authors. Whether this is a zone of true tension cannot be ascertained by the type of measurements used at Straight Creek. However, it does appear to be a zone where there is a maximum amount of displacement towards the tunnel and, therefore, would tend to be the decompressed area termed the Trompeter or Weber zone by many European authors. The zone appears to develop a maximum amount of "tension" at anywhere from 1/6th to approximately 1/2 the diameter away from the opening. Table 2 shows the location of this zone for those MPBX stations at Straight Creek where it appears to occur. The "tension arch" phenomenon warrants further study. The difficulty, however, is to design the physical or mathematical predictive model that would adequately simulate this type of stress distribution. Such a model apparently would have to incorporate the influence of joint orientation and frequency, ambient stress conditions, and variations in deformation moduli between different geologic strata.

Table 2

Station	MPBX No.	Anchor No.	Distance from Opening
43 + 85	2030	1	2 feet
43 + 85	2032	2 & 3	3 to 6 feet
43 + 85	2028	3	10 feet
49 + 27	2026	2	4 feet
49 + 27	2025	2 & 3	4 to 6 feet
65 + 94	2099	1	2 feet
69 + 81	2018	1	7 feet
73 + 57	2014	1	2 feet
83 + 93	2010	1	4 feet
83 + 93	2012	1	6 feet
114 + 53	2001	1	2 feet
114 + 53	2002	2	4 feet
114 + 53	2003	1 & 2	8 to 10 feet

4.23. Attempted Correlation. The magnitudes of the calculated displacements appeared to have little or no relationship to the magnitudes of measured displacements. However, it was decided to determine if there was a statistically definable relation between these two variables. This was done by calculating the correlation coefficient,  $r$ , between the magnitudes of the average and the maximum measured displacements and the magnitudes of the average and maximum calculated displacements, respectively. (In making the analysis the one set of apparently extreme values for MPBX 2008 were omitted.) The average values generally were obtained by only a visual approximation from the displacement plots; the maximum values were scaled from the plots.

The resulting values were an  $r$  of 0.202 where the variables were the magnitudes of the average measured and the calculated displacements; and an  $r$  of 0.037 where the variables were the magnitudes of the maximum measured and calculated displacements. Because these coefficients are

Table 3

Numerical Comparison Between Measured and Calculated Displacements

MPBX No.	Measured (in)		Calculated (in)		MPBX No.	Measured (in)		Calculated (in)		No. times Measured Value > Calculated	No. times Measured Value > Calculated
	Avg.	Max.	Avg.	Max.		Avg.	Max.	Avg.	Max.		
Straight Creek											
2001	.3	.5	.002	.003	150	133					
2002	.3	.6	.006	.006	50	100					
2003	-.5	-.75	.01	.01	*	*					
2004	.25	.5	.0035	.004	71	125					
2005	.4	.75	.006	?	66	?					
2006	.4	.8	.006	.007	66	114					
2008	(2.0)	(2.5)	(.02)	(.025)	(100)	(100)					
2010	.8	1.7	-.012	-.01	**	**					
2011	-.6	-1.05	-.01	-.015	60	70					
2012	.9	1.8	-.06	-.055	**	**					
2013	-.4	-.6	-.01	-.01	(400)	60					
2014	.15	.55	.01	.02	15	27					
2015	.07	.21	.009	.01	77	21					
2018	.13	.28	.01	.015	13	18					
2020	.2	.55	.005	.005	40	111					
2021	.02	.05	.01	.01	2	5					
2025	.25	.5	.003	.004	83	125					
2026	.07	.21	.006	.009	11	23					
2027	-.13	-.2	-.0005	0	260	-					
2028	0	-.22	-.01	-.013	∞	17					
2029	.07	.10	-.007	-.008	**	**					
2030	-.03	-.22	.002	.002	*	*					
2031	.30	.25	-.005	-.005	*	*					
2032	-.02	-.045	-.01	-.01	2	5					
2099	.03	.18	.01	.02	3	9					
Pacheco											
2208*	-.11	-.68	.0012	.002							
2209*	-.04	-.077	.001	.0025							
Morrow Point											
2201	.015	.028	.10	.13							
2202	.10	-.42	.08	.11							
2203	.17	.40	.09	.11							
2206	.01	.025	-.005	-.005							
2207	.02	.06	-.04	-.05							
2215	.22	.28	.015	0							
2217	.025	.225	-.03	-.03							
Green River											
2106	.20	.38	.02	.01							
2107	.04	.21	.14	.12							
2108	.10	.33	.07	.035							
2101	-.40	-3.2	.7	.9							
2105	-.07	-.21	.17	.14							
2104	.015	.05	.015	.04							
2033	.07	.45	.16	.13							
2103	.23	.32	.08	.10							
2100	-.13	-.55	.03	-.01							
2024	-.03	-.06	.2	.6							
2023	.03	-2.0	.25	.4							
2035	0	-.12	.09	.08							

Note: Values in ( ) were omitted in determining correlation coefficient

\*\*\* The calculated values were > than the measured values

\*\* Values not included because measured value was (+) and calculated value was (-)

\* Values not included because measured value was (-) and calculated value was (+)



considerably below the 5% level of significance for the number of data sets, there appears to be no useful relationship between the aforementioned variables.

This analysis was performed only for the Straight Creek Tunnel data. There were insufficient data points to make a realistic analysis of other tunnels. Also, it was not deemed advisable to incorporate all of data from all of the tunnels into one correlation analysis because there was no way to accurately weight the influence of the different tunnel geometries and geological environments.

#### Pacheco Tunnel

4.24 This tunnel is being built by the U.S. Bureau of Reclamation for the purpose of transporting water on the San Luis Project near Los Banos, California. The tunnel is a modified horseshoe with maximum span of 17 ft. and a maximum height of 18 ft. 9 in. The tunnel has a length of 54,400 feet.

#### Geology (Figure 16)

4.25 The two major rock types at the site are Cretaceous metasandstone and metashale. The major faults are steeply dipping and intersect the tunnel axis at nearly right angles. Shear zones associated with the faults range up to 2 ft. in thickness. Groundwater inflow during the excavation ranged between 2 and 40 gpm. Much of the tunnel rock is severely fractured; some of the rock contains quartz veins with a porous or vuggy structure. The foliation is contorted and there is considerable variation in the dip of the joints. At Station 132 + 50 the metasandstone strikes N50°W and dips 30° to 55°NE. The bedding is thin to thick and dip of joints usually is greater than 75°. The joints are coated with yellow-brown oxides. At Station 151 + 68.1 the metasandstone strikes from N20° to 80°W and dips 5° to 20°NE. The bedding is thick to massive; the joints are spaced 1 to 3 feet and have some surfaces that are weathered grey-brown. The joints adjacent to faults have a yellowish-brown clay film. There is 10 to 20% metashale interbedded with the sandstone and this contains both calcite and quartz in veinlets up to a 1/2 inch in thickness.

### Rock Properties

4.26 It was difficult to obtain accurate tests on the rock because of the severe foliation, the quartz stringers, and frequent fracturing. However, the results of static and dynamic tests performed at the Purdue University rock mechanics laboratory gave the results shown in Table 4.

Table 4<sup>8/</sup>

ROCK PROPERTIES (Physico-Mechanical) and Types of Tests Used (laboratory); Static and dynamic tests. (Tests by rock mechanics laboratory, Purdue University.)

Specimen No.	Rock Type	Young's Modulus, E, x 10 <sup>6</sup> psi	Poisson's Ratio	Density, pcf
1	Metasandstone	6.2	0.318	173
2	Metasandstone	5	0.21	
3	Metasandstone	4.9	0.394	

### Instrumentation

4.27 Two MPBX's were installed in boreholes drilled vertically from the surface prior to excavation of the tunnel. Because of severe fracturing in the rock, the drill hole containing MPBX 2208 was cemented and re-drilled to insure positive anchor setting.

### Analytical Model

4.28 The elastic model used in the finite element analysis is shown in Figure 17. The rock properties used as input were an E of 5,000,000 psi and a  $\nu$  of 0.20. The depth of cover at both sections was 90 ft.

### Comparative Analysis

4.29 The measurements plotted on these two sections (Figures 18 and 19) are of considerable interest because they record the displacements as the excavation approached the instrument. These were the only MPBX's in the entire study that had been installed prior to actual excavation. Therefore, it is reasonable to assume that the measured displacements represent absolute values of displacement

4.30 The large difference between the calculated and the measured displacements is not unexpected because a two-dimensional static analysis cannot reflect the behavior of this rock system as the tunnel approaches the instrument. Also, it is believed that for Pacheco rock the modulus of elasticity of the intact rock tested in the laboratory is considerably higher than the modulus of the rock system in situ.

#### Navajo Tunnel No. 1

4.31 This tunnel was constructed by the U.S. Bureau of Reclamation on the Navajo Indian Irrigation Project, San Juan County, New Mexico. The tunnel is 10,079 feet long and has a circular cross-section with a diameter of approximately 21 feet. This tunnel was excavated full face by a boring machine.

#### Geology (Figure 20)

4.32 The formations at the site are alternating beds of Cretaceous sandstones and shales. The structure generally is massive and there is no evident joint system although at Station 18 + 84.5 there were randomly oriented slickensided joints in the shale. The sandstone is fine to medium grained with occasional pockets of medium to coarse sandstone. There are occasional lenses of silty, slightly limey, carbonaceous or shaley sandstones. The rock generally is moderately hard to moderately friable and poorly laminated to cross-bedded. The shale is silty to clayey, slightly carbonaceous, partly sandy, moderately hard and laminated and fissile to blocky. There is a transition material of shaley sandstone that is fine to medium grained, silty, carbonaceous and moderately hard to moderately friable and is laminated to poorly laminated. The beds generally have a very low dip or are horizontal. A continuum model would appear to closely approximate this geological environment.

#### Rock Properties

4.33 Laboratory tests gave secant E values at a first loading of 1000 psi of 507,000; 567,000; and 572,000 psi for the sandstone. Its compressive strength averaged 3,010, 5,730 and 1,820 psi, respectively<sup>8/</sup>.

### Instrumentation

4.34 The instruments consist of one MPBX at each of three stations and convergence-measuring plugs at two stations. (Information on the latter may be found in Reference 2.)

### Analytical Model

4.35 The elastic finite element model is shown in Figure 21. Rock property input values were an E of 500,000 psi,  $\nu$  of 0.2<sup>\*</sup>, and a density of 160 pcf. The depth of cover at all three stations was 350 ft.

### Comparative Analysis

4.36 Station 7 + 46 (Figure 22). The MPBX was installed in an old heading that had been excavated 1-1/2 years prior to the installation of the instrument. This long delay probably resulted in most of the strain being relieved prior to installation of the instruments.

4.37 Station 14 + 76 (Figure 23). This MPBX was installed 16.5 ft behind the advancing face. Since the tunnel was being driven full face by a boring machine, the instrument probably was installed within 24 hours after the machine had passed the instrument point. Despite this rapid installation of the instrument, the amount of measured displacement is so small as to approach the accuracy of the instrument, and for that reason may not represent a true measure of the absolute displacement.

4.38 Station 18 + 85 (Figure 24). This instrument was installed 19.3 feet behind the advancing face; the latter means that it probably was installed within 24 hours of the time the tunneling machine had passed the instrument station. Although there is an order of magnitude difference in magnitude, the directions of the measured and the calculated displacements are the same. The lack of comparison with Station 14 + 76 is not readily explainable.

4.39 An overall interpretation of the instrument behavior at Navajo is that the rock may have behaved as an elastic continuum; if so, there would be an almost complete release of strain prior to the time the instruments were installed. If this assumption is true, it then supports our earlier statements that for accurate displacement measurements, it is essential for instruments to be installed prior to the actual excavation of an opening; the latter particularly would be true when the behavior and composition of a rock system approaches or equals that of an elastic continuum.

---

\*In the absence of a laboratory value for  $\nu$ , this value was assumed as representative of the sandstone.

### Green River Tunnels

4.40 The Green River Tunnels were excavated by the Wyoming Highway Department; they are twin tunnels for U.S. Highway I-80 through Castle Rock Ridge near Green River, Wyoming. Each tunnel is a horseshoe shape with an excavated diameter of approximately 34 feet, a height from invert to springline of 9.66 feet, and a length of 1100 feet.

### Geology (Figure 25)

4.41 The rock in the tunnels consists of marlstone, siltstone, silty sandstone and shale of the Tertiary Green River formation. The beds are predominantly flat with local  $1^{\circ}$  to  $4^{\circ}$  dips resulting from general folding on northerly trending axes. The maximum overburden is approximately 250 feet. The rock varies in hardness with the shales being the weakest and bedding planes tend to be weak. Prolonged exposure causes some local slacking but does not produce excessive disintegration or volume change. Generally the tunnels were dry although there was a small amount of seepage near the west end of the east bound tunnel. The joint sets have vertical dips and are oriented  $N22^{\circ}W$  and  $N80^{\circ}E$ .

### Rock Properties

4.41 Laboratory tests gave the physico-mechanical properties shown in Table 5.

Table 5<sup>8/</sup>

ROCK PROPERTIES (Physico-Mechanical) and Types of Tests Used (laboratory):

<u>Property</u>	<u>Average</u>	<u>Range</u>
Density, pcf	130	125-136
Unconfined Compressive Strength, psi	1,300	550-3,200
Modulus of Elasticity, $\times 10^6$ psi	0.10-0.19 (2 tests)	

### Instrumentation

4.43 At each of the four instrument stations there were prop load cells and three MPBX's. The MPBX's had a range of 0 to 1.0 in and a sensitivity of .0002 inches.

### Analytical Model

4.44 The elastic finite element model used for our analysis is shown in Figure 26. The rock properties used as inputs were an E of 150,000 psi, a  $\nu$  of 0.1, and a density of 130 pcf. For this analysis the depths of cover for the various sections were rounded off to 90 ft for 98 + 35, 240 ft for 103 + 51 and 105 + 05 and 208 ft for 105 + 54.

### Comparative Displacements

#### 4.45 Station 98 + 35 (Figure 27), (80' cover)(South Tunnel):

There is relatively good agreement in both magnitude and direction of displacement between the measured and the calculated values; the exception to this is that the movements of MPBX 2108 anchors 6 to 8 are in the opposite direction from that calculated for these anchors. There does not appear to be a reasonable explanation for this contradiction. It is of interest that a "tension arch" appears to have developed between anchors 2 and 4 and at anchor 6 in MPBX 2107 and between anchors 3 and 6 and anchor 7 in MPBX 2106.

#### 4.46 Station 103 + 51 (Figure 28), (247' cover)(South Tunnel):

There generally is good agreement in the magnitude of the calculated and the measured displacements. However, there is a reversal in direction in the measured data on MPBX 2101. The calculated displacement using a K of .11 appears to provide the closest simulation to the measured points. MPBX's 2104 and 2105 both indicate the possible development of a "tension arch" at anchors 3 through 5 in 2104 and anchors 5 and 6 in 2105. The movement of the tunnel crown away from the opening, as demonstrated by the measurements in MPBX 2101, is not readily explainable.

#### 4.47 Station 105 + 05 (Figure 29), (233' cover)(North Tunnel):

There is relatively good agreement in the direction of displacements between the measured and calculated values. However, the magnitudes vary considerably. It is of particular interest to note that for MPBX 2100 the reversal in direction of displacement as shown by the calculated plot has, except for anchors 1 and 2, a comparable directional change in the measured displacements.

4.48 Station 105 + 54 (Figure 30), (208' cover)(South Tunnel):

There is generally good agreement between the orientation and the magnitudes of the measured and the calculated displacements except for MPBX 2024 where the measured displacement is in an opposite direction from that calculated.

4.49 In general there is good agreement between the measured and calculated displacements for the measurements at Green River Tunnel. The anomalies probably can be explained by observation of the time-displacement plots which appear to indicate large movements occurring within a relatively few hours; therefore, a significant amount of movement probably occurred before the instruments had been installed. A major reason for the relatively good agreement between the measured and the calculated data is that this tunnel is located in a geological environment that has had only relatively modest amounts of orogenic disturbance and there are no major faults or shear zones. Thus, it is reasonable to assume that the in situ behavior would approximate that of an elastic continuum.

Morrow Point Underground Powerplant

4.50 The chamber for this plant was constructed by the U.S. Bureau of Reclamation on the Gunnison River some 20 miles east of Montrose, Colorado and adjacent to the Morrow Point Dam. The chamber is 206 ft long, 57.4 ft wide, 65 to 134 ft high and is about 400 feet beneath the ground surface.

Geology (Figure 31)

4.5 The chamber is in a region of anticlinal folding and is intersected by several shear zones. The chamber is intersected by a major shear zone that has a strike of  $N28^{\circ}W$ , a dip of  $35^{\circ}NE$ , and an average thickness of 2.5 feet. A second major shear zone intersects the upper east end of the chamber and lies above the remainder of the chamber. The orientation of the three major joint sets that intersect the openings are:  $N37^{\circ}E$ ,  $80^{\circ}NW$ ;  $N63^{\circ}W$ ;  $80^{\circ}SW$ ; and  $N4^{\circ}E$ ,  $42^{\circ}SE$ . The rock types primarily are biotite and mica schist, quartzite and pegmatite.

### Rock Properties

4.52 Laboratory and field tests were performed to determine physico-mechanical properties of the rock. A summary of the results of these tests are shown in Table 6.

Table 6<sup>8,10/</sup>

ROCK PROPERTIES (Physico-Mechanical) and Types of Tests Used (in-situ and laboratory):

Rock Unit	Rock Type	Young's Modulus, <sup>6</sup> E, x 10 <sup>6</sup> psi	Poisson's Ratio	Ultimate Strength, psi	Number of Tests
A	(Biotite Schist	0.86	0.02	3,615	2
	(Mica Schist	1.20	0.04	6,385	24
B	(Micaceous Quartzite	4.14	0.06	15,590	20
	(Quartzite	8.84	0.14	28,820	4
C	Pegmatite	2.68	0.05	17,700	4

### Instrumentation

4.53 Precise leveling techniques were used to determine the absolute displacement of 25 points on the rock arch. Movements of the walls of the excavation were measured for nine pairs of points. Permanent reference points were established above and below shear zone A at two stations to determine if excessive movement of the A-line rock wall was confined to the shear zones. Twenty-five instrumented rock bolts were installed (20 feet long) in the walls. 7 MPBX's were installed; 3 in the arch, 2 at the springline, and 2 in the walls. Two single-position borehole extensometers were installed to a maximum depth of 115 feet. The displacements shown for the sensor head ("anchor" 0) were obtained from the plots in Reference 11; all other measurement data were supplied directly by the U.S. Bureau of Reclamation.



#### Analytical Model

4.55 The elastic finite element model is shown in Figure 32. Three types of materials appeared to have significantly different elastic parameters; the properties adopted for these are as follows:

$$\begin{array}{lll} \text{Rock Type A: } E = 2.5 \times 10^6 \text{ psi} & & \\ \text{B: } E = 3.5 \times 10^6 \text{ psi} & \nu = 0.03 & \\ \text{C: } E = 0.1 \times 10^6 \text{ psi}^* & & \end{array}$$

The mesh in Figure 32 was used for the initial calculation and displacements prior to the removal of material. The second mesh in which the elements in the excavated area were removed was used for the second computation. The area of particular interest in Figure 32 is that zone in which the elements are smallest.

#### Comparative Analysis

4.55 MPBX's 2201 and 2202: (Figures 33 and 34). The considerable axial extension between anchors 1 and 6 on these instruments may be indicative of the so-called "tension arch". For MPBX 2201 the measured displacement is less than the calculated displacement; for MPBX 2202 the calculated average displacement is less than the measured average displacement. These contradictions are not readily explainable. It should be recognized, however, that these instruments are in the hanging wall of the shear zone and do not appear to be intersected by any fault. Any movement, therefore, should be due to loosening of joints and fractures in the rock. In the one case (MPBX 2202), it is suggested that a considerable part of the elastic strain was not released during the period of measurements; whereas for MPBX 2201, a considerable portion of elastic strain may have been released prior to installation of the instrument. However, of most value is that, with the exception of the sensor head, the direction of the measured displacement is in agreement with that predicted by the calculated displacements. No reasonable explanation could be found for the apparent inconsistency in the direction of movement of the sensor heads for these MPBX's.

---

\*This "C" material represents the shear zone material and is not the same rock unit as "C" in Table 6.

4.56 MPBX 2215: (Figure 35). In this section the measured movement was in the same direction but several times greater than that predicted. This sharp increase in magnitude may have been caused by the shear zones intersecting the instrument. This latter conclusion is supported by other field observations that indicated a large wedge of rock in this part of the wall was moving toward the chamber, and its boundary was between anchors 6 and 7<sup>11</sup>/<sub>1</sub>. If the latter assumption is correct, then this type of inelastic displacement would not have been predictable by our use of an elastic model in the finite element analysis.

4.57 MPBX's 2203, 2206, 2207 and 2217: (Figure 36). The wide variance between the measured and the calculated displacements for MPBX 2203 may be attributed to the same situation described for Figure 33 and 34; i.e., loosening of joints in the rock would have caused considerable displacement and the influence of joints was not introduced in the finite element analysis. Measurements for MPBX 2206 and 2207 apparently indicate the development of a tension arch and, if so, this would not have been predicted by the elastic model used in the finite element analysis. Also, the direction of movement probably was controlled by the joint system around the opening. The large measured displacement shown for MPBX 2217 probably was caused by this instrument being located in the same large wedge of moving rock as MPBX 2215. The fact that the direction of the motion for 2217 is opposite to that for 2215 might be attributed to the possible rotation of the block during its movement. In either case a finite element analysis based upon an elastic model would not be expected to predict these anomalies.

## 5. CONCLUSIONS

### The Instrumentation

1. The usefulness of the MPBX measurements to some extent depends upon how its axis is oriented with respect to the direction of jointing, faults and shear zones.
2. A reasonable assumption is that a considerable release of elastic strain occurs immediately upon excavation of an opening; therefore, the measuring instrument should be installed as rapidly as possible after the excavation of a tunnel section is completed.
3. Displacement data probably can be lost because of the time lag between the excavation process and the installation of the instrument; therefore, it would be desirable to install strain-or displacement-measuring instruments ahead of the excavation. To minimize construction disturbances to the instrument, the most desirable installation method would be to place the instrument in a hole bored from the ground surface to the perimeter of the proposed excavation; then the behavior of the rock system can be recorded as the excavation approaches and then passes the instrument.
4. It is possible that significant but unrecorded strains may occur in the intervals between readings. To minimize the loss of such data, it would be desirable to attach continuous recorders to each instrument. If this does not prove feasible, it would be worthwhile to explore the development of a "maximum-minimum" strain recorder that would be permanently attached to each cantilever on the MPBX; it would act in a manner somewhat analogous to a maximum-minimum thermometer, i.e., it would be designed to indicate the maximum and the minimum strains that occurred in the time intervals between periodic readings of the cantilevers.

Preceding page blank

### Comparative Analysis

5. The results from our study indicate that a finite element method of analysis that is based upon an elastic continuum tends to predict displacements that can be one or more orders of magnitude less than what actually occurs, and occasionally is larger.

6. The preceding conclusion appears to particularly apply when the rock system contains numerous joints and/or faults, and secondly when the rock properties used as input to the analysis are derived from intact laboratory specimens rather than from in situ field tests.

7. When the rock system is relatively homogeneous from an elastic viewpoint and contains few joints and no faults, the finite element analysis generally but not always can predict the direction of the displacements that may occur during excavation although there still may be discrepancies between the magnitudes of the measured and the predicted displacements.

8. In general, since our study indicates that the accuracy of the finite element prediction for underground openings appears to be highly sensitive to the geological environment, finite element analyses based upon elastic models of such openings should be used with considerable caution. The predictive accuracy of the finite element method should be significantly improved if (1), a method can be found to quantify all significant geological factors so they can be used as direct inputs in the finite element model, and (2) data are available on the orientations and magnitudes of the ambient stresses around the opening.

#### REFERENCES

1. Wallace, G. and W. Ortel, "Tests for Tunnel Support and Lining Requirements", 12th Symp. on Rock Mechanics, Rolla, Mo., Nov. 1970 (Preprint)
2. Clough, R. W., The Finite Element Method in Structural Mechanics, "Stress Analysis", O. C. Zienkiewicz & G. S. Hollister, eds., Section 2.2, J. Wiley & Sons, Ltd., London, 1965 (Chapter 7).
3. Zienkiewicz, O. C. and Y. K. Cheung, The Finite Element Method in Structural and Continuum Mechanics, McGraw-Hill, London, 1967.
4. Wilson, E. L., "Finite Element Analysis of Two-Dimensional Structures", Ph.D. Thesis, Univ. of Calif., 1963.
5. Perloff, W. H., "Strain Distribution Around Underground Openings - Tech. Report No. 1, Finite Element Analysis of Underground Openings", Purdue Univ. Sch. of Civ. Eng., Lafayette, Indiana, June 1969. (Available from Defense Documentation Center as AD 701 764)
6. Obert, L., "Determination of Stress in Rock - A State of the Art Report", ASTM STP 429, 1967.
7. Robinson, C. S. and E. T. Lee, "Preliminary Report on the Engineering Geology of the Straight Creek Tunnel Pilot Bore, Clear Creek and Summit Counties, Colorado", U.S. Geological Survey Open-File Report, 1965.
8. Brown, L. A., "Strain Distribution Around Underground Openings - Tech. Report No. 3 Data Bank: Underground Openings Rock Deformation Measurements - Abstracts", Purdue Univ. Sch. of Civ. Eng., Jan. 1970. (Available from Defense Documentation Center as AD 701 087)
9. Abel, J. F. Jr., "Tunnel Mechanics", Colo. Sch. of Mines Qtly, V.62, N.2, April 1967.
10. Redmond, M. C., "Laboratory Tests of Foundation Rock Cores, Morrow Point Dam site", U.S. Bureau of Reclamation Report C-1157, 1965.
11. Dodd, J. S., "Morrow Point Underground Powerplant Rock Mechanics Investigation", U.S. Bureau of Reclamation Report, March 1967.

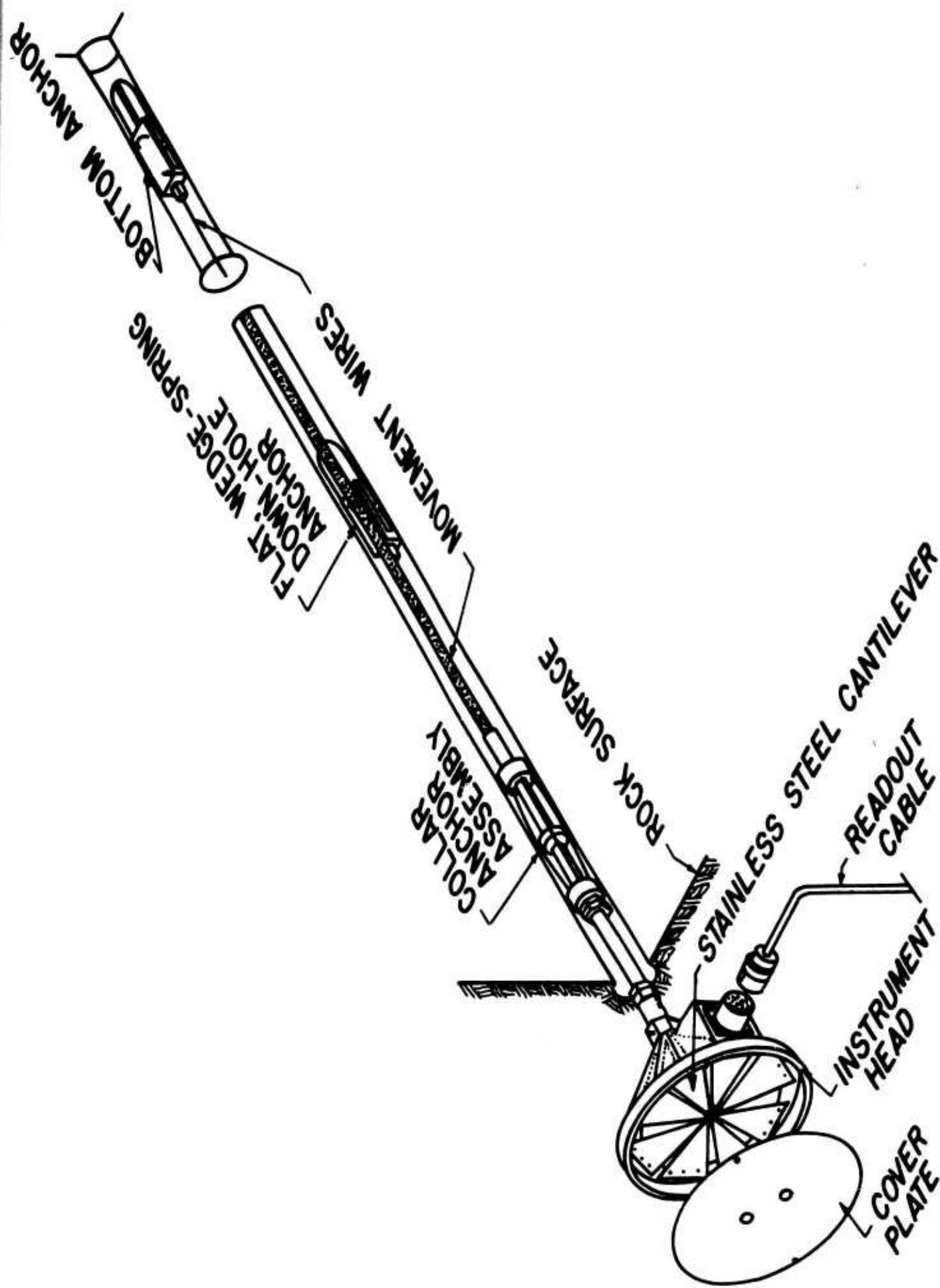


Figure 1. Schematic of MPBX Assembly  
(Courtesy Teledyne Terrametrics)

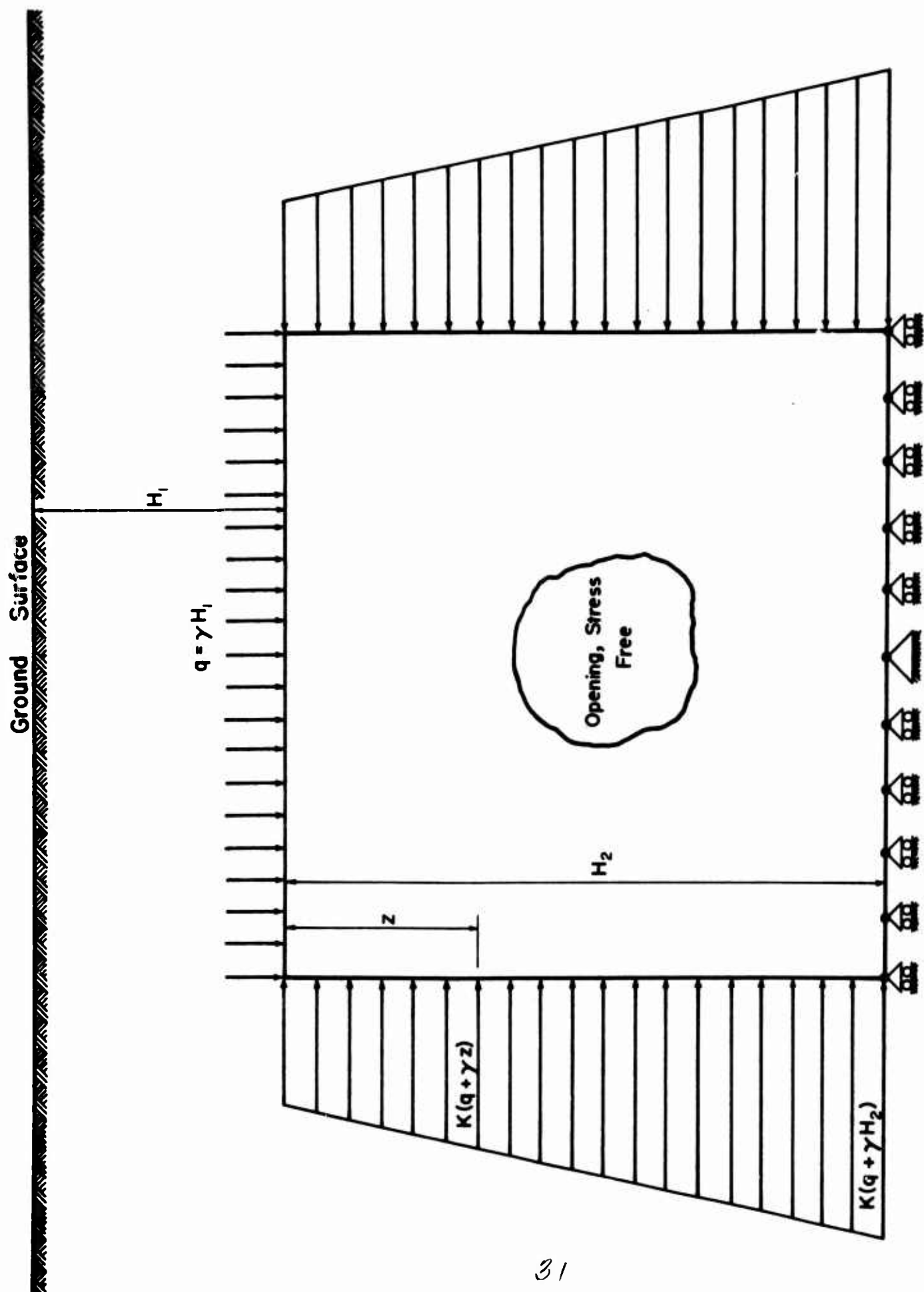


Figure 2. Boundary Conditions for Plane Strain Analysis of Underground Openings

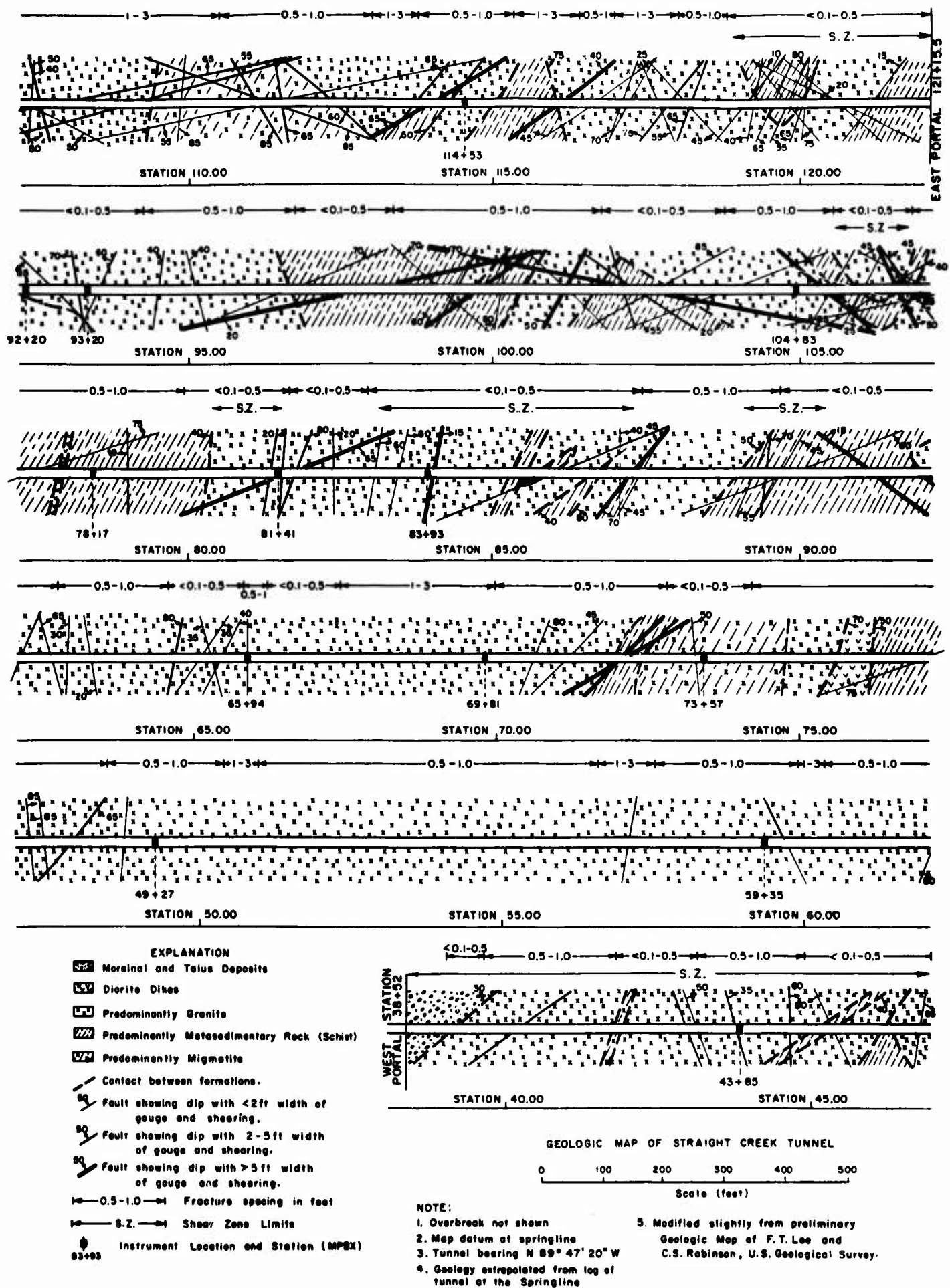


Figure 3. Straight Creek Tunnel - Geologic Log



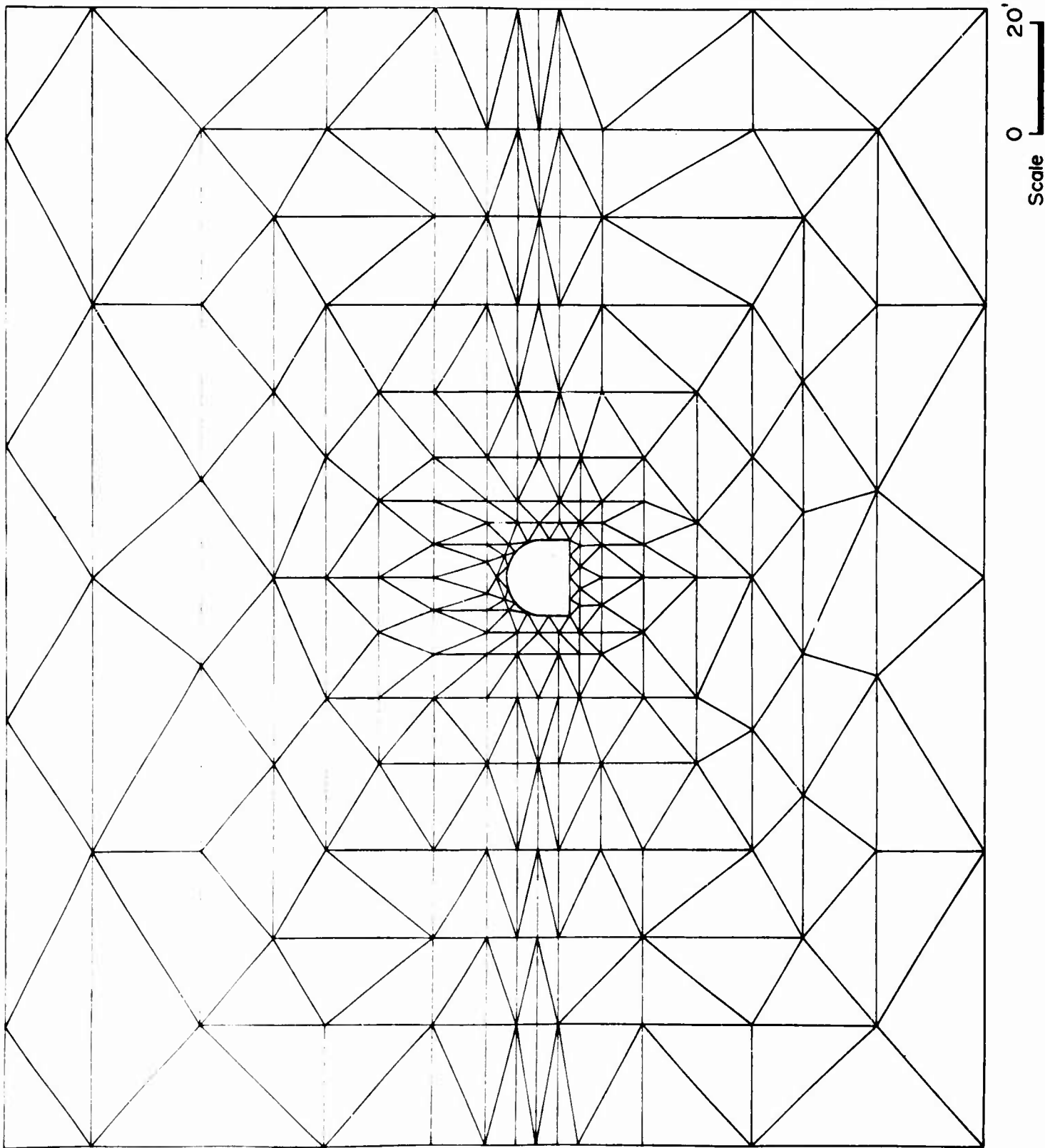
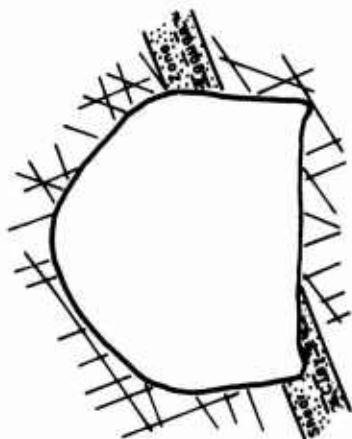


Figure 4. Straight Creek Tunnel - finite element mesh



NOTE:

1. Granite, iron stained, unbroken to moderately sheared, 0-20% biotite schist and gneiss.
2. Joint spacing averages 0.5-1.0 feet.
3. Joint traces are diagrammatic and do not represent actual locations.
4. Steel supports 6' c.c., 20% lagged.

Scale for opening and anchor depths (feet)

0 5 10

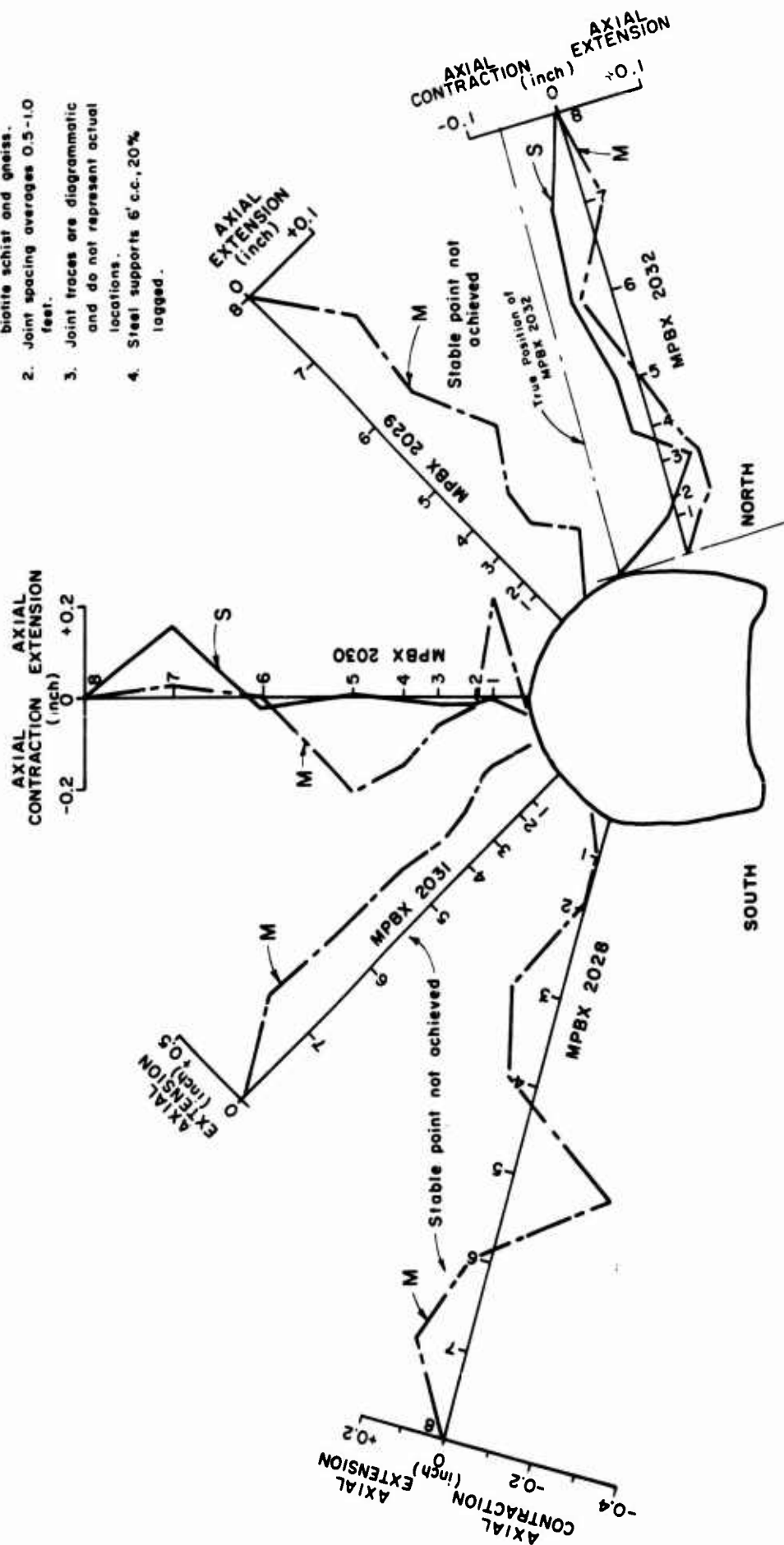


Figure 5A. Straight Creek Tunnel - Sta. 43 + 85 - Measured Displacements

Scale for opening and anchor depths (feet)

0 5 10

NOTE:  
 Because of the large differences  
 between the magnitudes, and the  
 measured data, the data on this  
 figure are plotted on a different  
 scale than used on figure 5A.

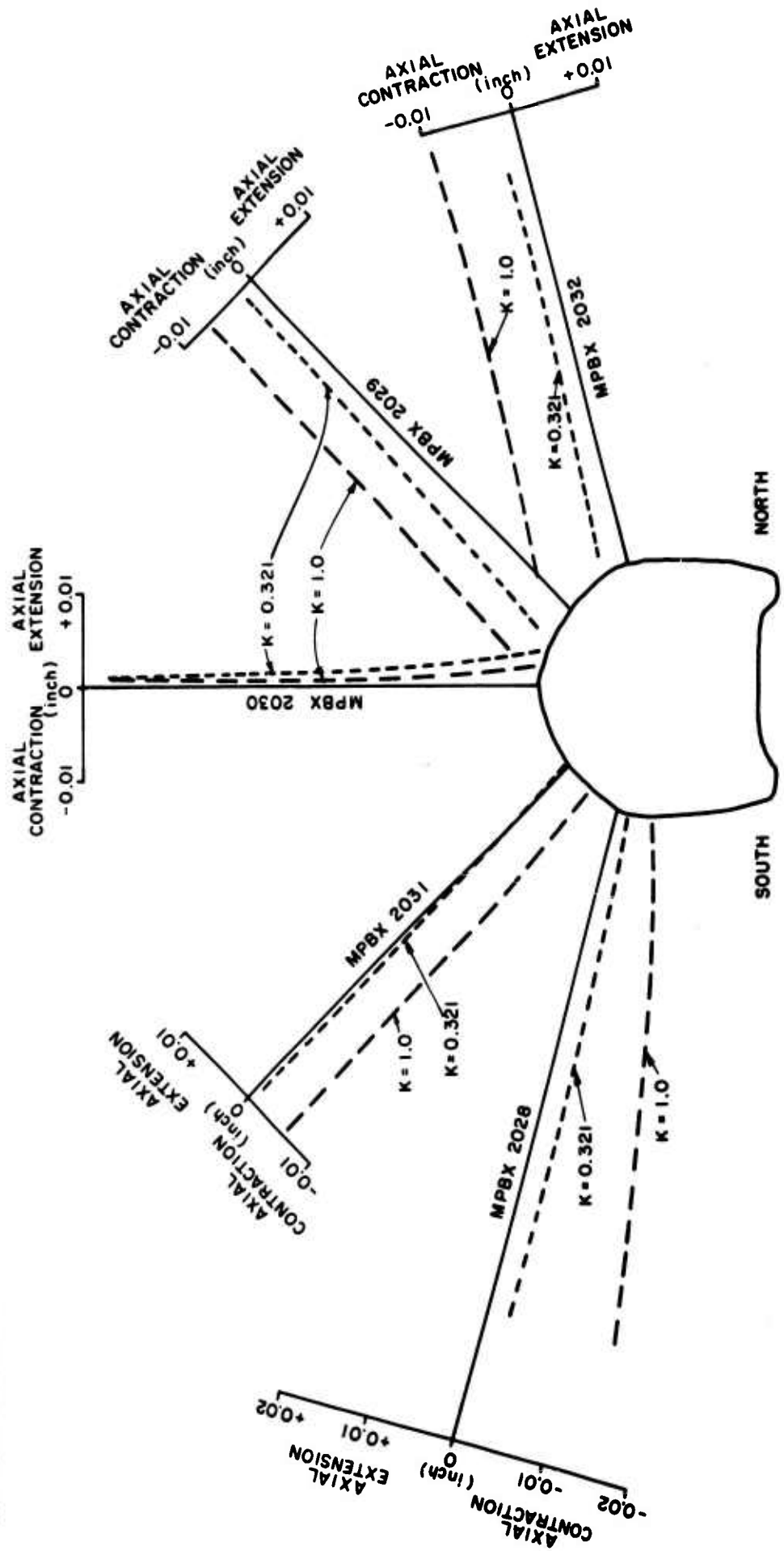


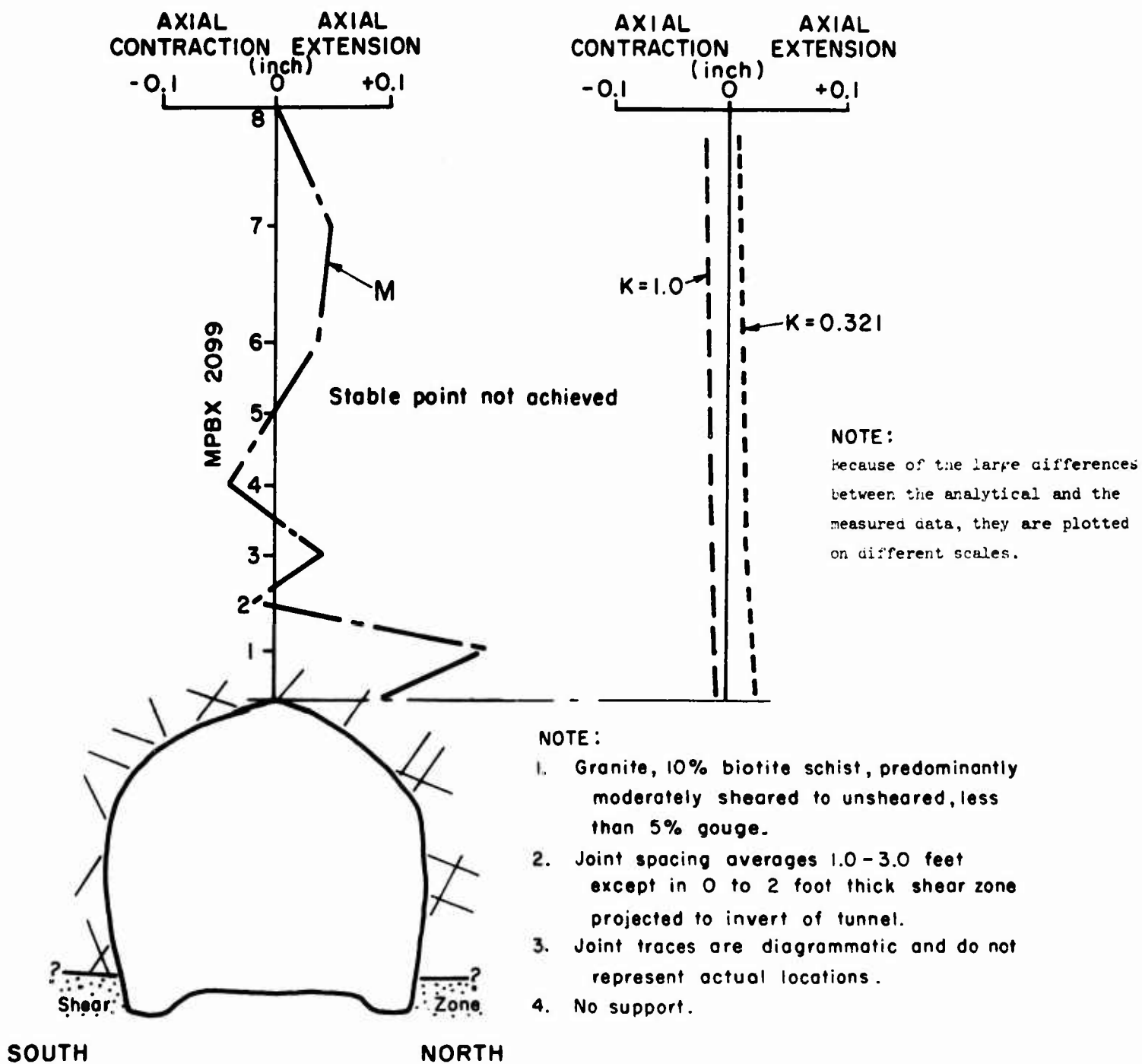
Figure 5B. Straight Creek Tunnel - Sta. 43 + 85 - Calculated Displacements







Scale for opening and anchor depths (feet)



38  
Figure 8. Straight Creek Tunnel - Sta. 65 + 94 - Displacements



Scale for opening and anchor depths (feet)

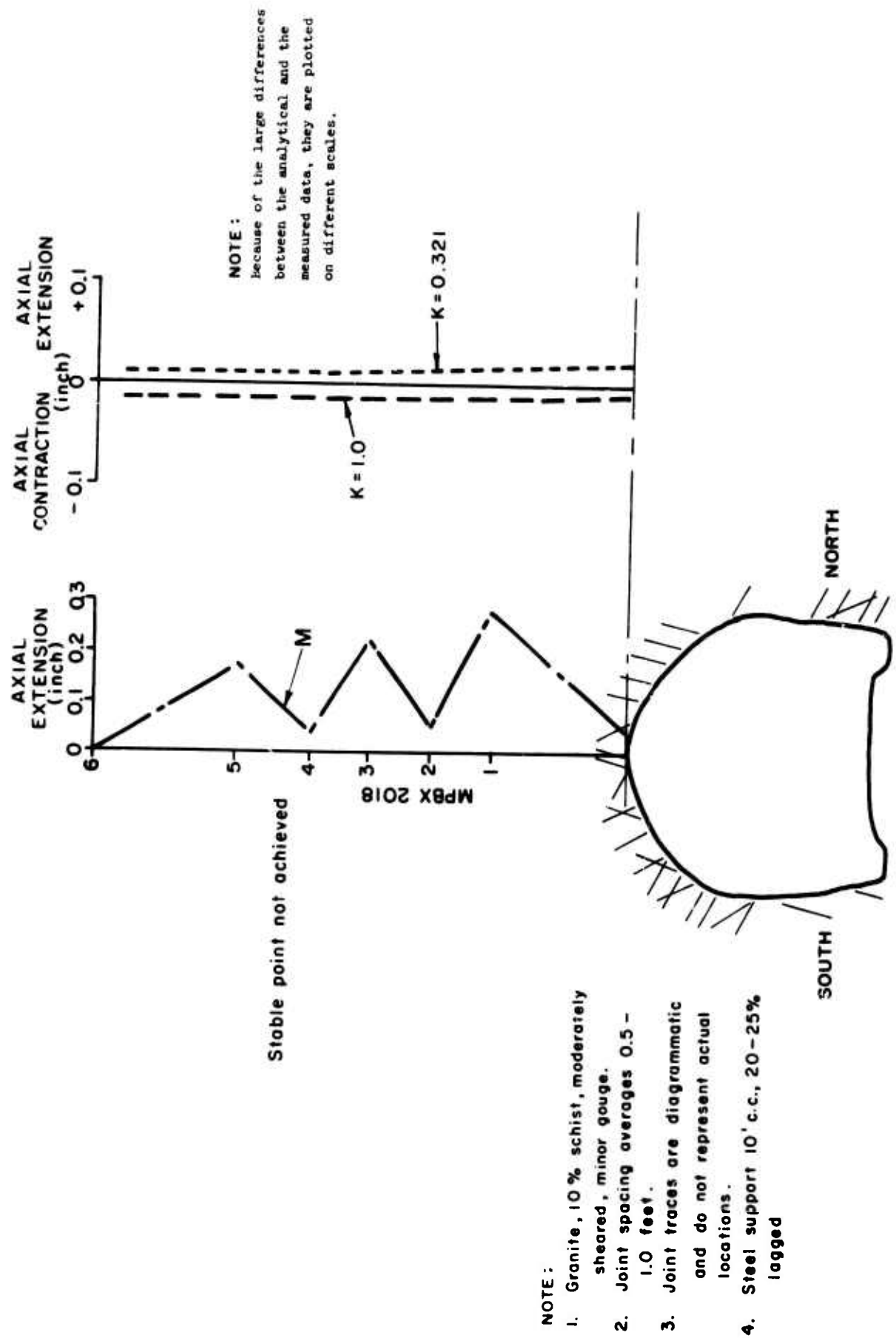
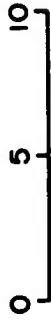
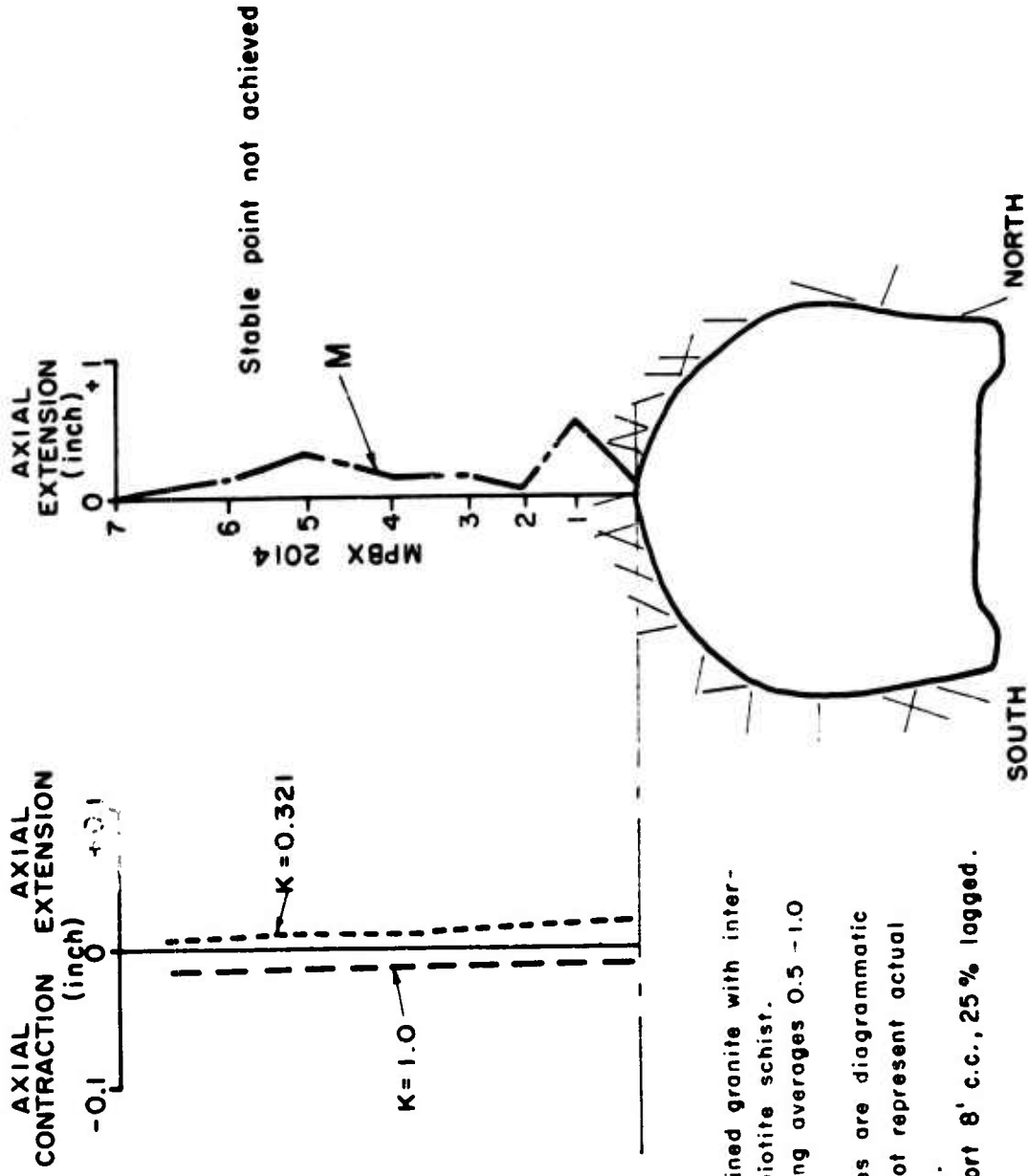


Figure 9. Straight Creek Tunnel - Sta. 69 + 81 - Displacements

"?" indicates questionable reading



Scale for opening and anchor depths (feet)



NOTE:

Because of the large differences between the analytical and the measured data, they are plotted on different scales.

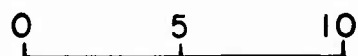
NOTE:

1. Coarse grained granite with inter-banded biotite schist.
2. Joint spacing averages 0.5 - 1.0 feet.
3. Joint traces are diagrammatic and do not represent actual locations.
4. Steel support 8' c.c., 25% logged.

Figure 10. Straight Creek Tunnel - Sta. 73 + 57 - Displacements



"?" indicates questionable reading



Scale for opening and anchor depths (feet)

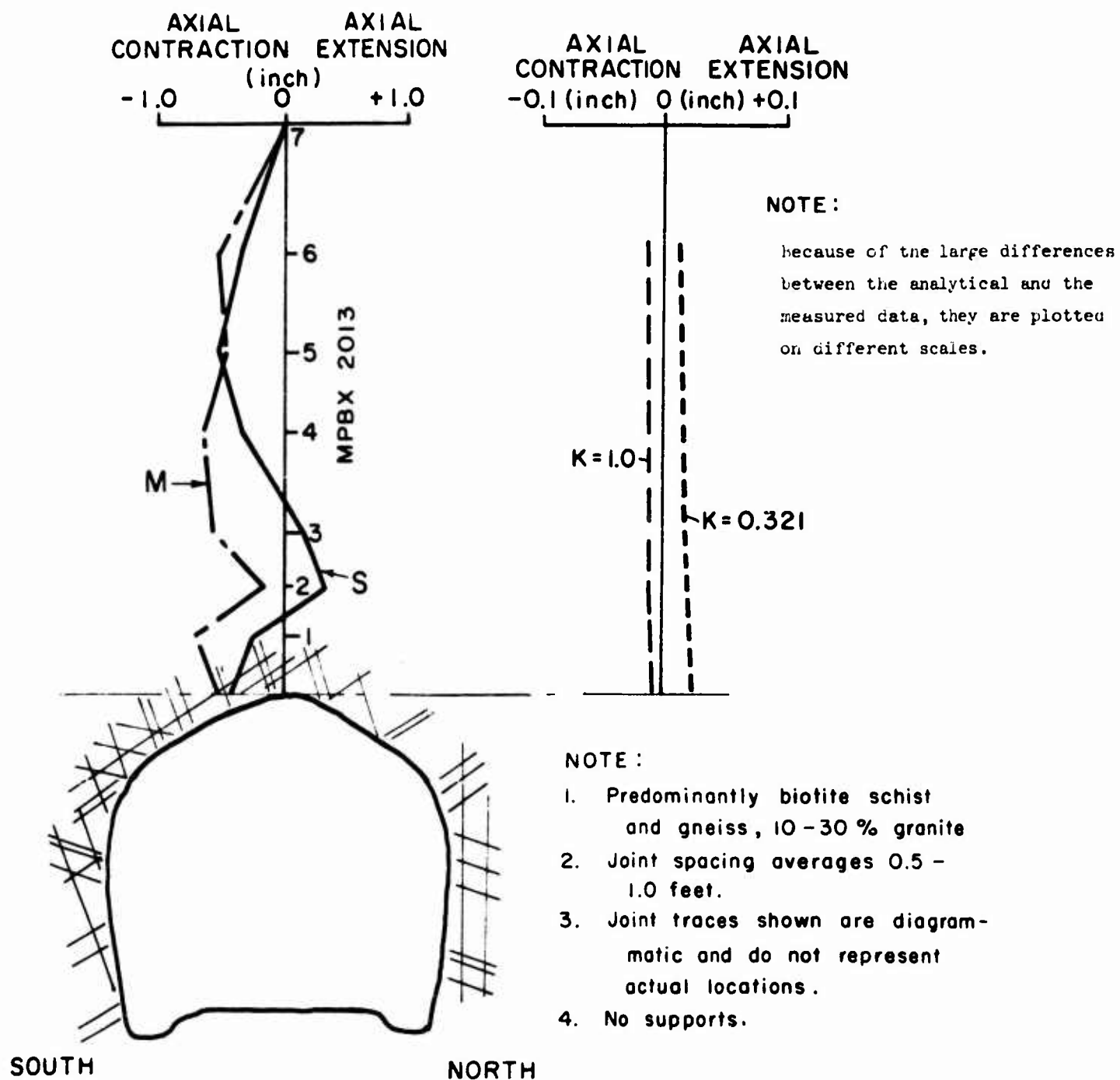
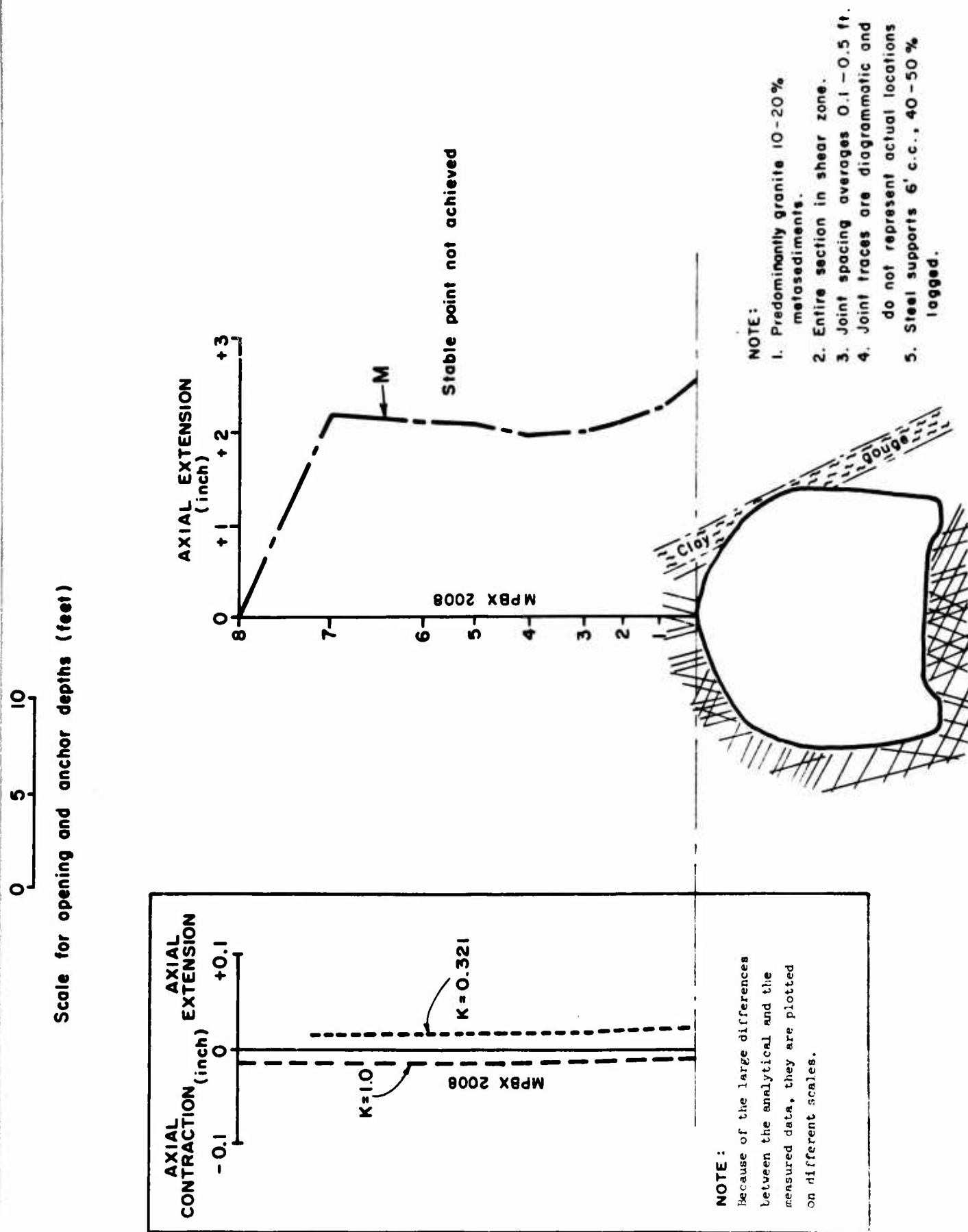


Figure 11. Straight Creek Tunnel - Sta. 78 + 17 - Displacements



**Figure 12. Straight Creek Tunnel - Sta. 81 + 41 - Displacements**



A vertical number line with tick marks at 0, 5, and 10.

Scale for opening and anchor depths (feet)

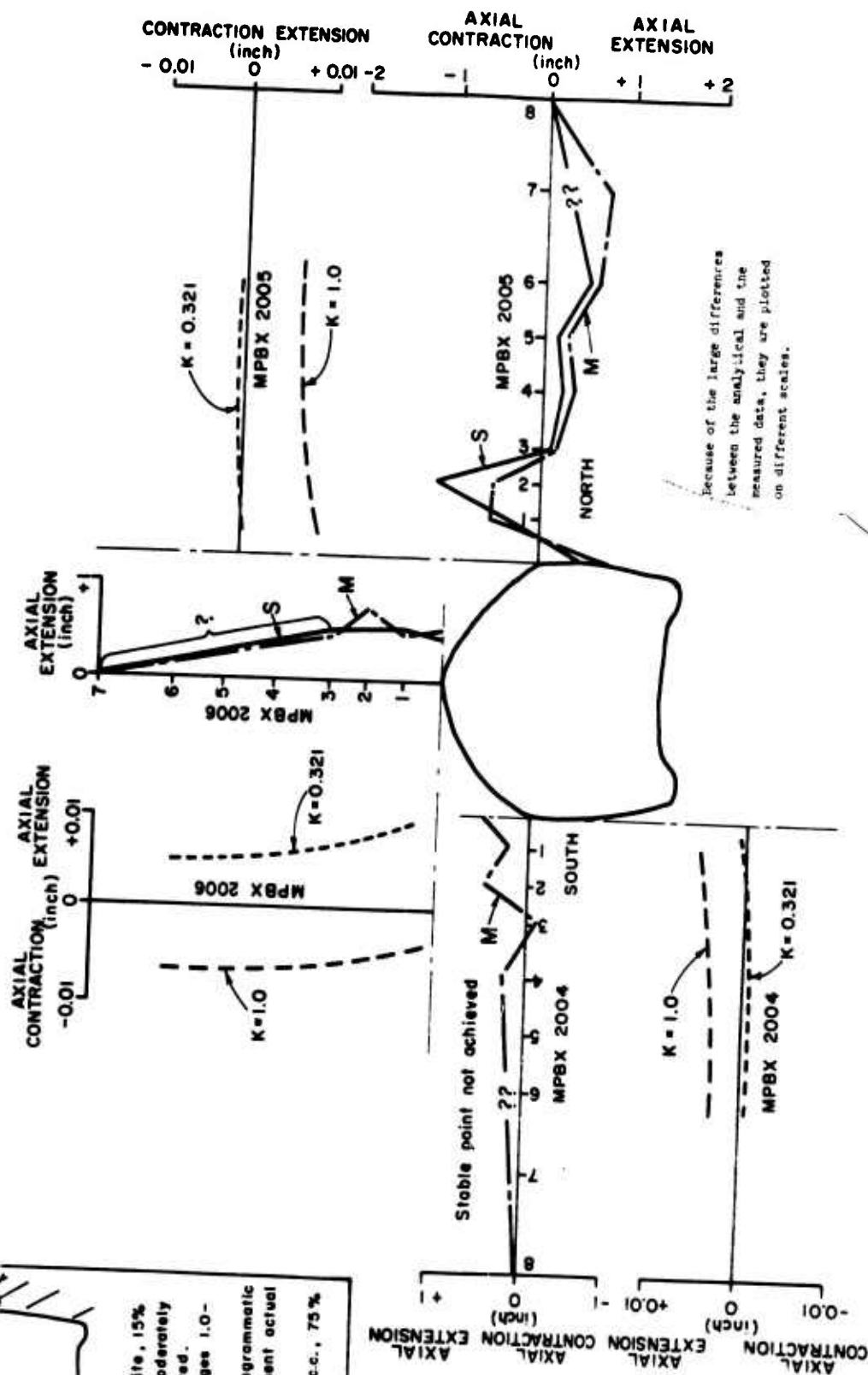
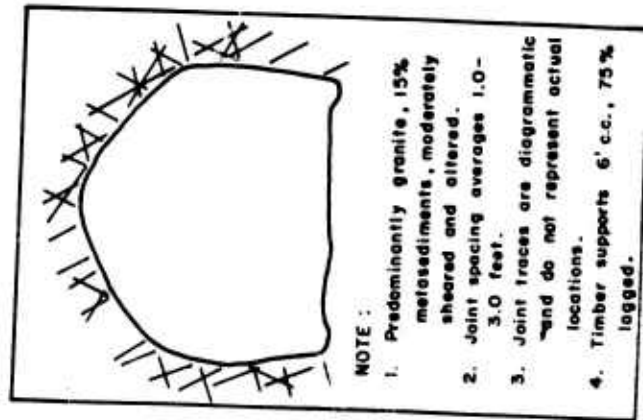
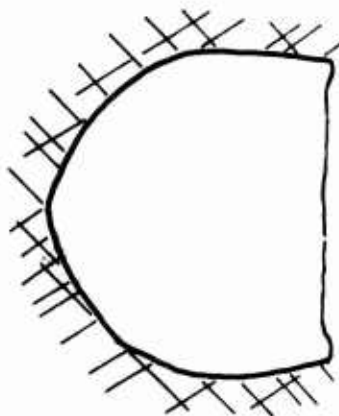


Figure 14. Straight Creek Tunnel - Sta. 104 + 83 - Displacements

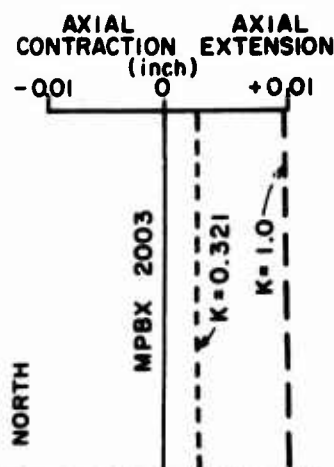
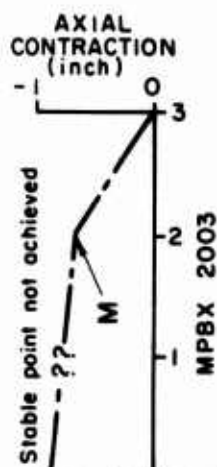
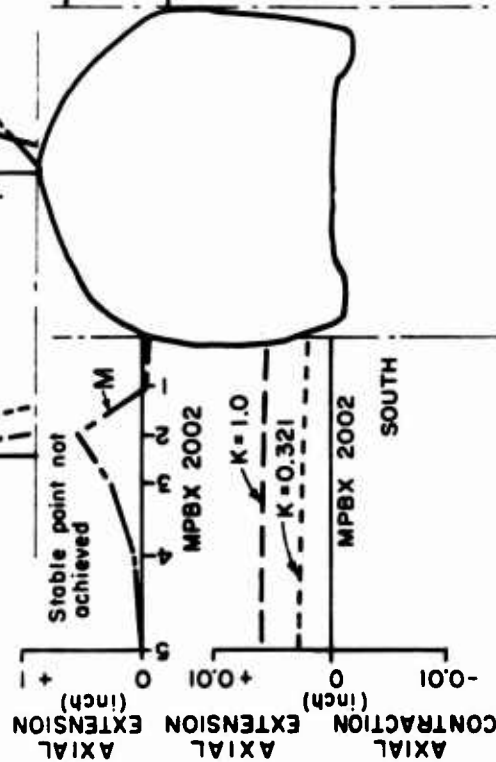
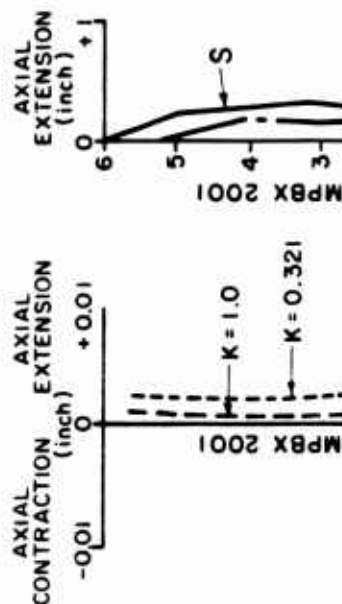


NOTE:

1. Predominantly granite
2. Joint spacing averages 1.0 - 3.0 feet.
3. Joint traces are diagrammatic and do not represent actual locations
4. Steel support 6' c.c., 75% lagged



Scale for opening and anchor depths (feet)



NOTE:  
Because of the large differences  
between the analytical and the  
measured data, they are plotted  
on different scales.

Figure 15. Straight Creek Tunnel - Sta. 114 + 53 - Displacements

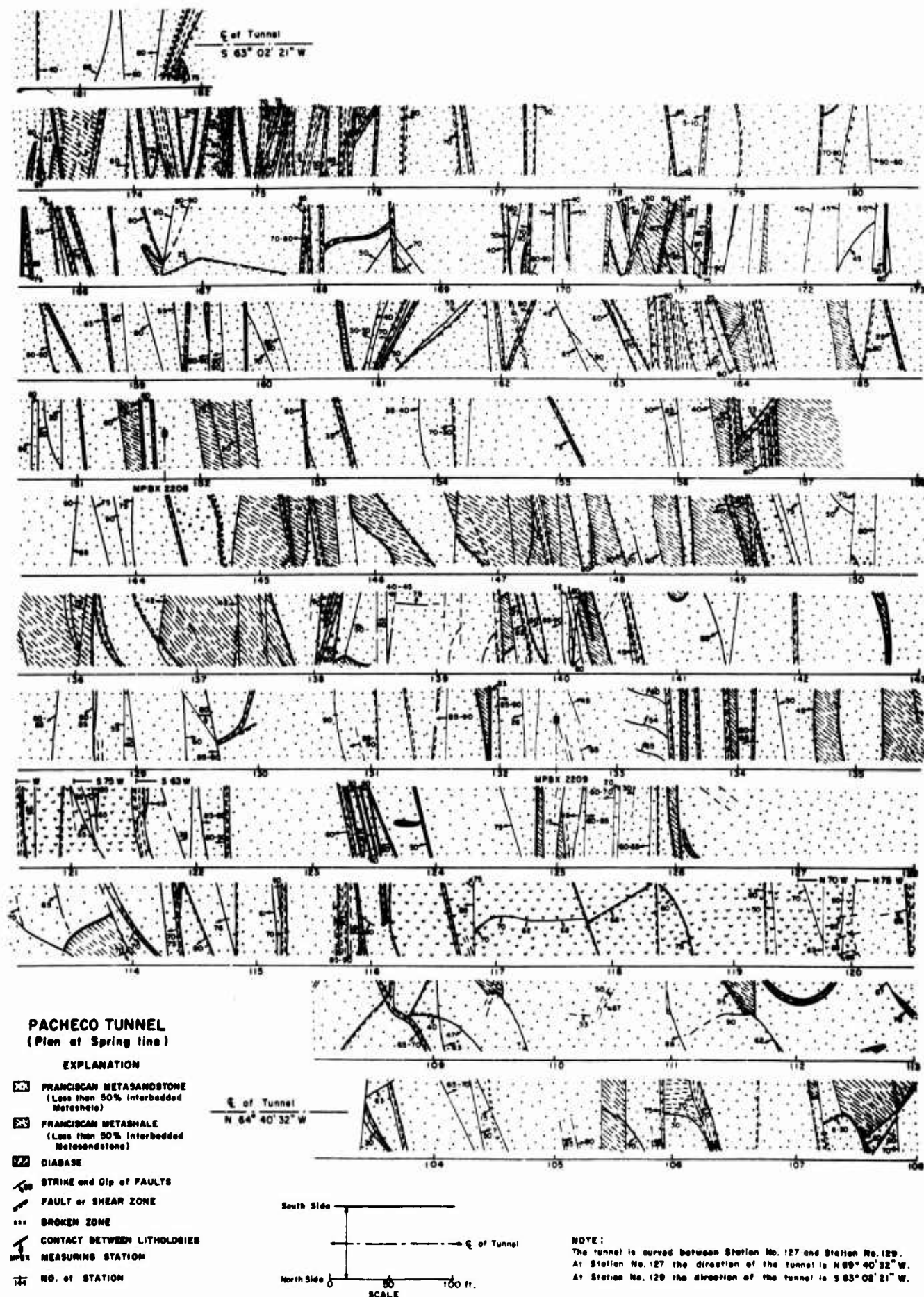
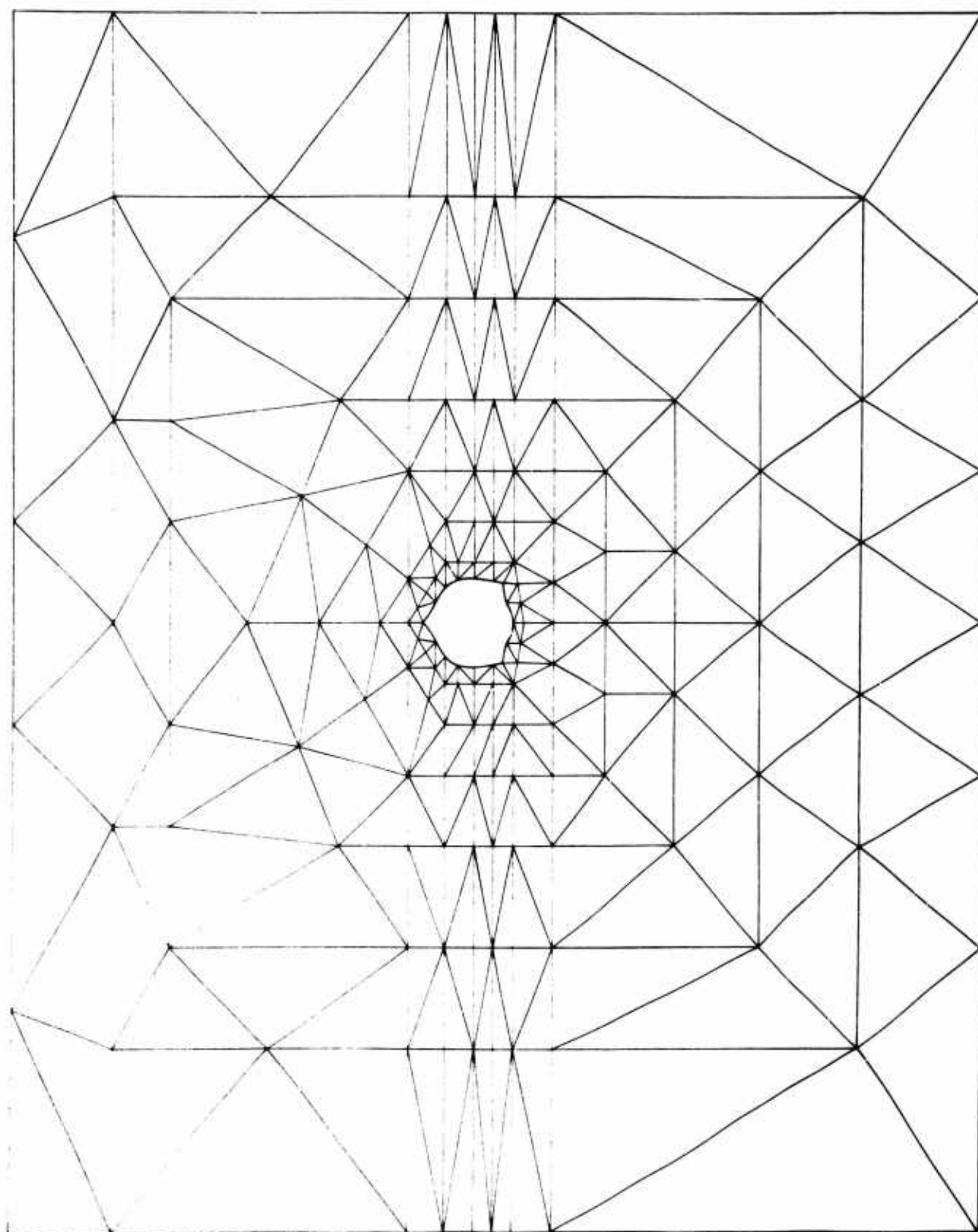
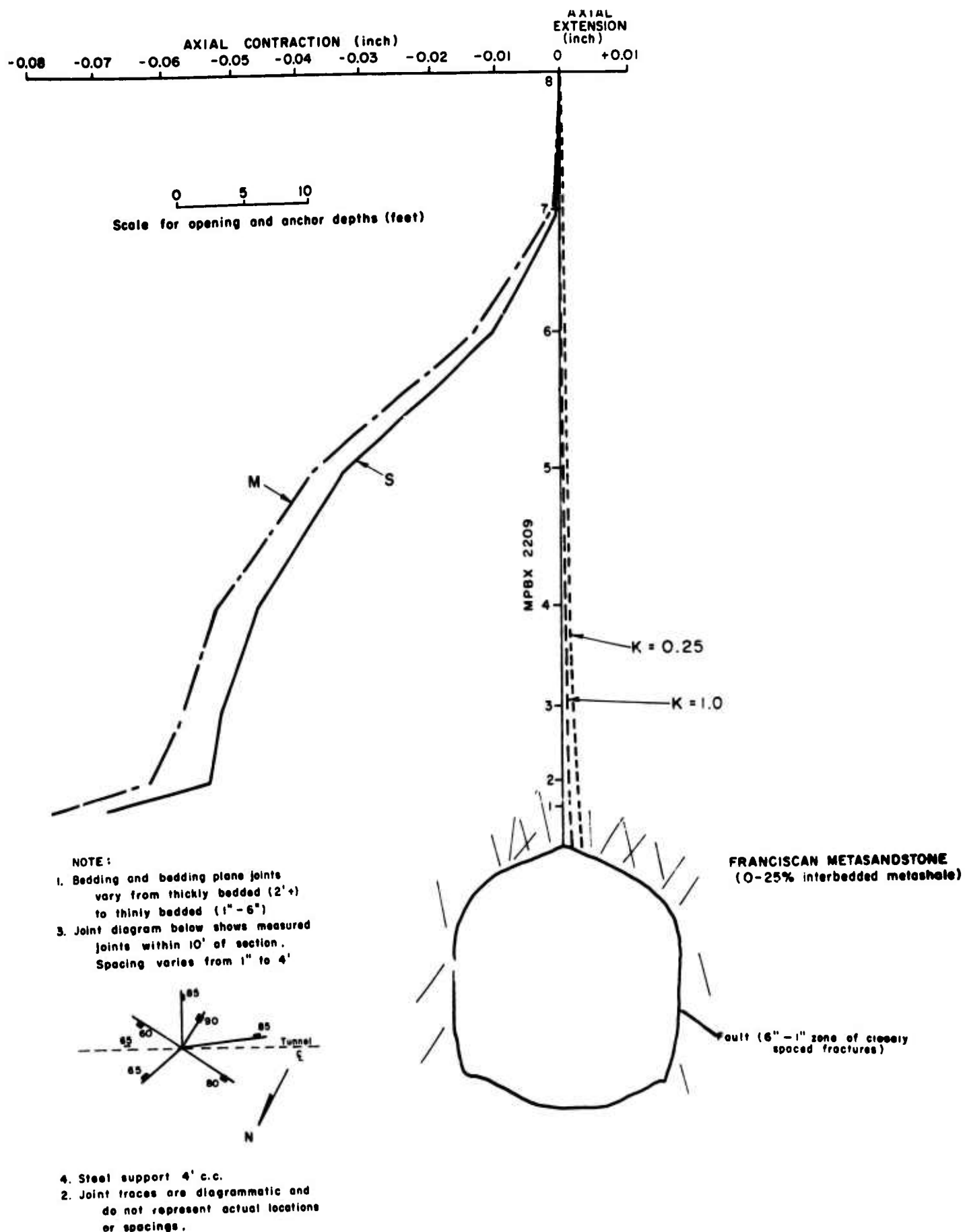


Figure 16. Pacheco Tunnel - Geologic Log



Scale 0 20'

Figure 17. Pacheco Tunnel - Finite Element Mesh



48

Figure 18. Pacheco Tunnel - Sta. 132 + 50 - Displacements



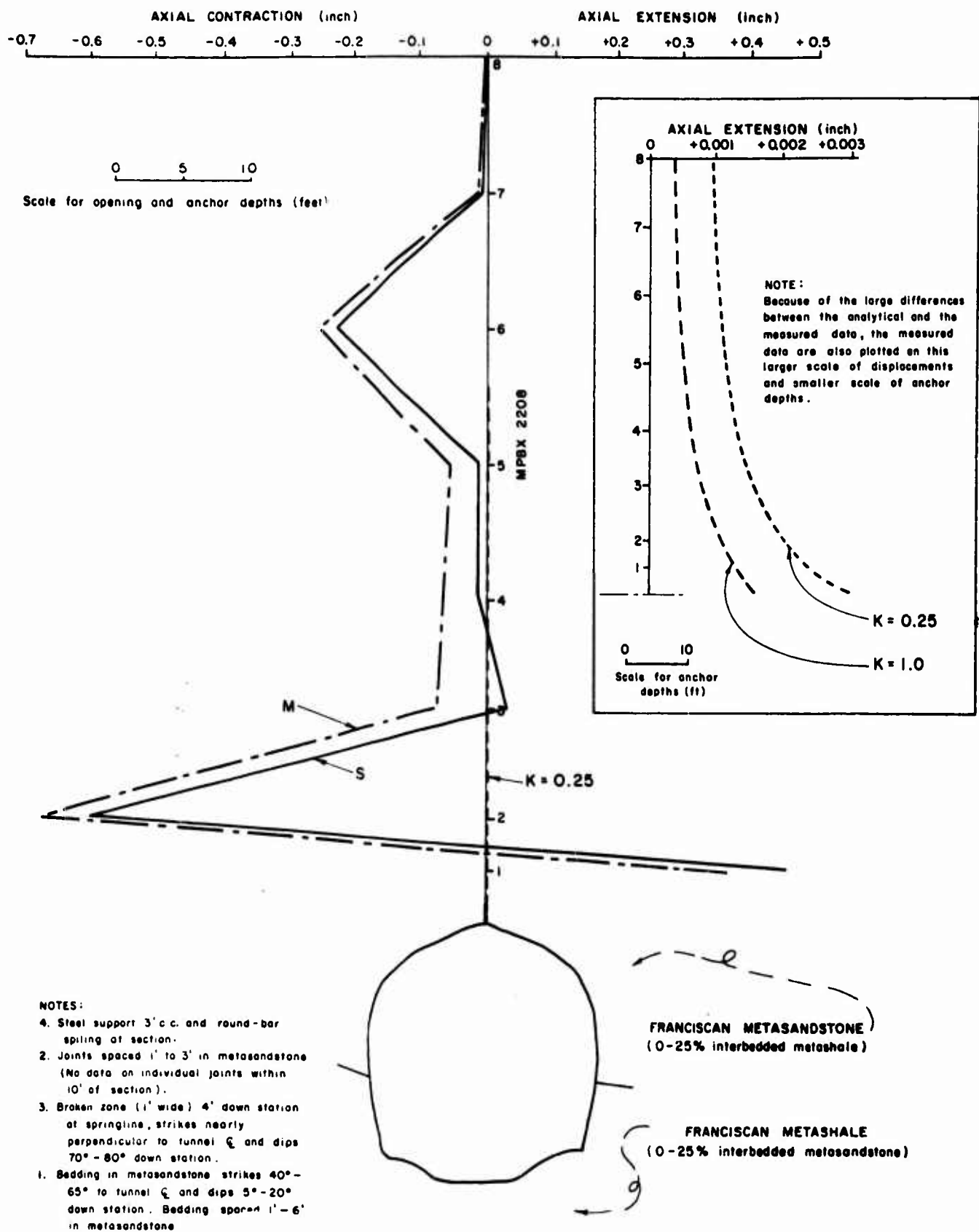


Figure 19. Pacheco Tunnel - Sta. 151 + 68.1 Displacements

# NAVAJO INDIAN GATION PROJECT - NEW MEXICO MAIN CANAL

## GEOLOGICAL CROSS SECTION AT TUNNEL ALIGNMENT

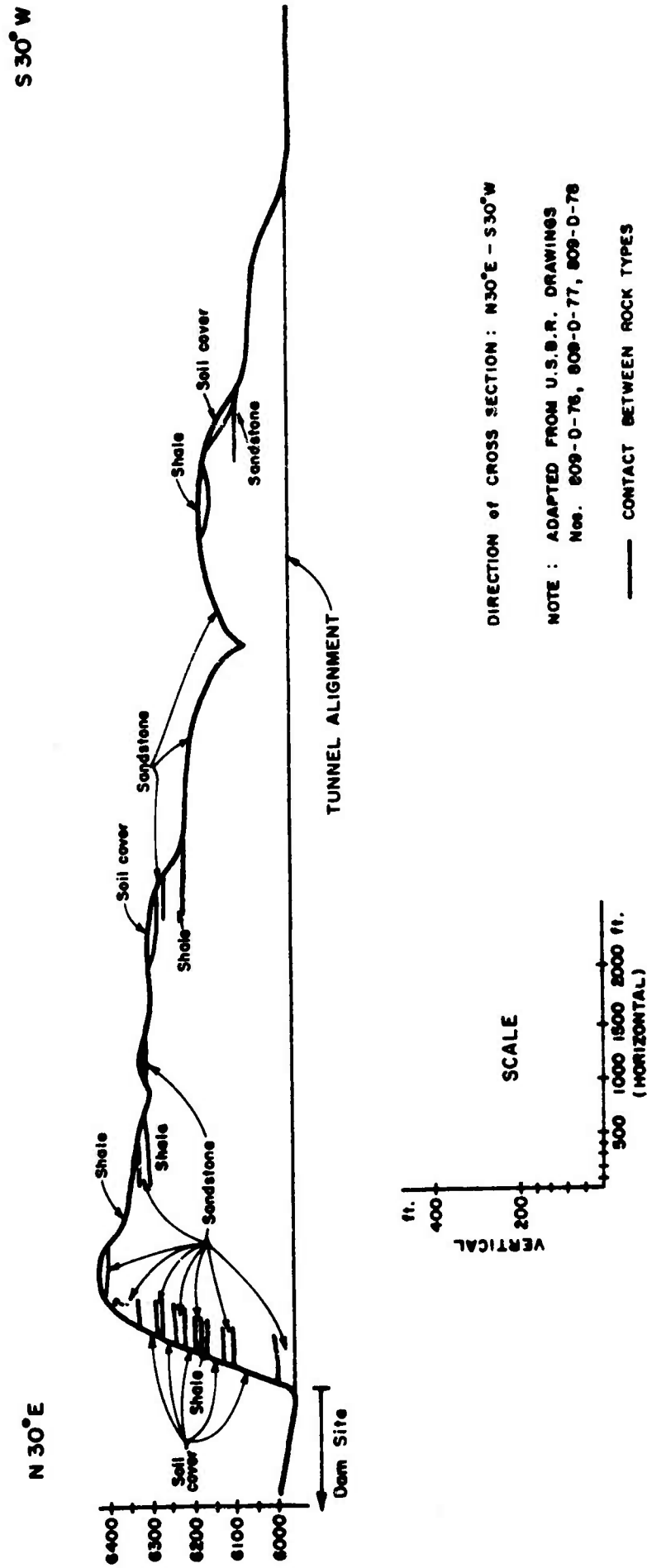


Figure 20. Navajo Tunnel - Geology

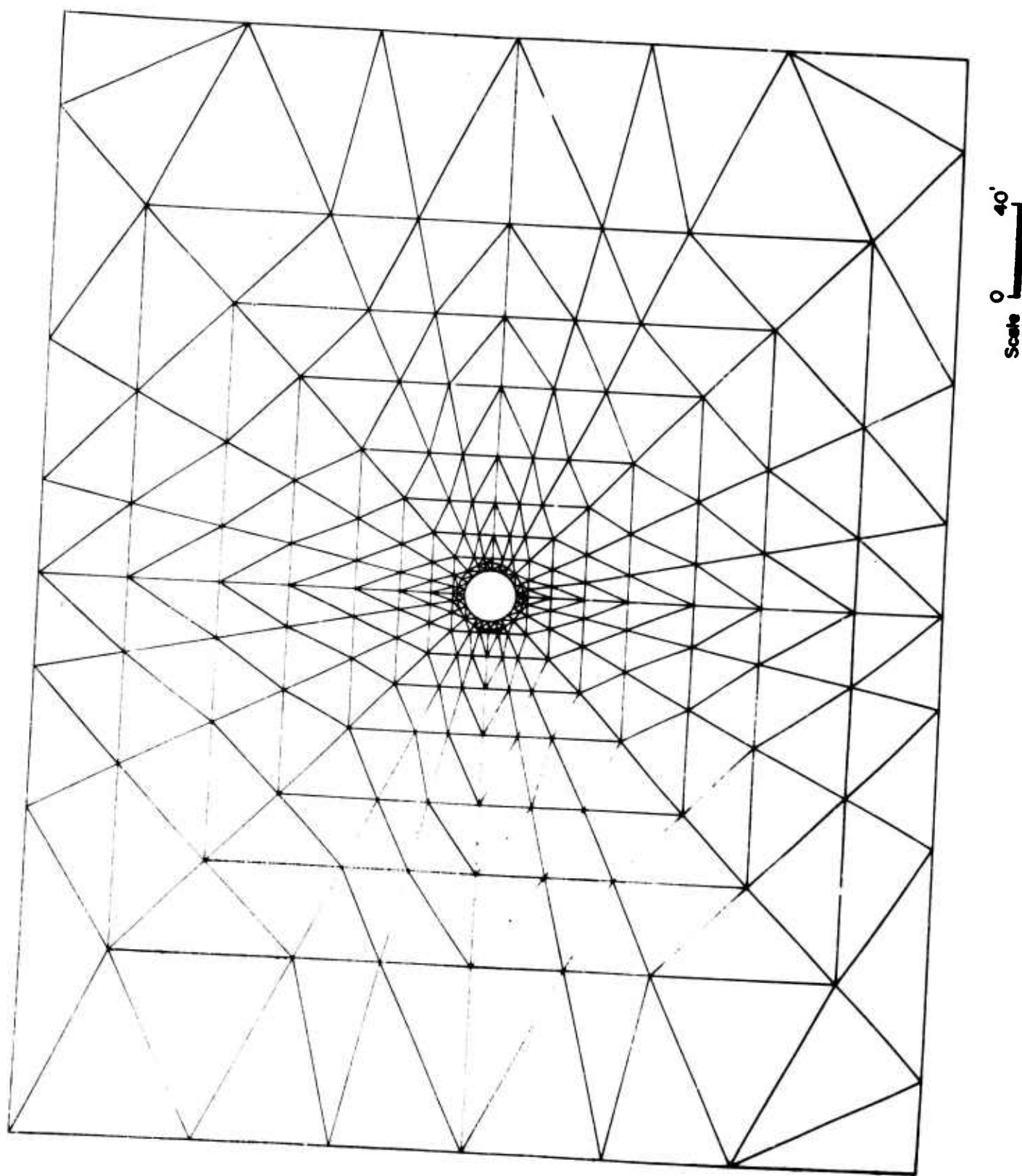
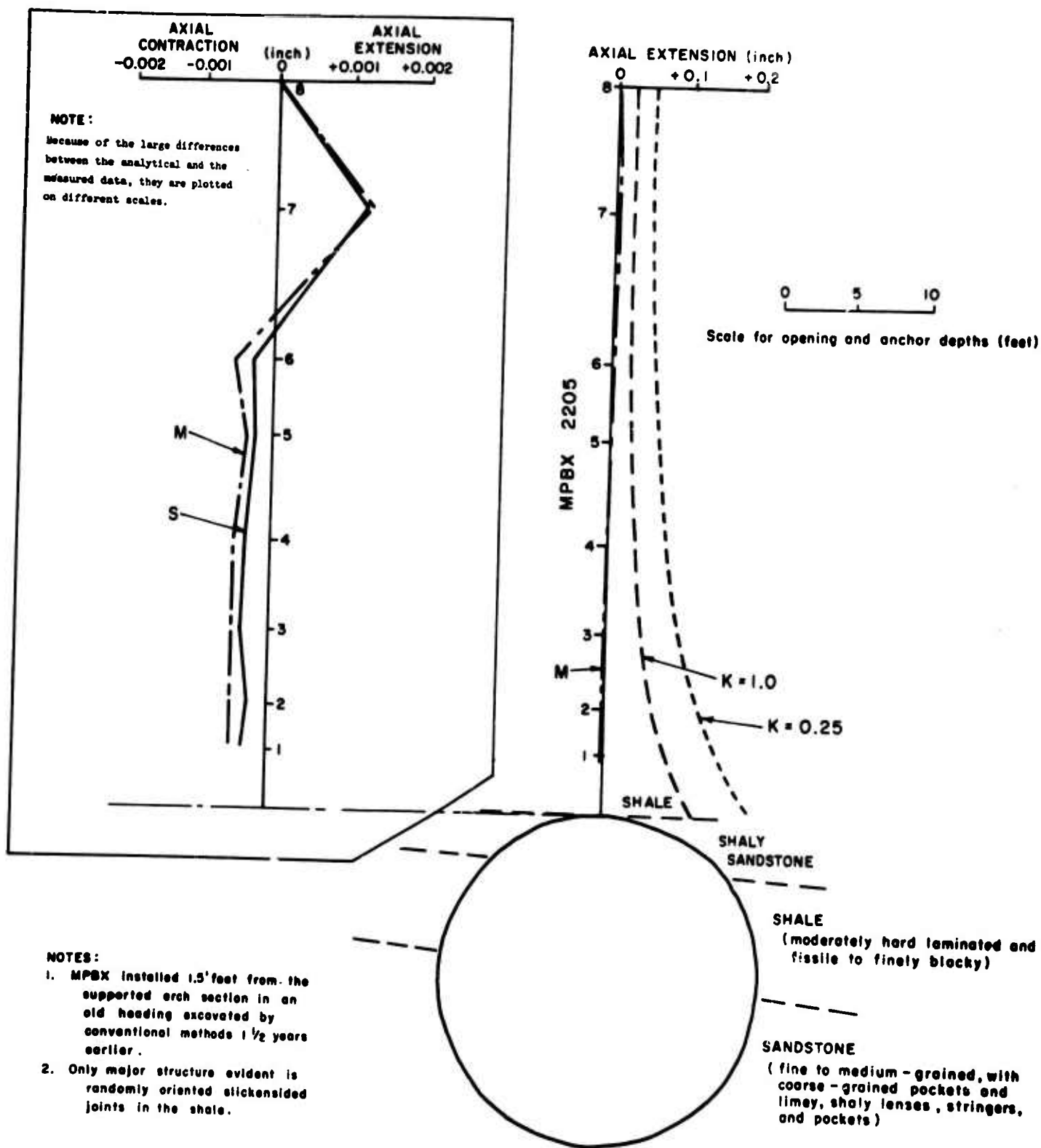


Figure 21. Navajo Tunnel - Finite Element Mesh



52  
Figure 22. Navajo Tunnel - Sta. 7 + 46 - Displacements

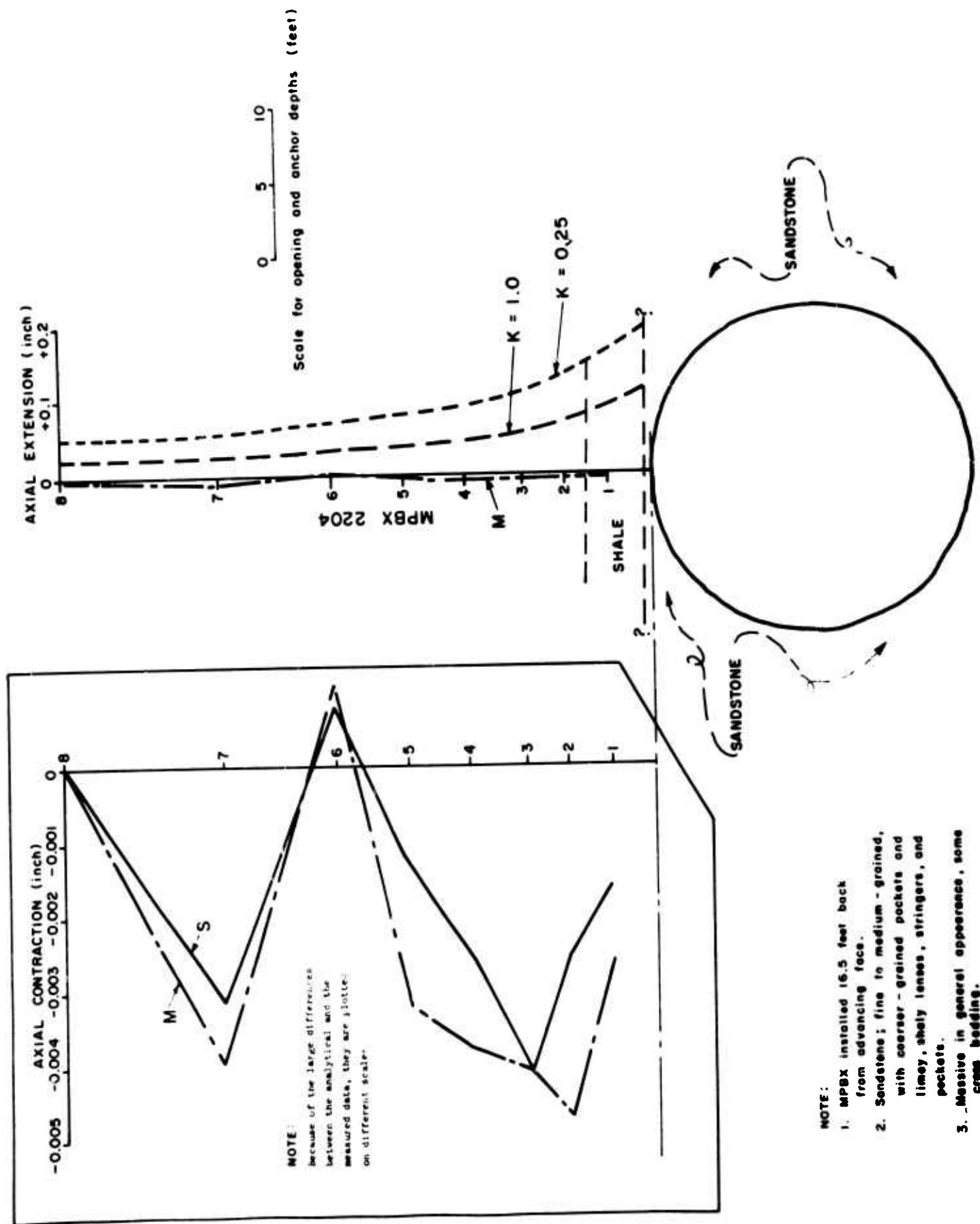
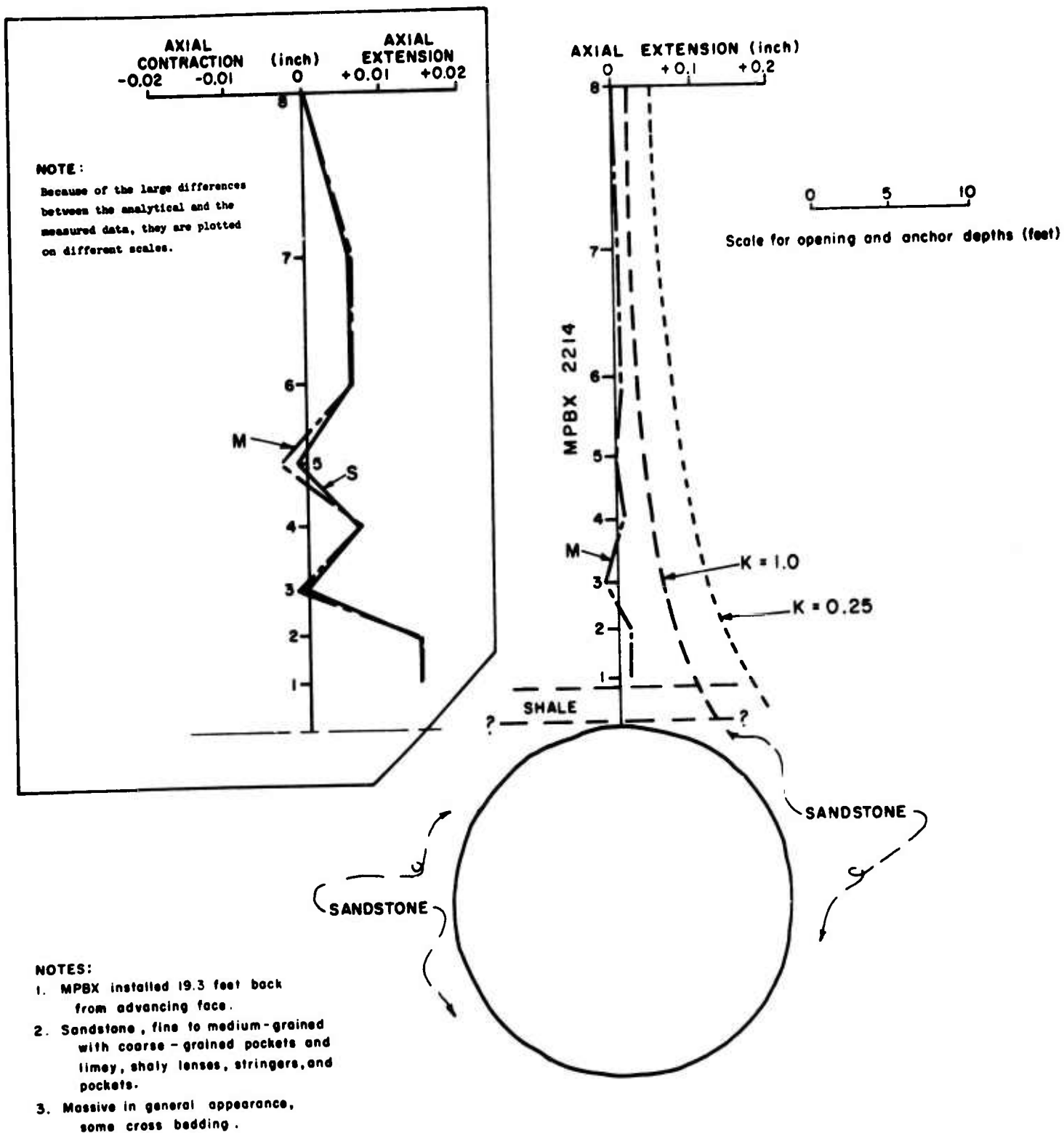
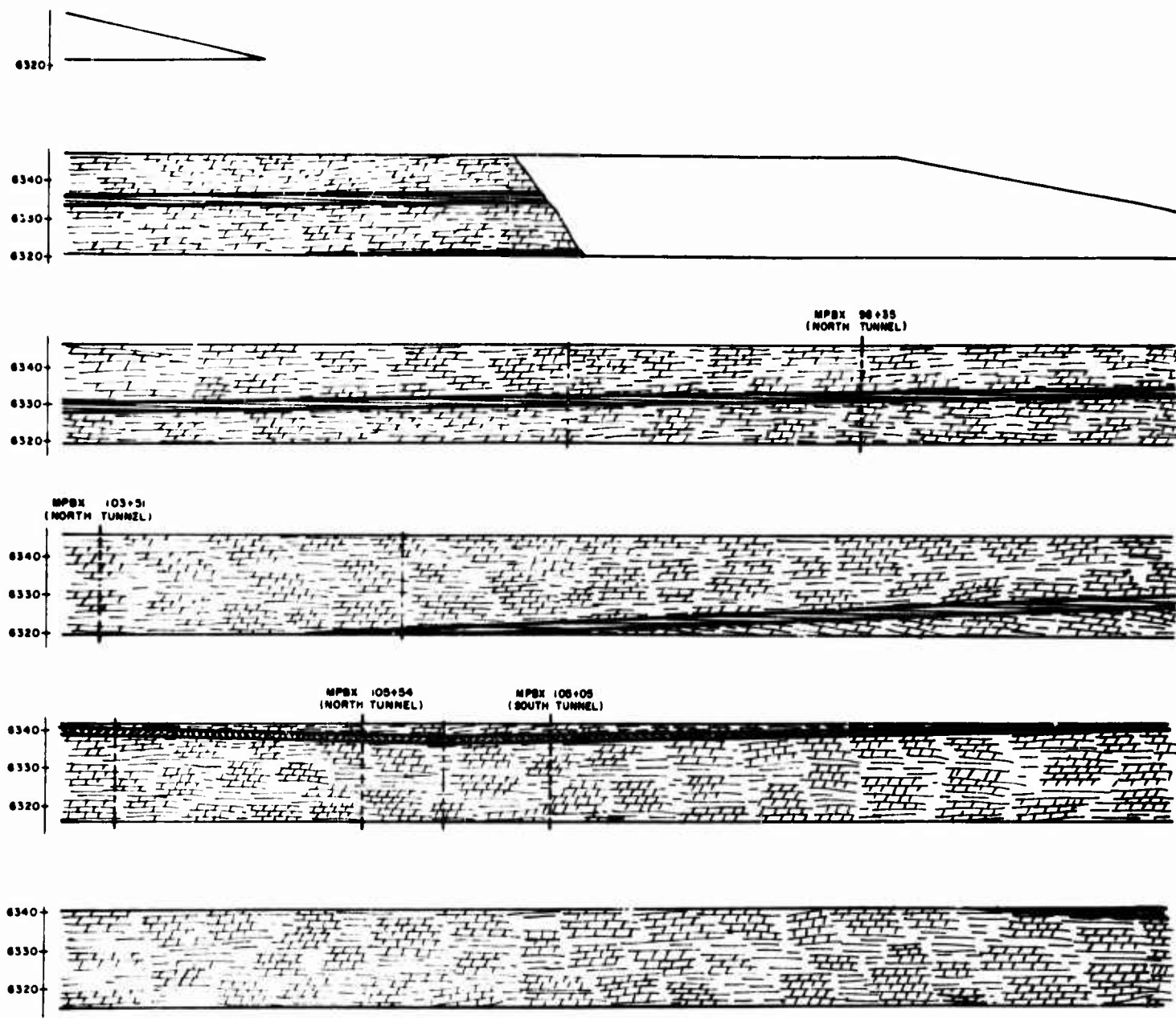


Figure 23. Navajo Tunnel - Sta. 14 + 76 - Displacements








54  
Figure 24. Navajo Tunnel - Sta. 18 + 85 - Displacements



# GREEN RIVER TUNNEL Geological Cross Section

0 10 20 30 40 50 ft  
Scale  
(Vertical and Horizontal)

-  Massive or Laminated Dolomitic Marlstone  
(Massive up to 10 ft. in thickness)
-  Dolomitic Shales
-  Tuffaceous Siltstone
-  Boundary Between Lithological Units
-  MPBX Stations

Note: Adapted from a report published in September 1962  
by the Wyoming Highway Department.

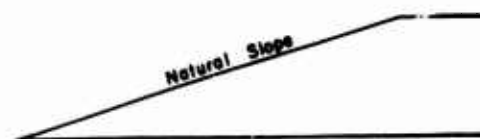
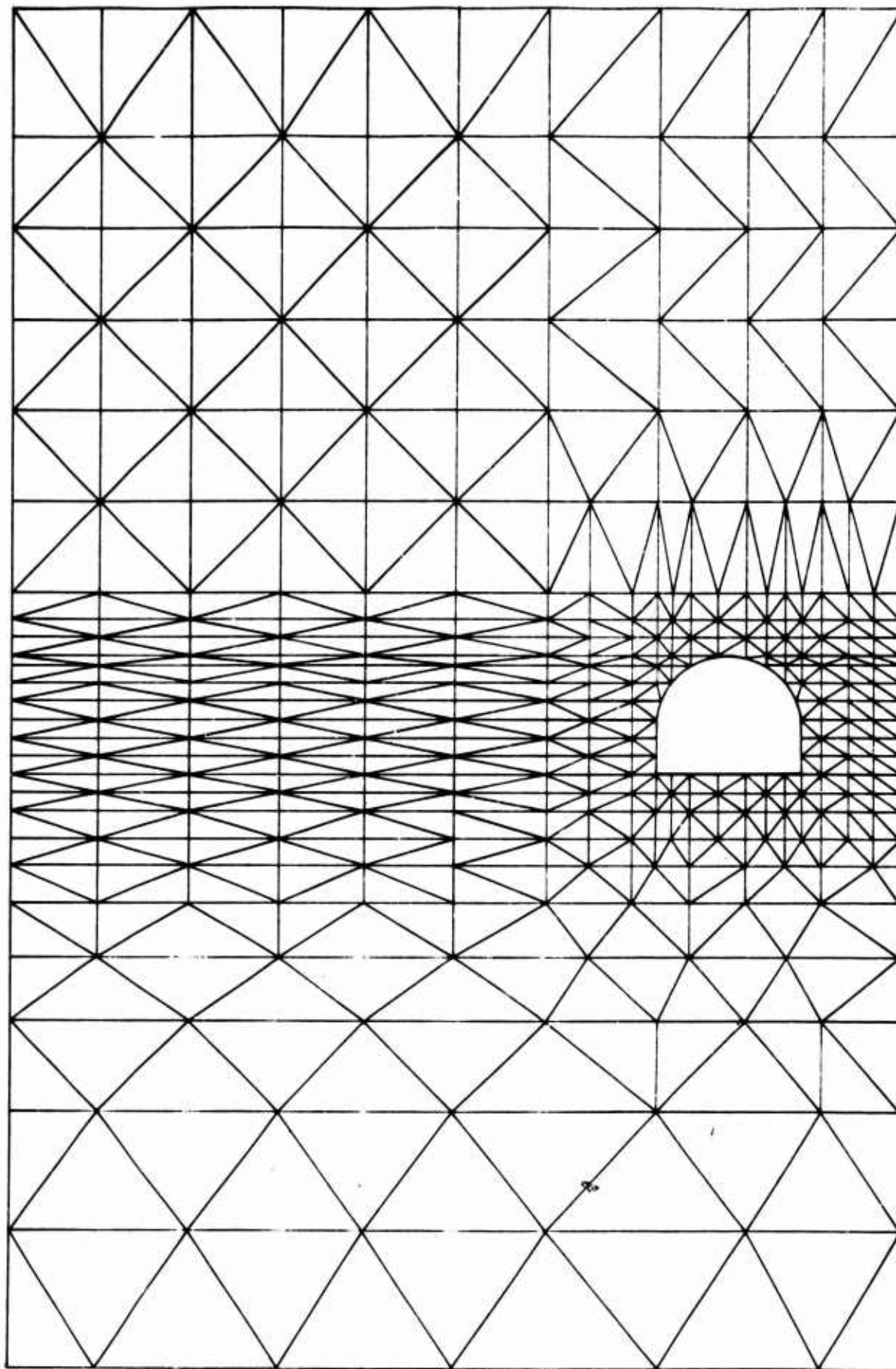


Figure 25. <sup>55</sup> Green River Tunnel - Geology



Scale 0 40'

56

Figure 26. Green River Tunnel - Finite Element Mesh



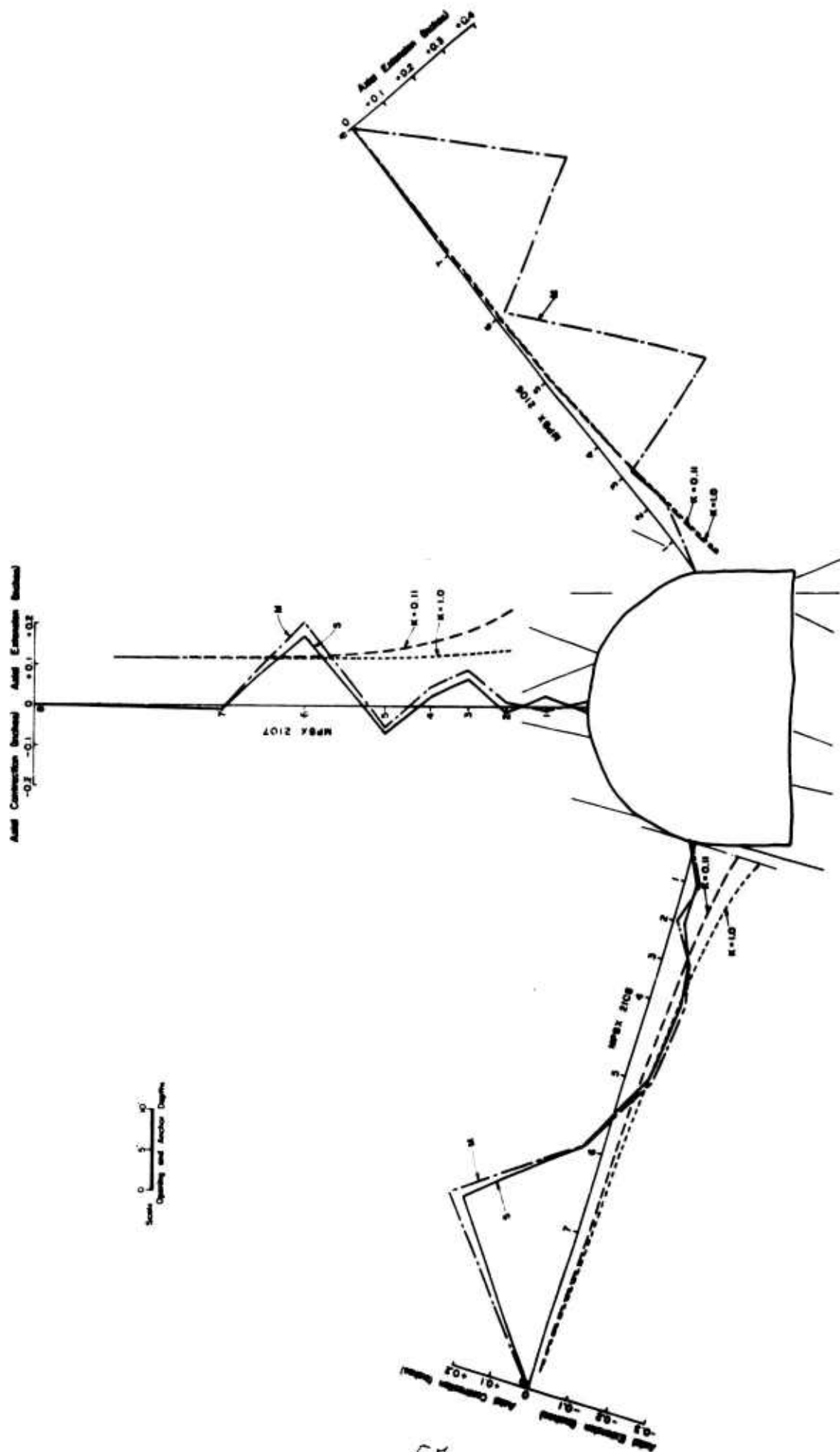


Figure 27. Green River North Tunnel - Sta. 98 + 65 - Displacements

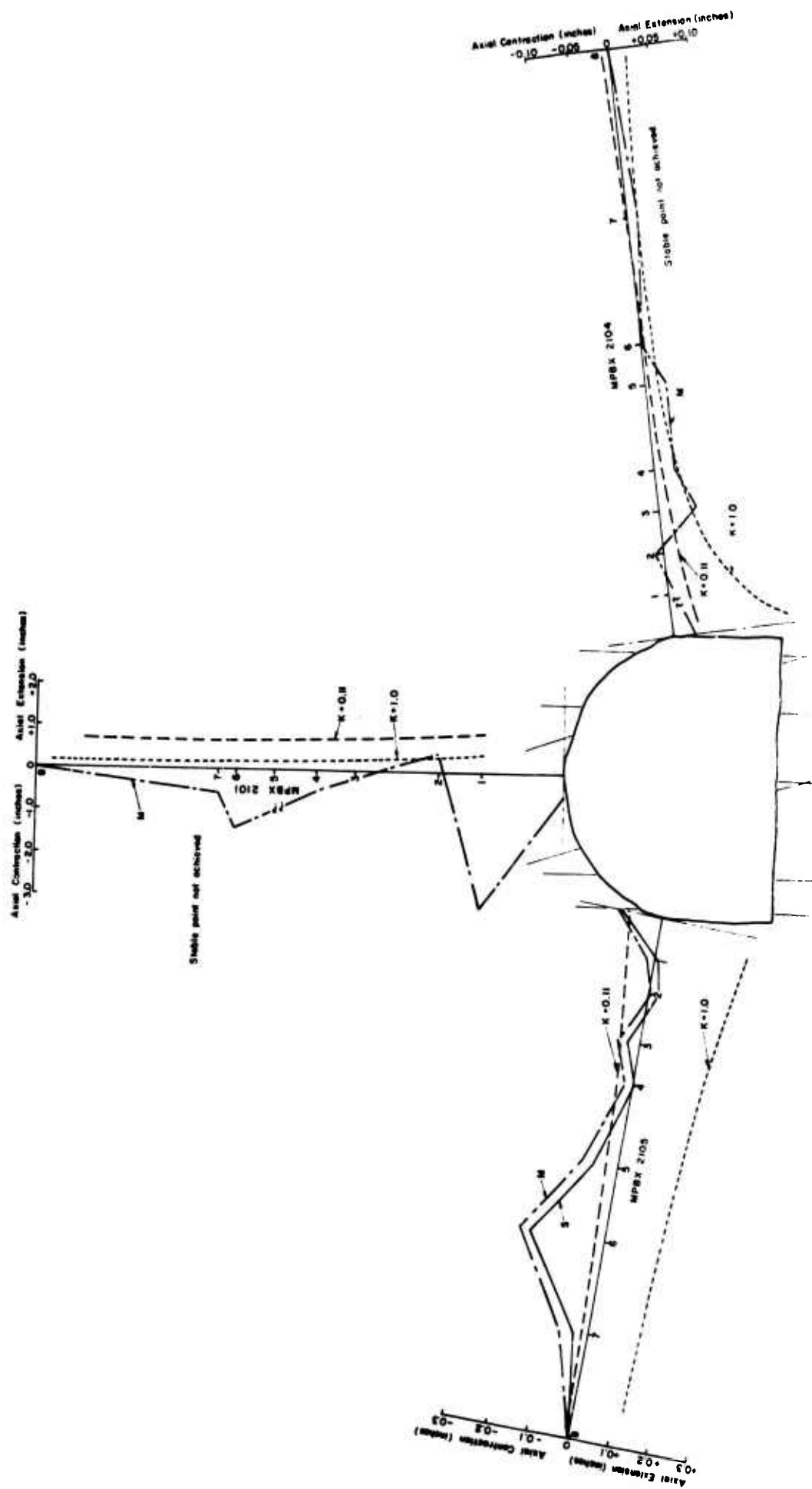


Figure 28. Green River North Tunnel - Sta. 103 + 51 - Displacements



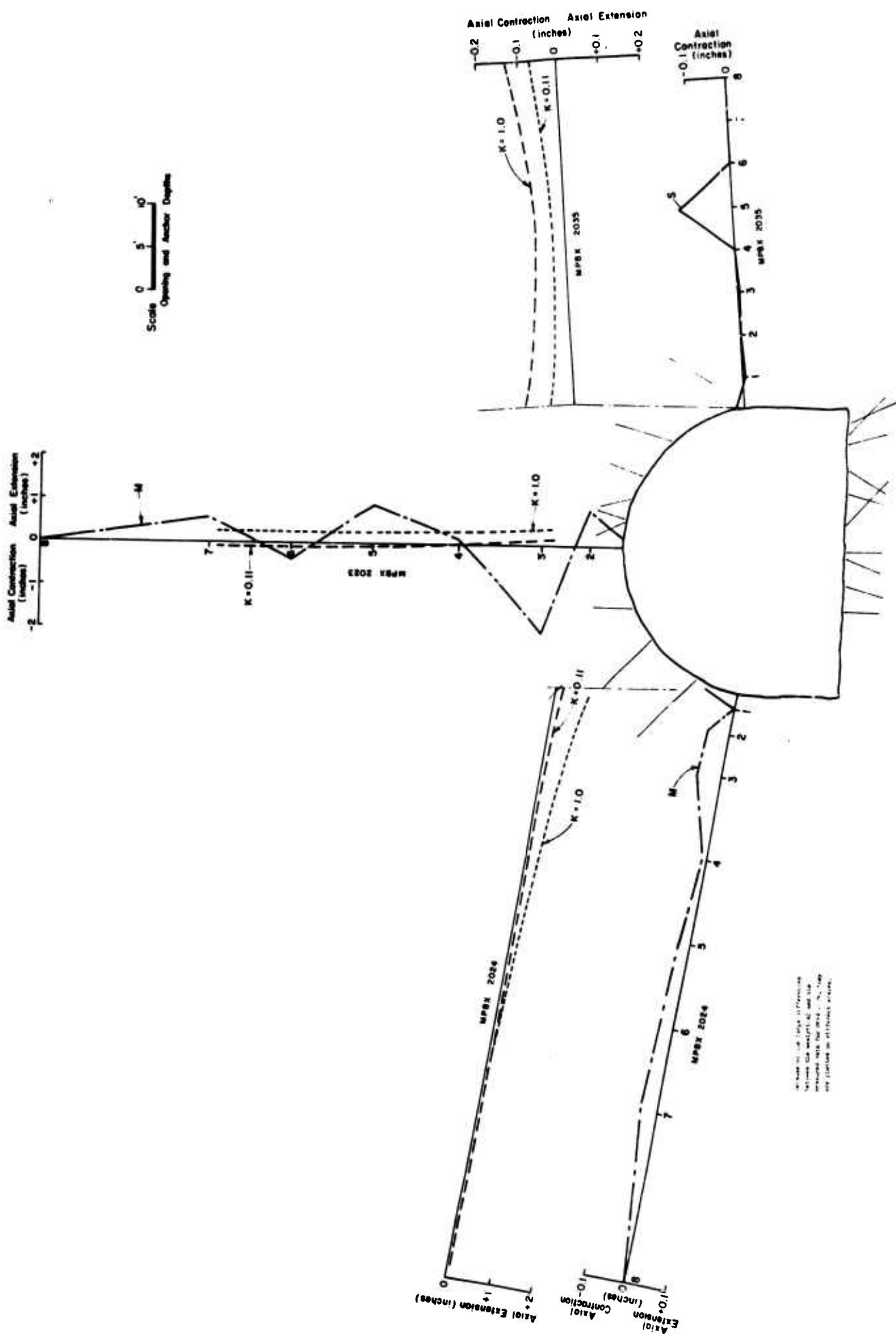
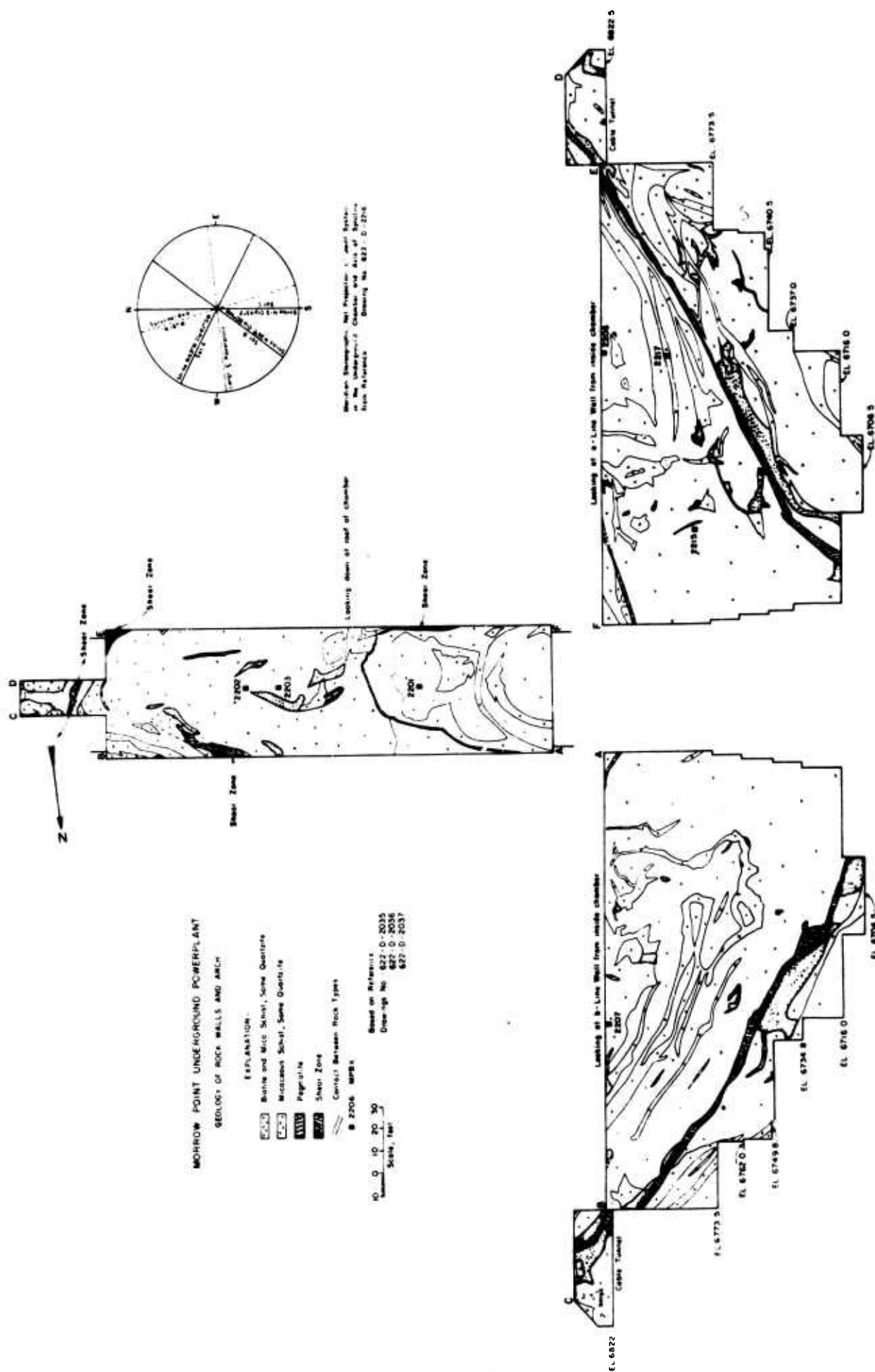


Figure 30. Green River North Tunnel - Sta. 105 + 54 - Displacements



**Figure 31. Morrow Point Powerplant - Geologic Log**

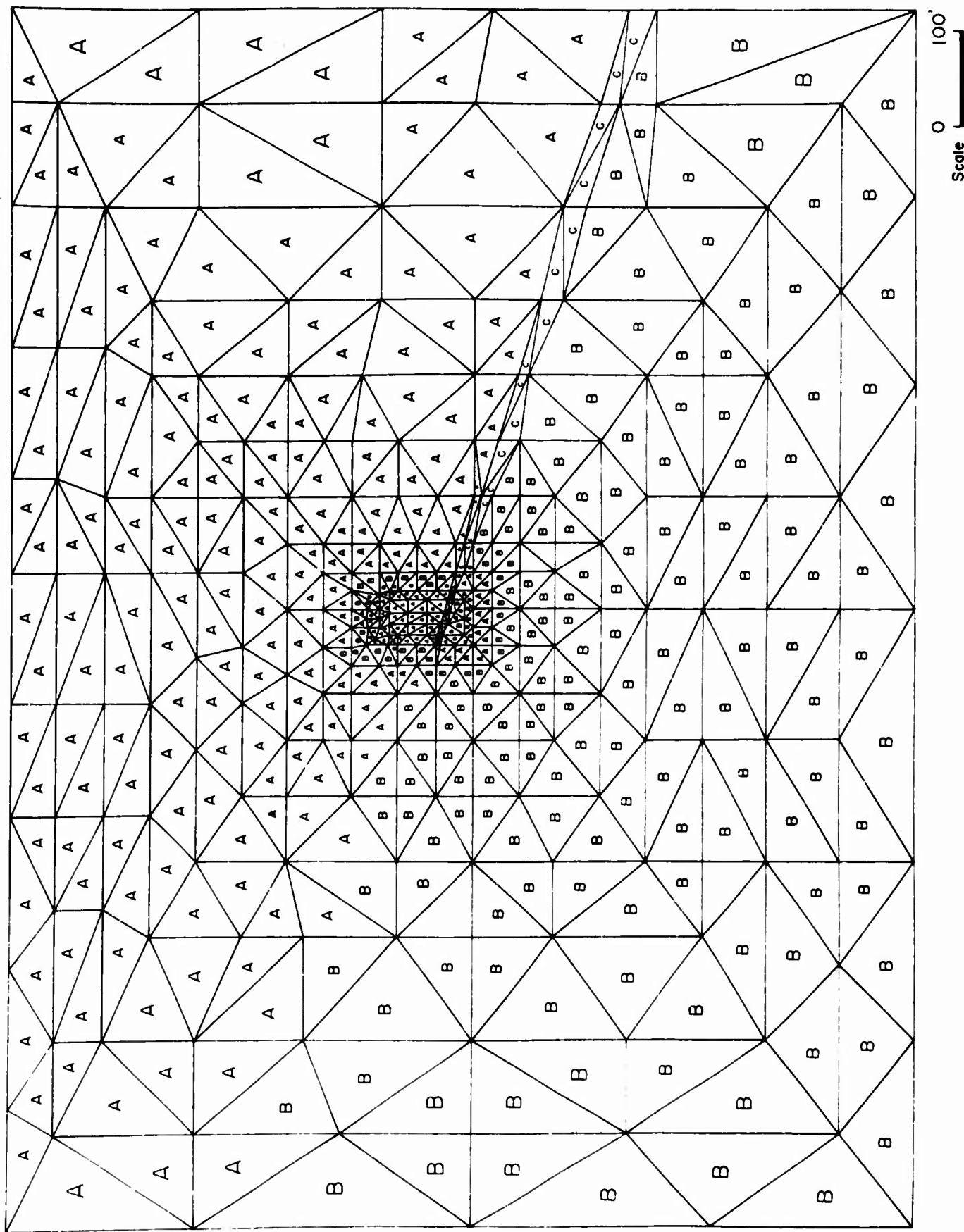


Figure 32. Morrow Point Powerplant - Finite Element Mesh

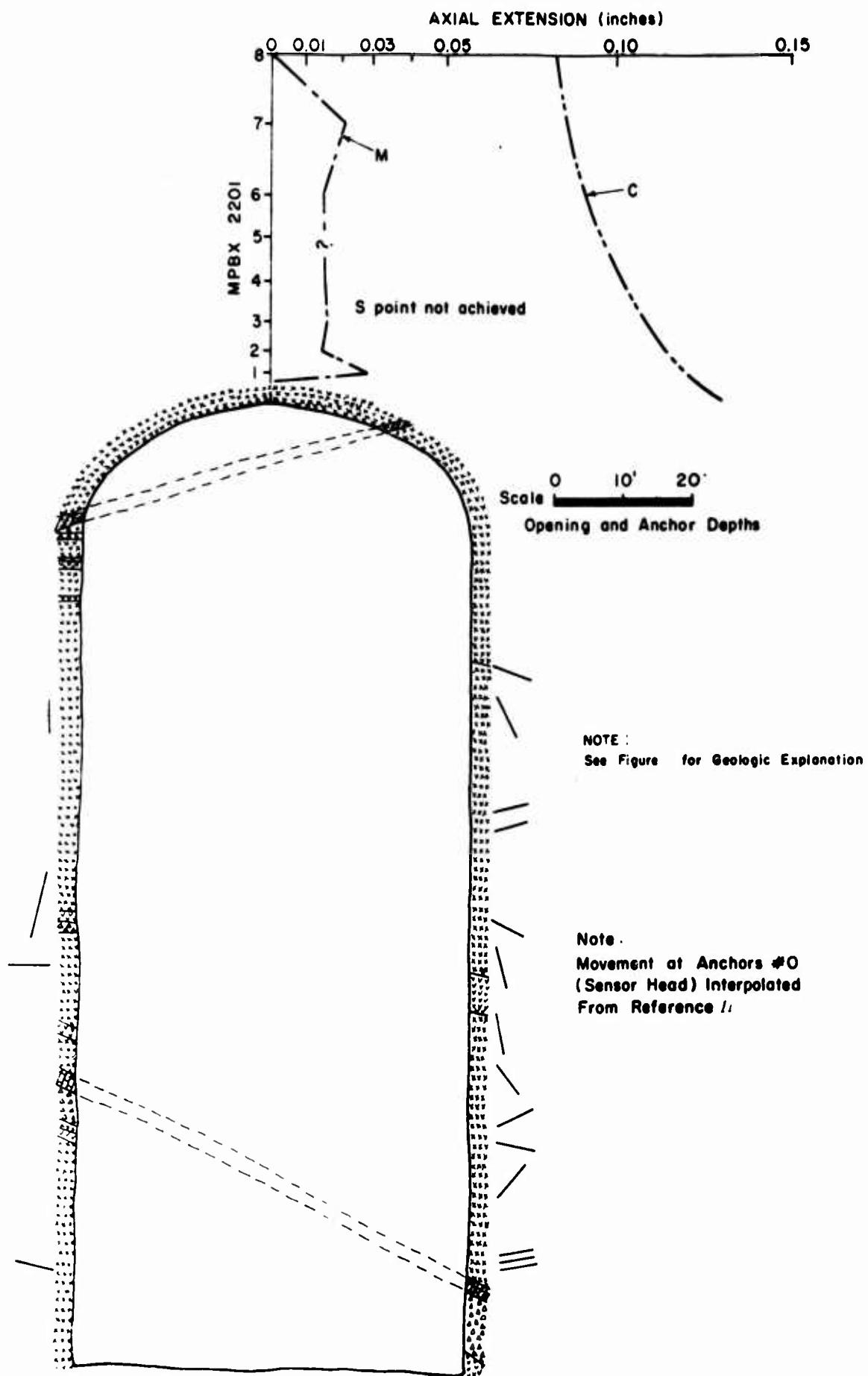


Figure 33. Morrow Point Powerplant - MPBX 2201 - Displacement

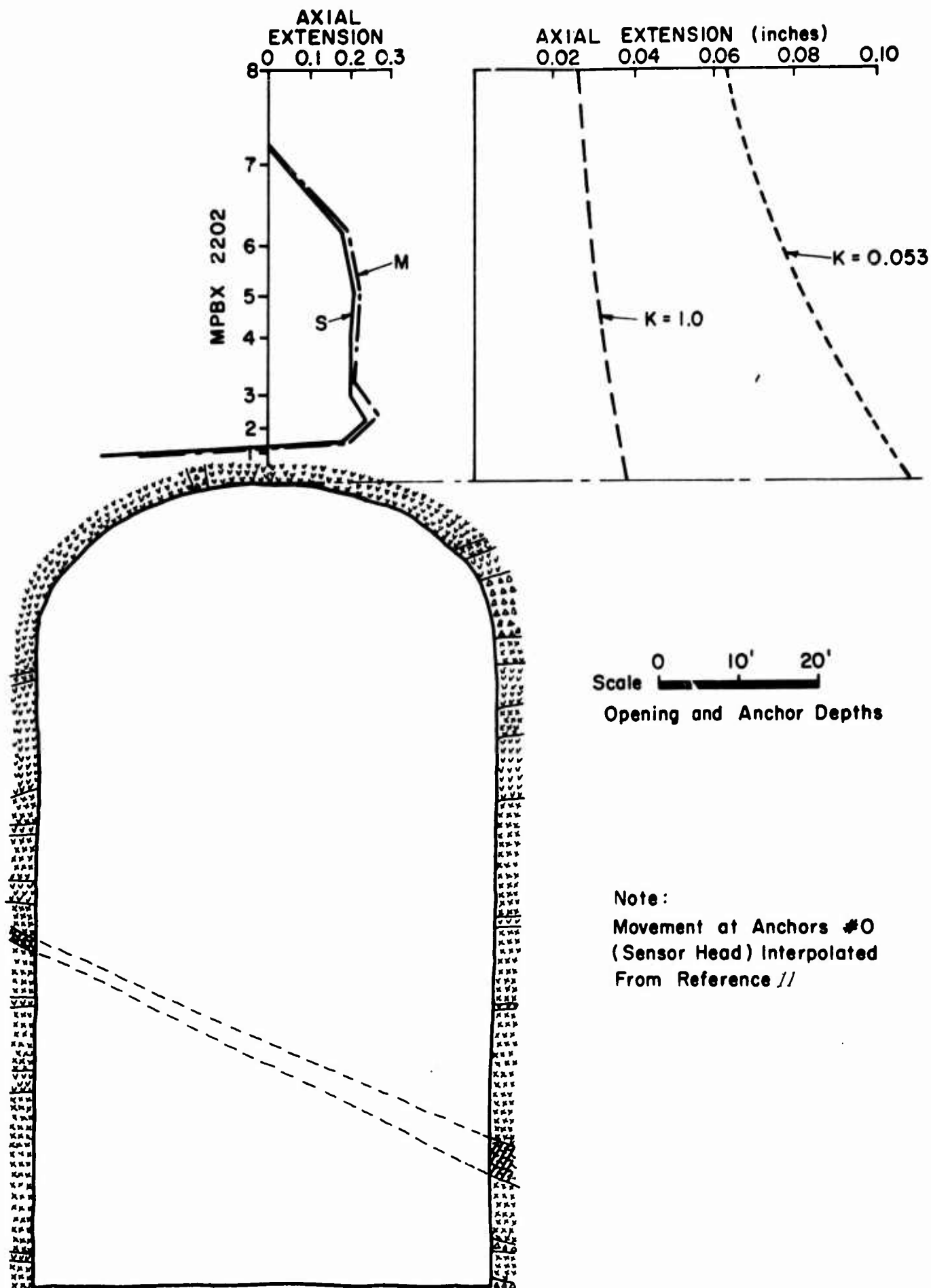


Figure 34. Morrow Point Powerplant - MPBX 2202 - Displacement



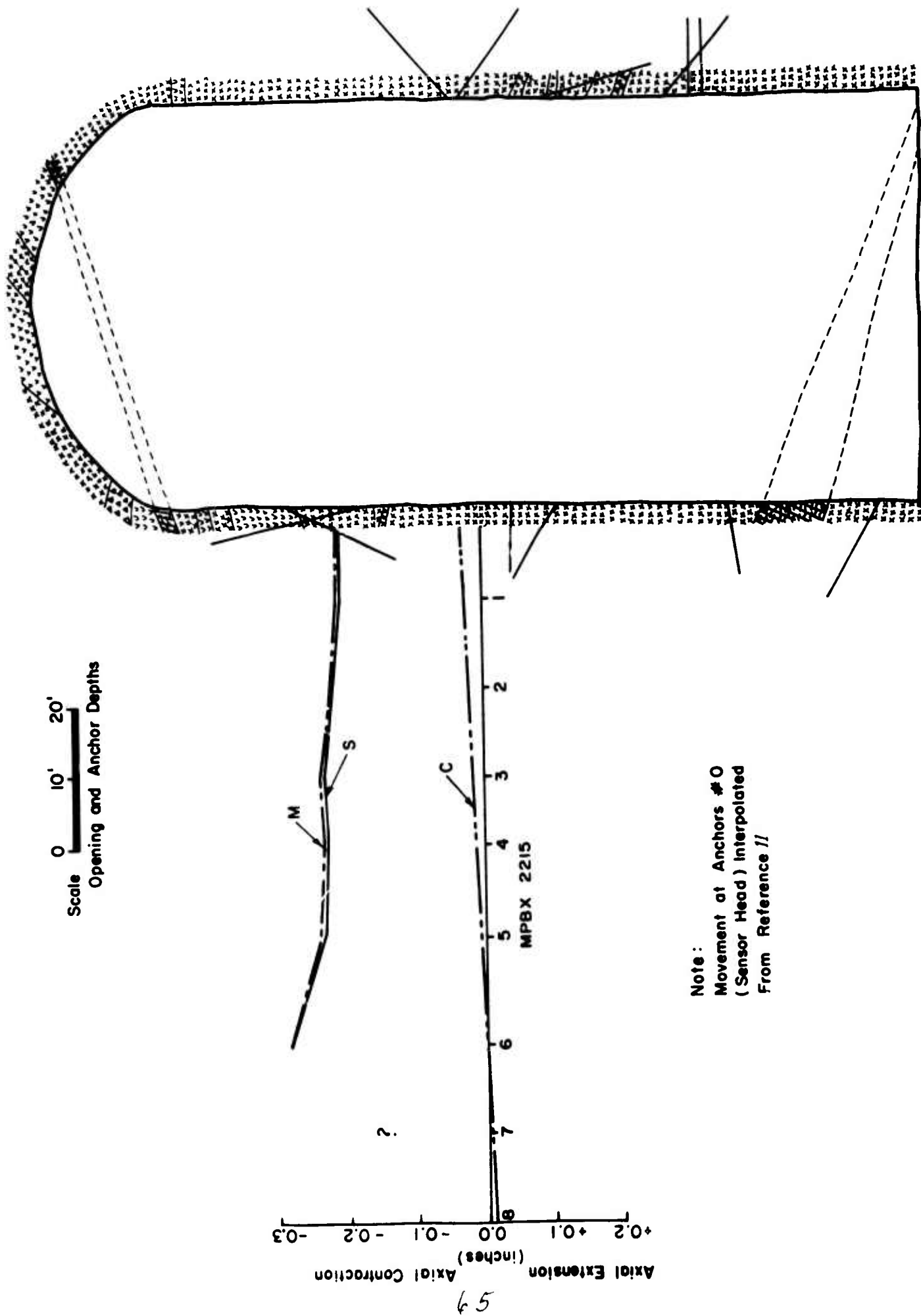


Figure 35. Morrow Point Dam, 1961

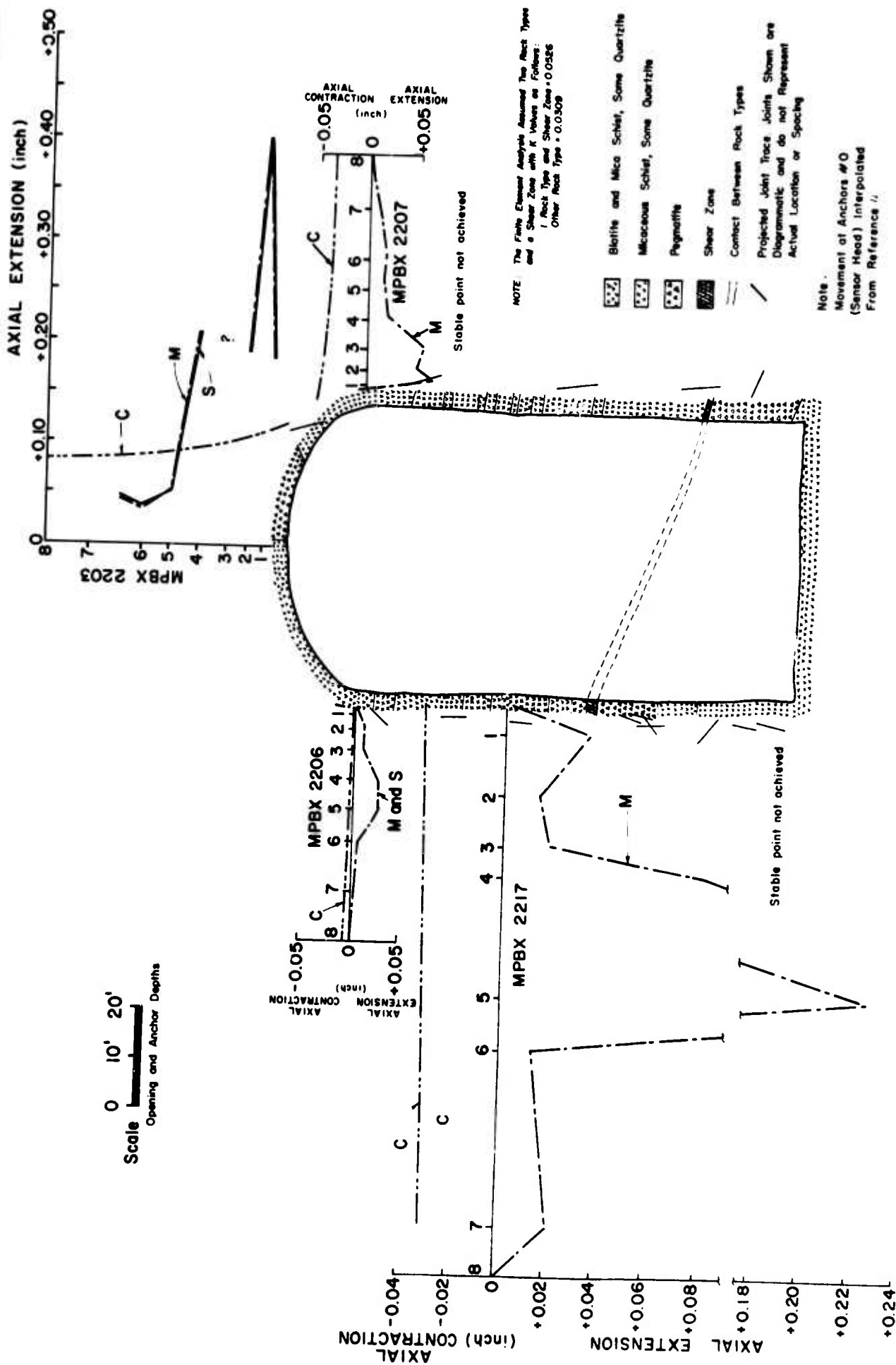
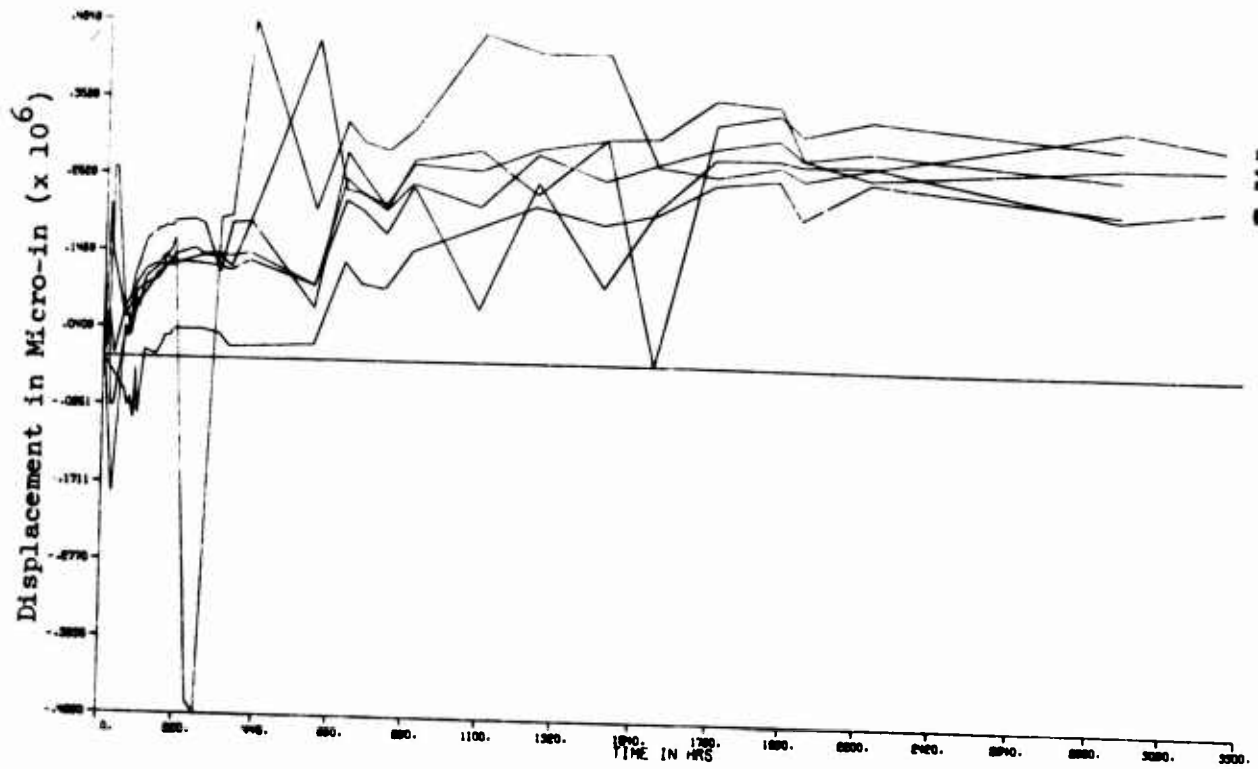


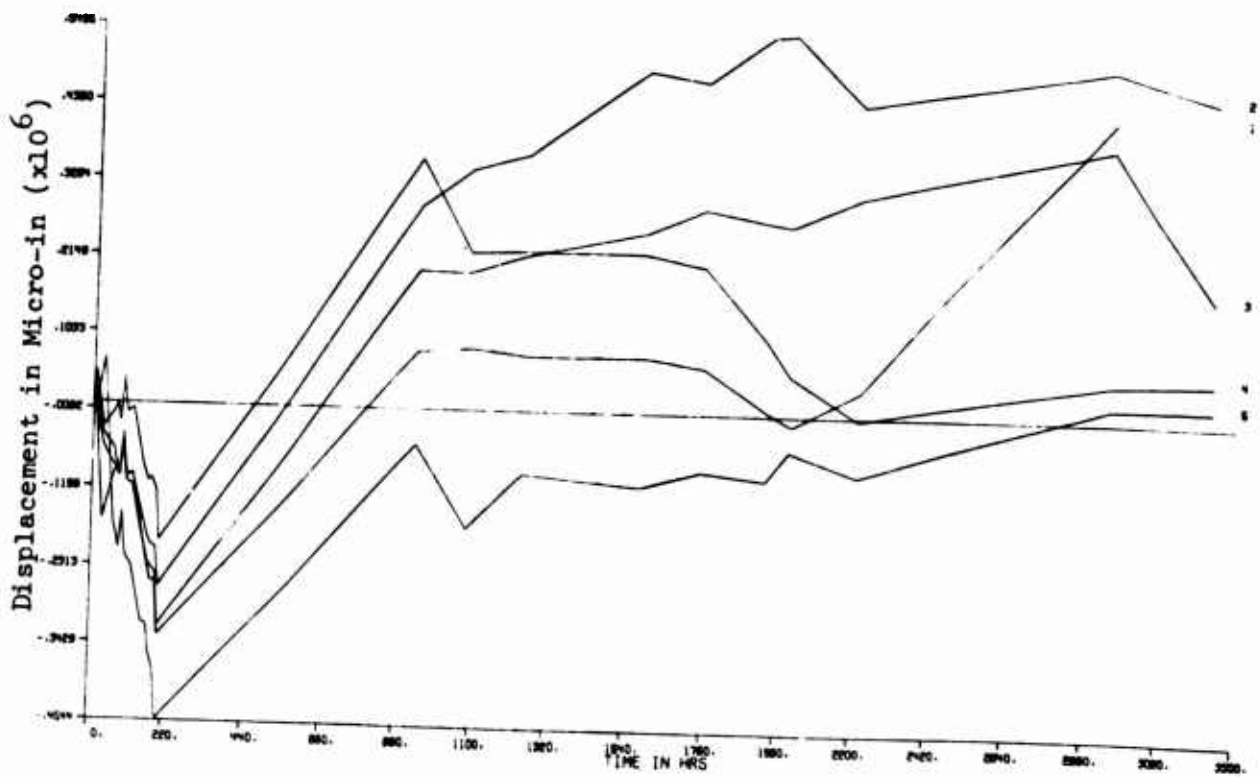
Figure 36. Morrow Point Powerplant - MPBXx 2203, 2206, 2207, 2217 Displacements

**BLANK PAGE**

SC-2001 114+53



SC-2002 14+53



## APPENDIX A

### TIME-DISPLACEMENT PLOTS

#### Explanation:

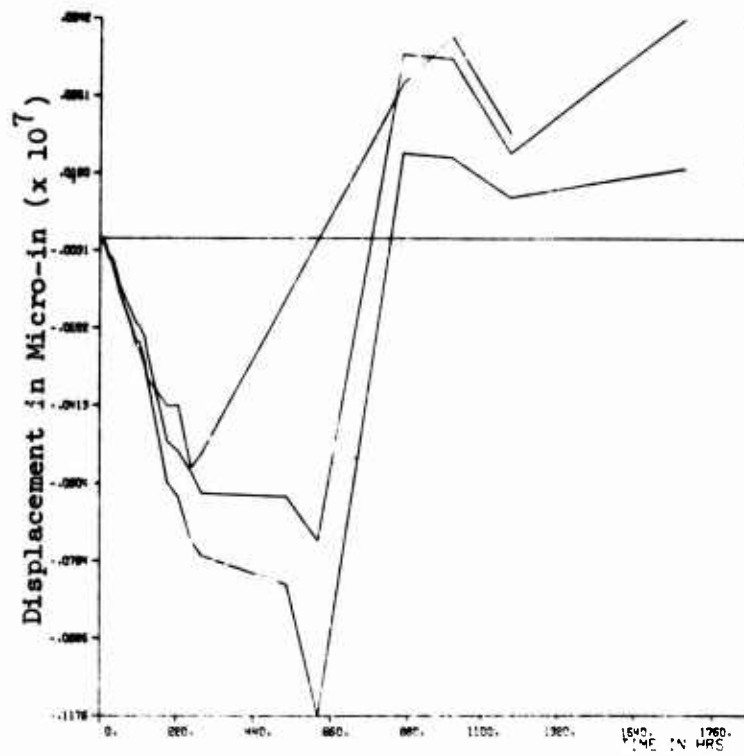
SC - Straight Creek Pilot Bore  
GR - Green River Highway Tunnels  
MP - Morrow Point Underground Powerhouse Chamber  
N - Navajo Tunnel  
P - Pacheco Tunnel

#### Example:

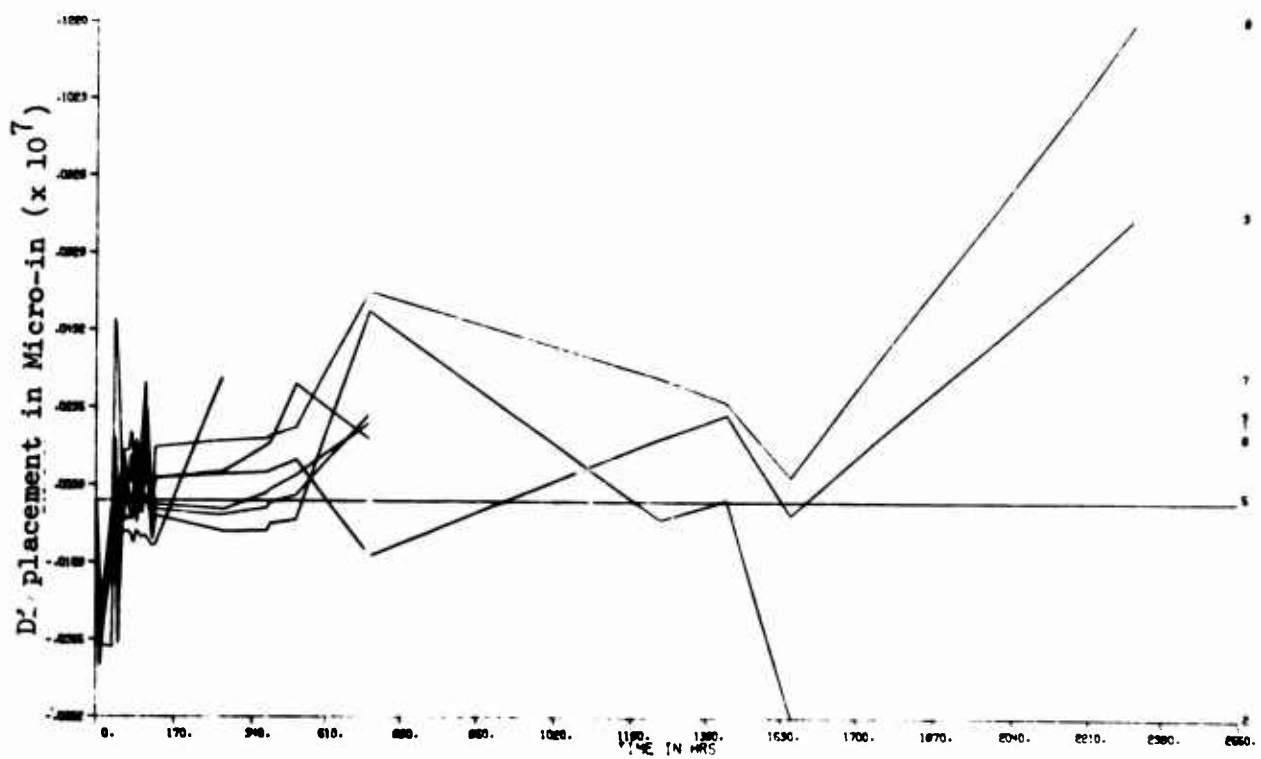
SC - 2001 114 + 53  
└─ Name of tunnel  
└─ Number of the MPBX  
└─ MPBX Location in the tunnel

The small numbers on the right side of each figure refer to the anchor represented by that particular plotted line. The reference anchor that is assumed not to move is the horizontal line that separates the (+) and the (-) displacements.

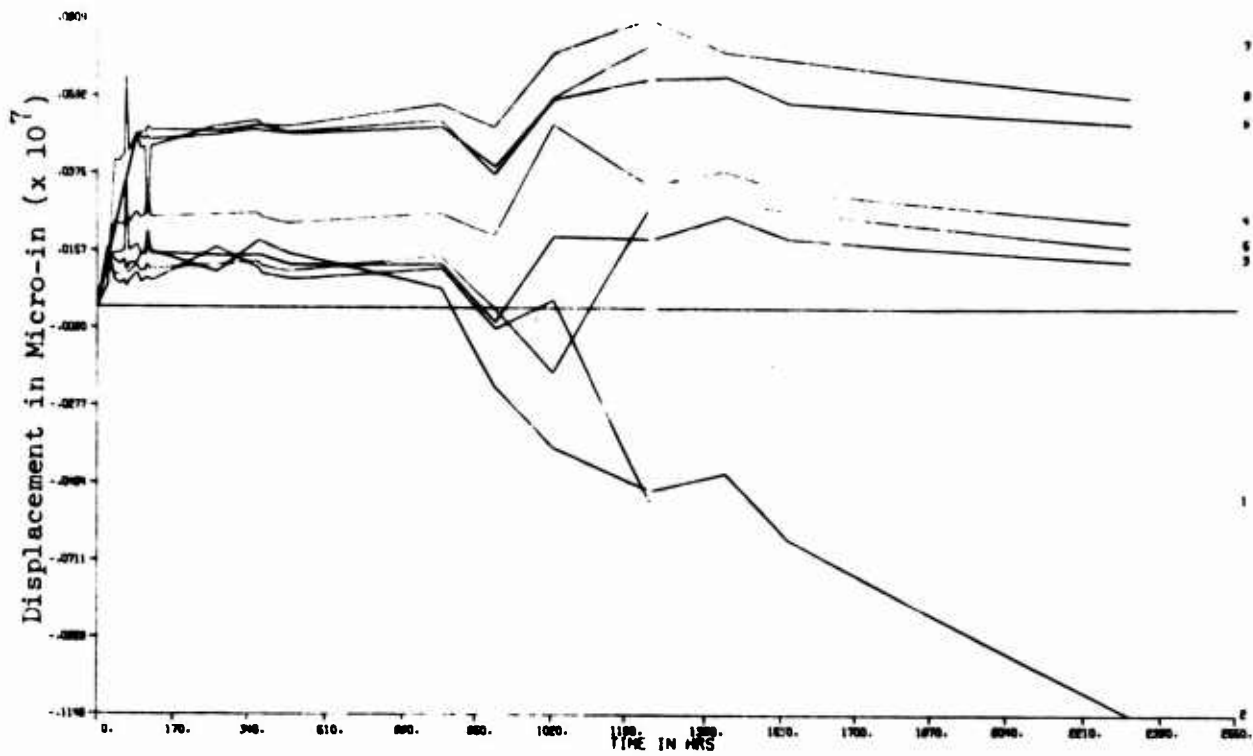
SC-2003 114+53



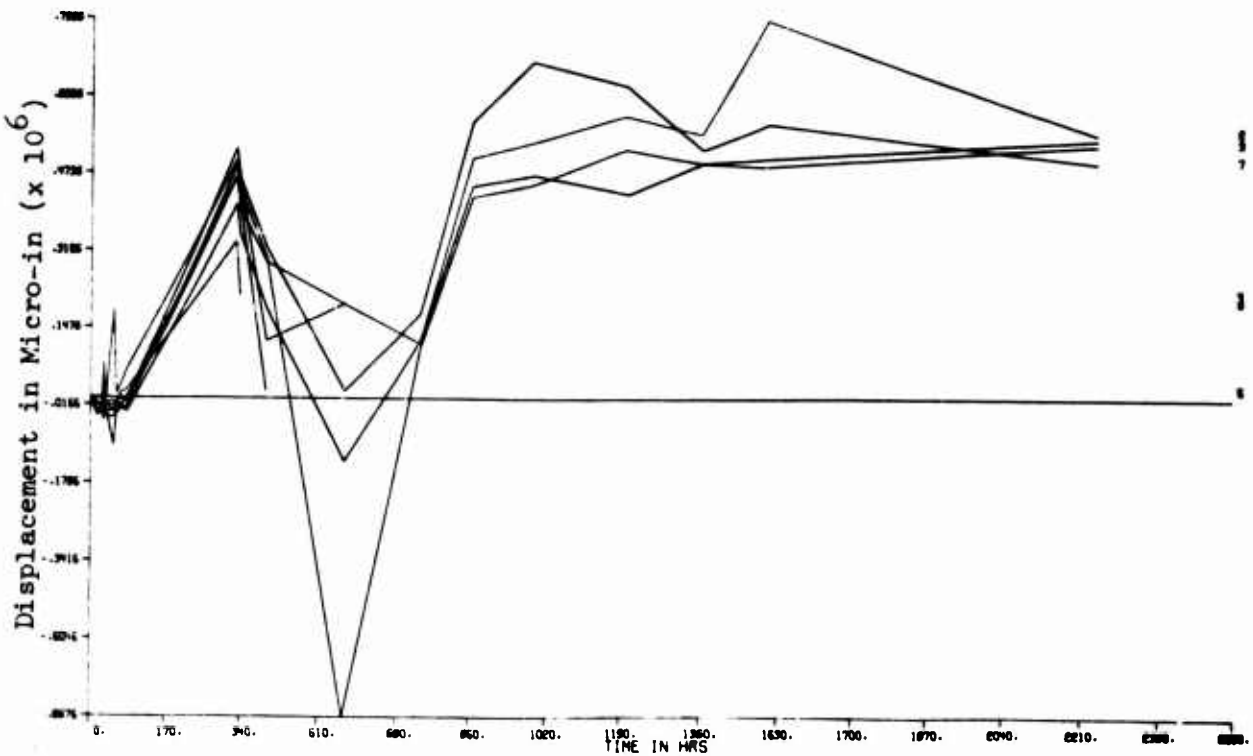
SC-2004 104+83



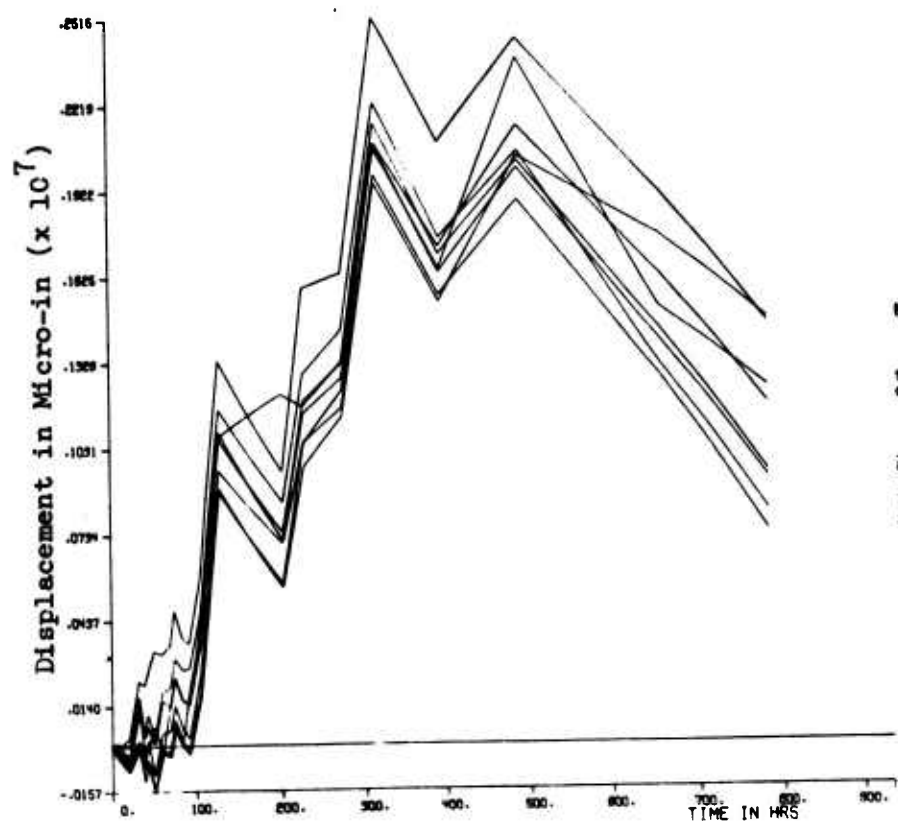
SC-2005 104+83



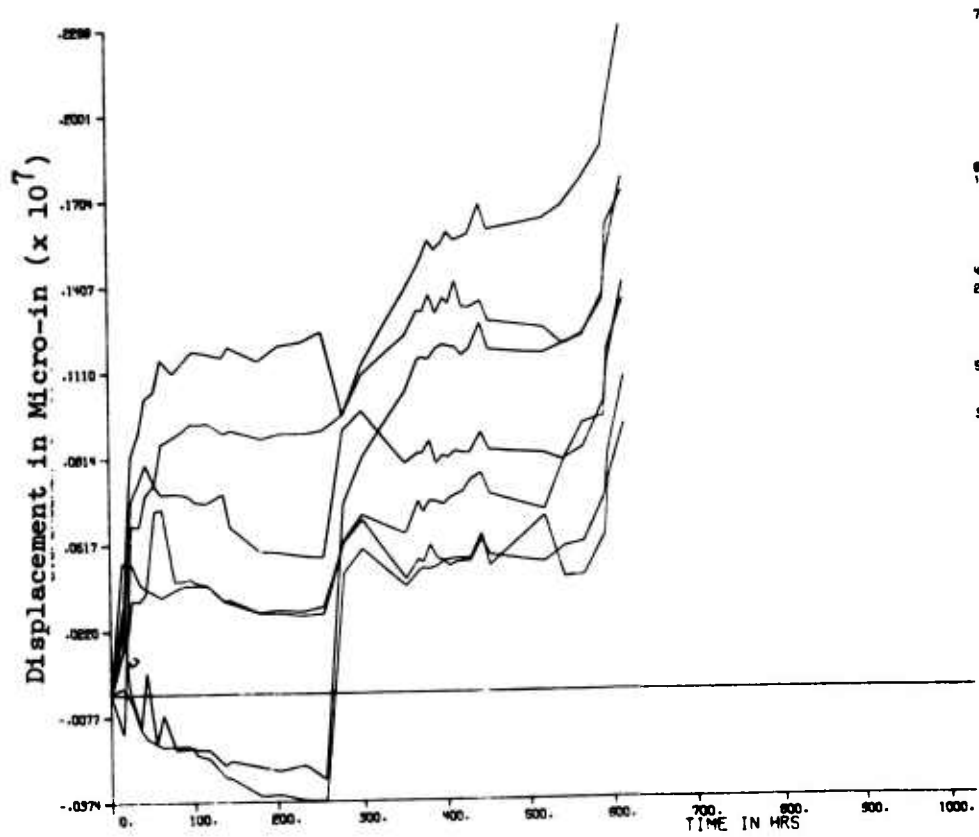
SC-2006 104+83



SC-2008 81+41

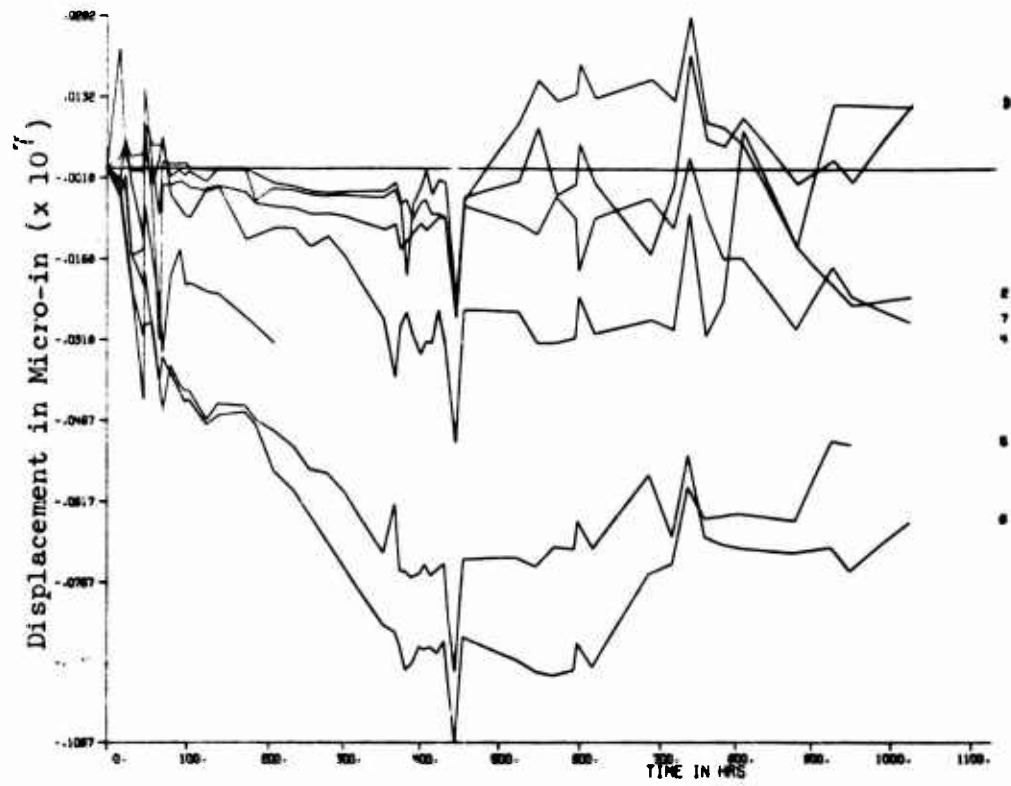


SC-2010 83+93

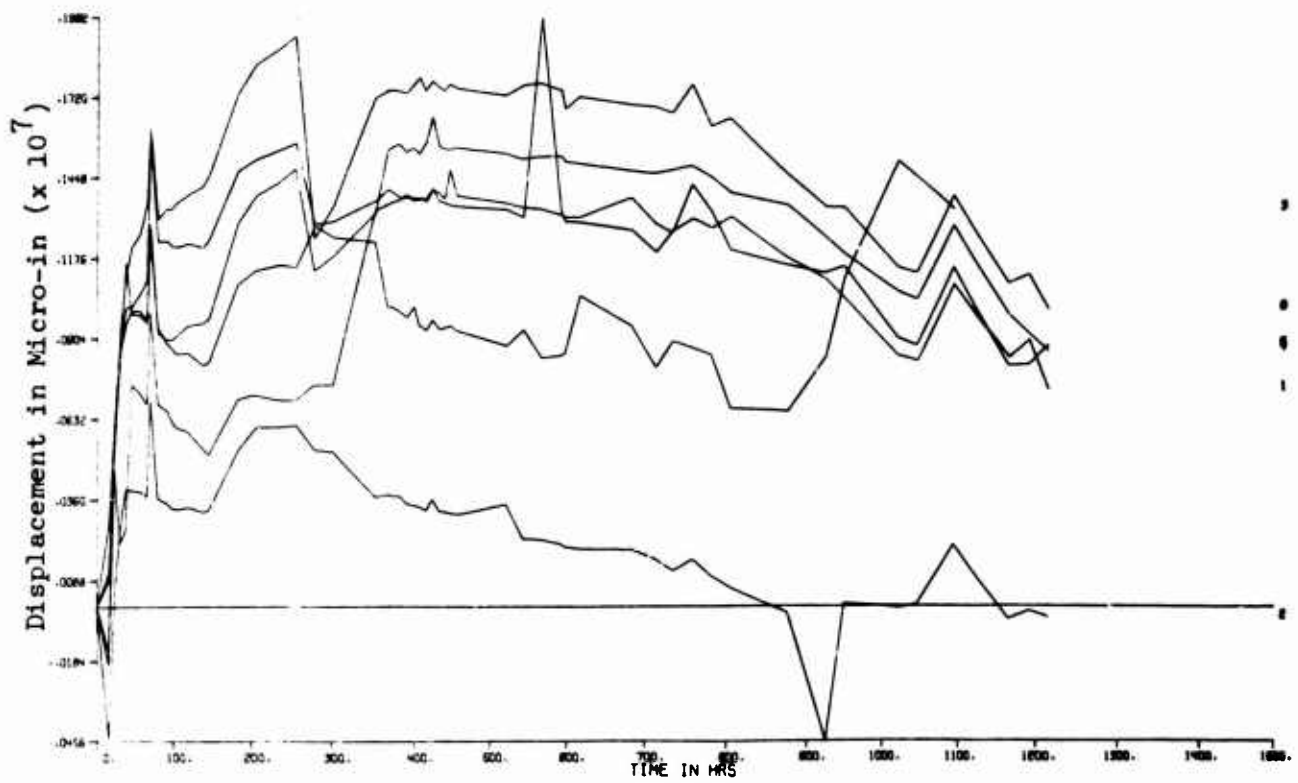




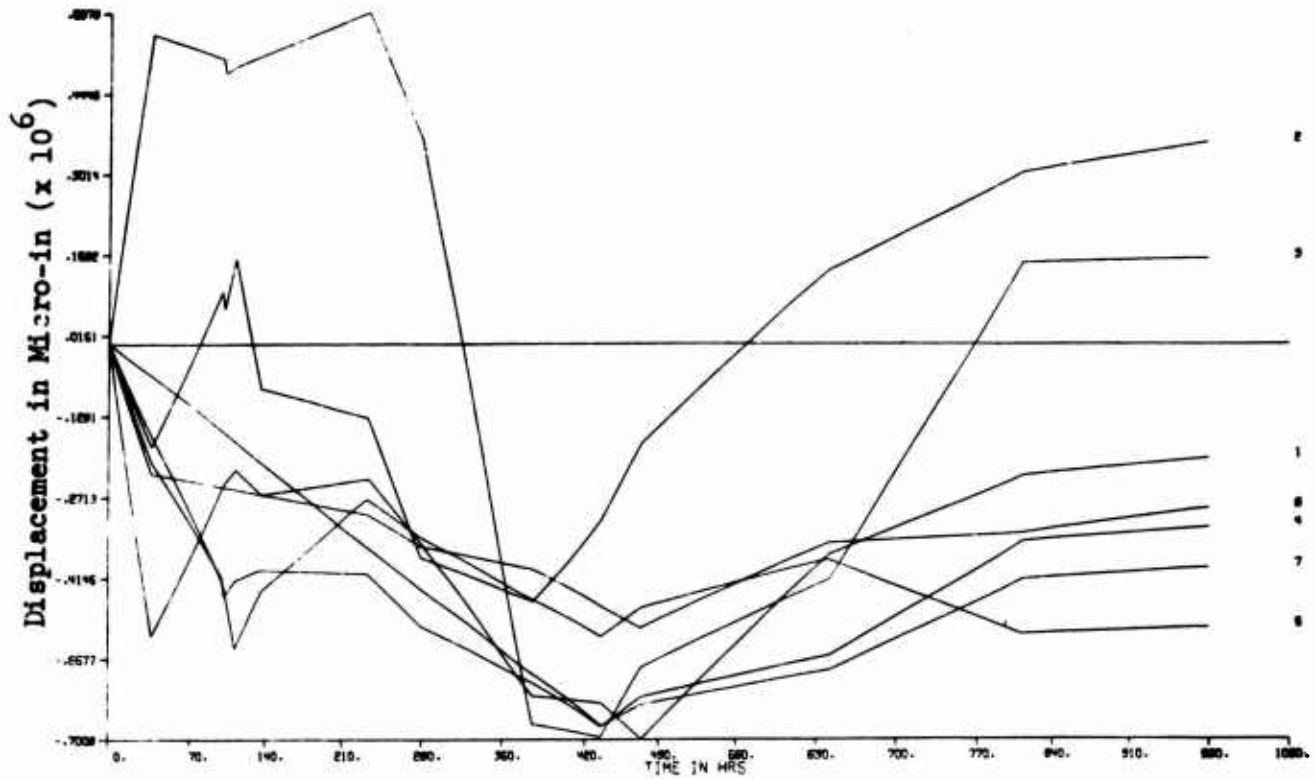
SC-2011 83+93



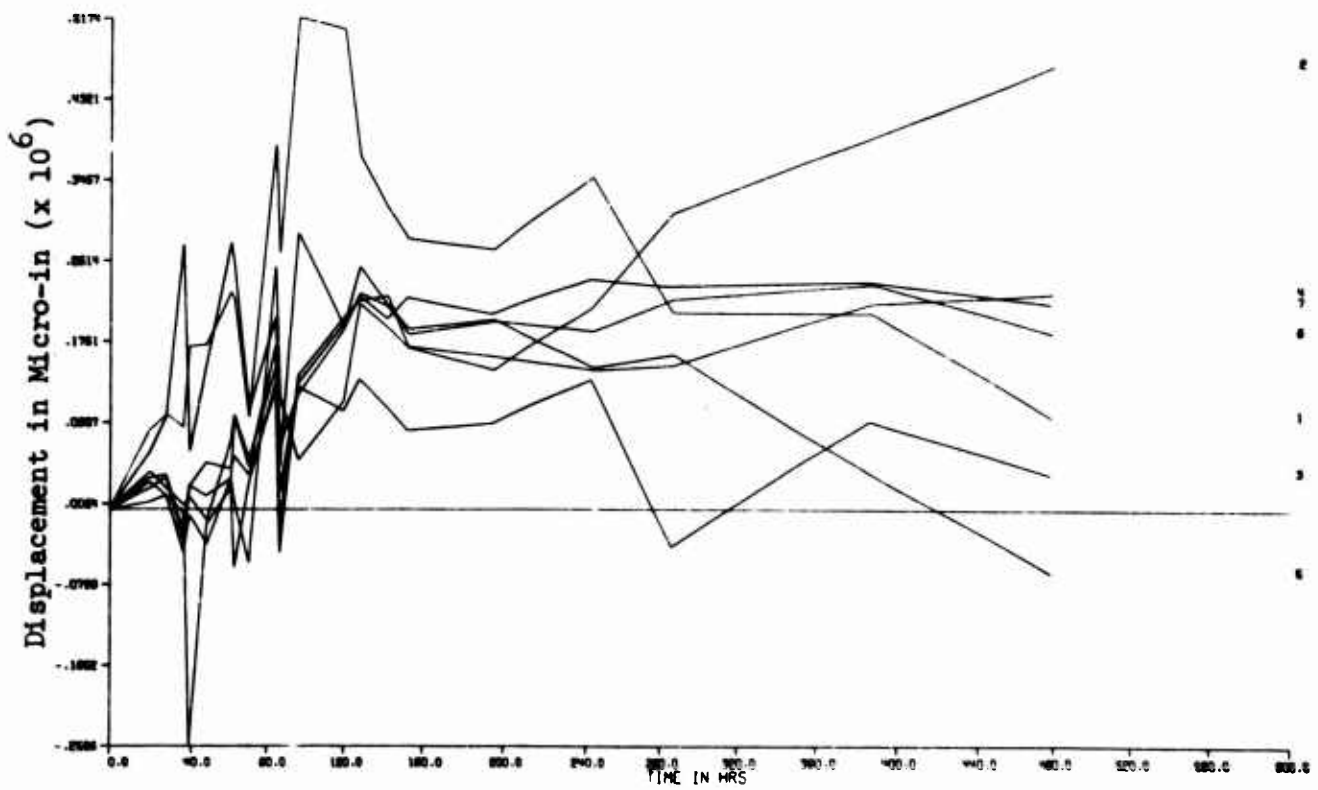
SC-2012 83+93



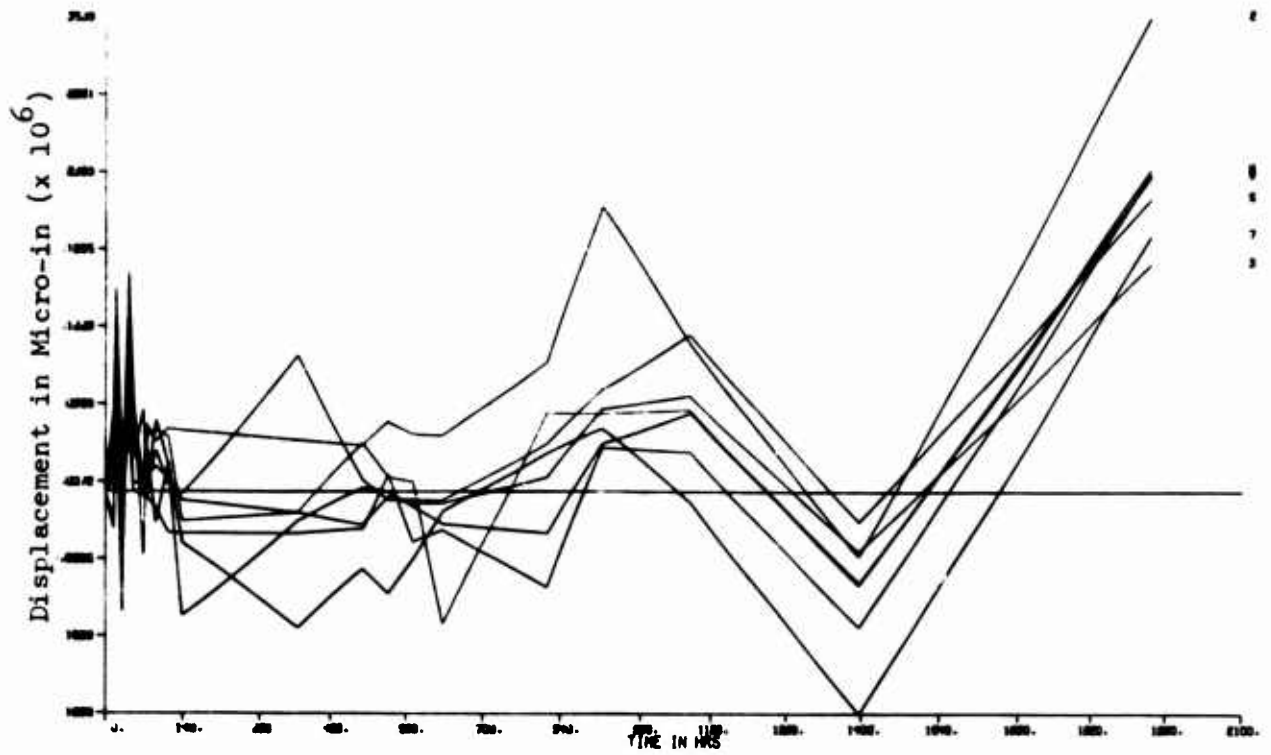
SC-2013 73+17



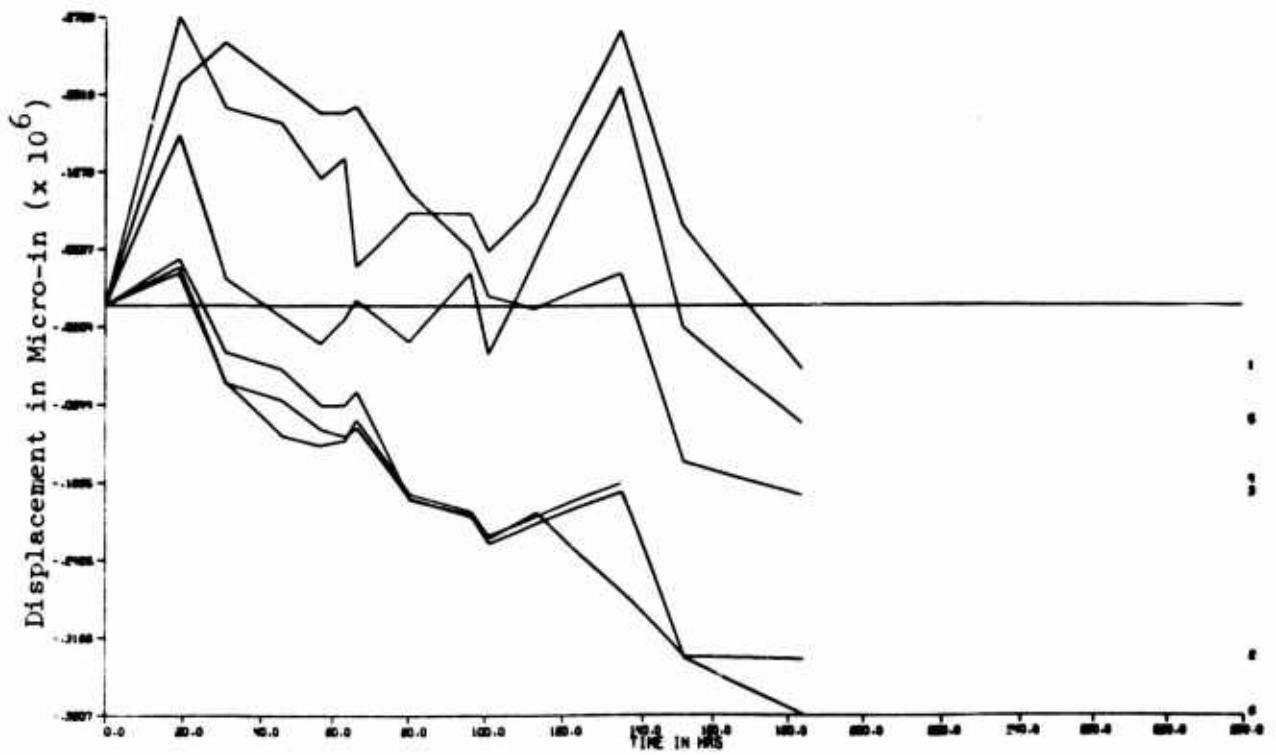
SC-2014 73+57



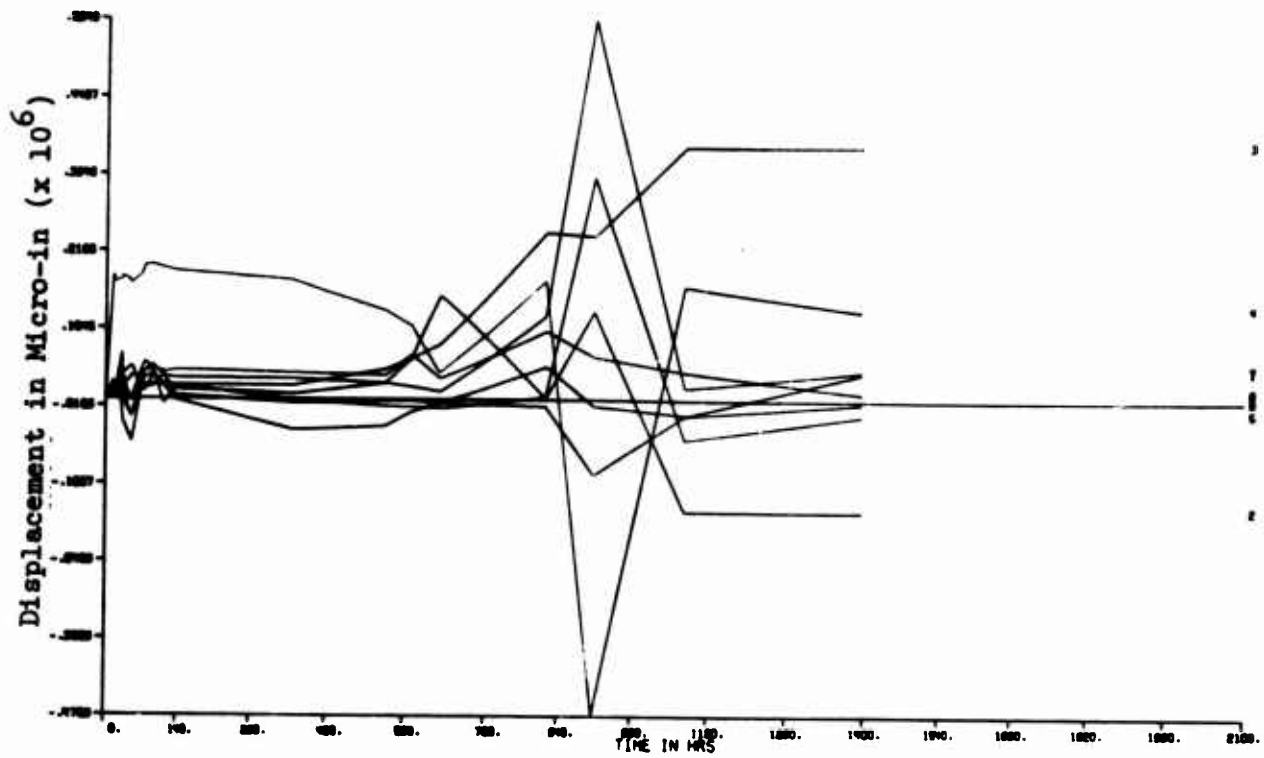
SC-2015 59+35



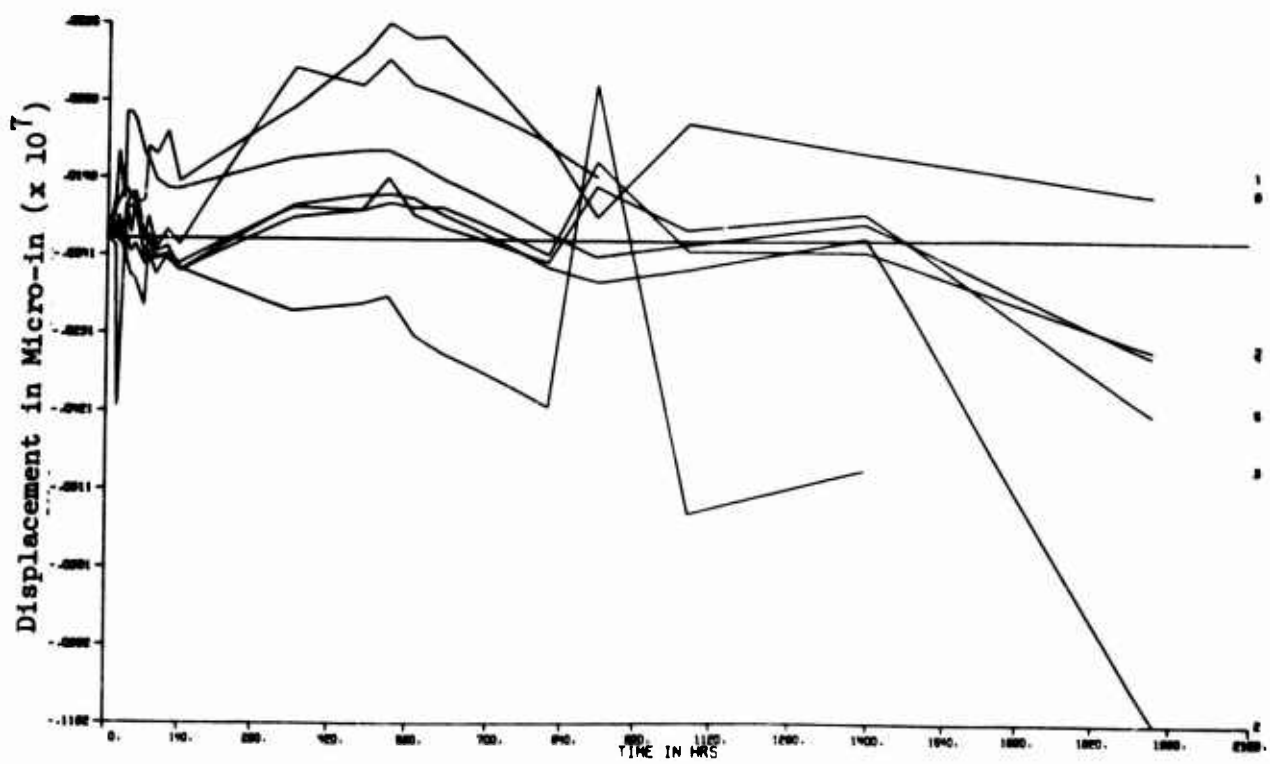
SC-2018 69+81



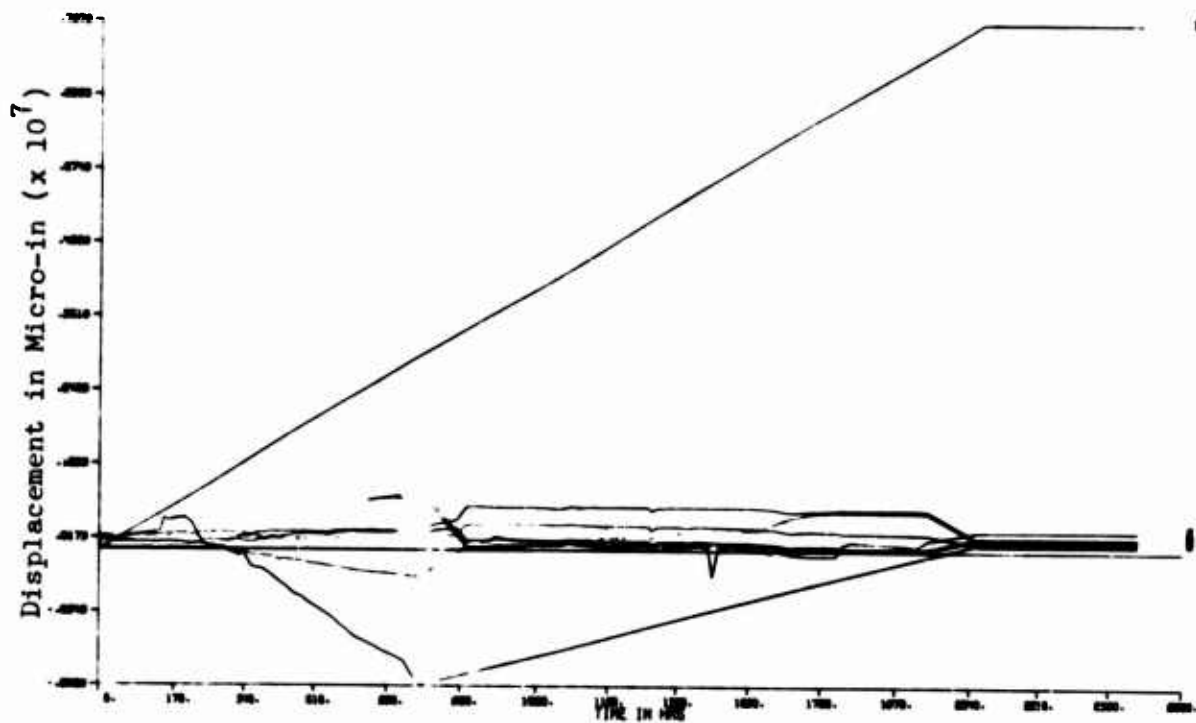
SC-2020 59+35



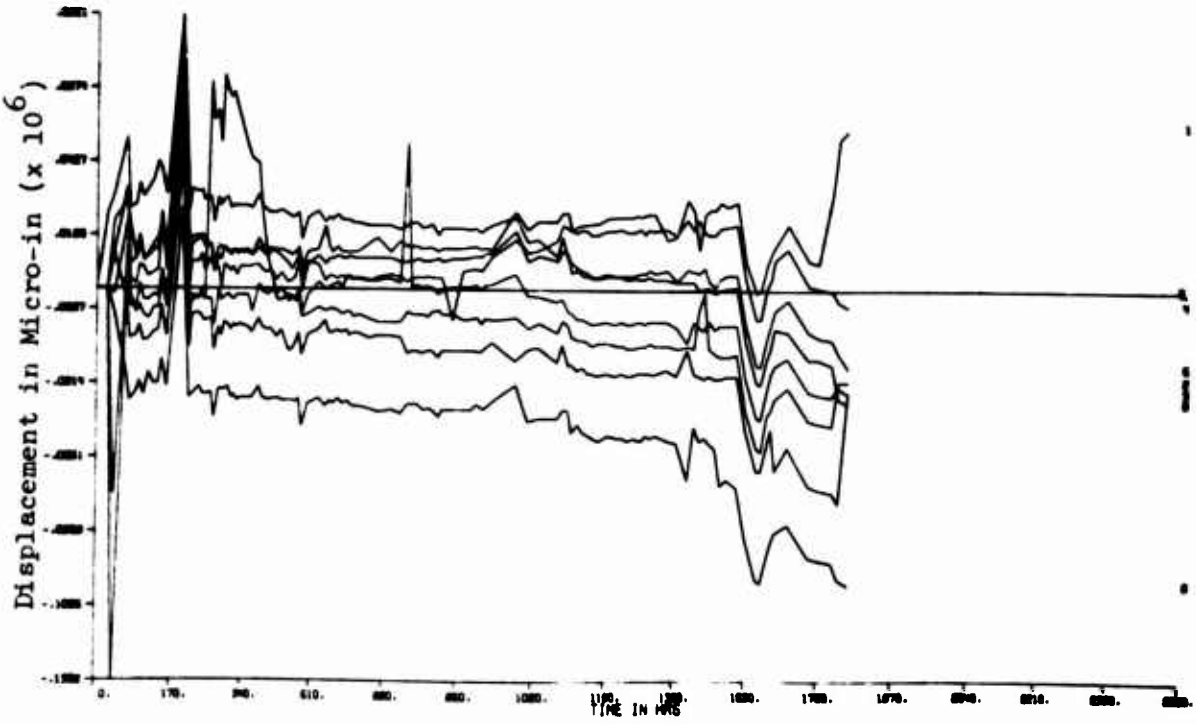
SC-2021 59+35



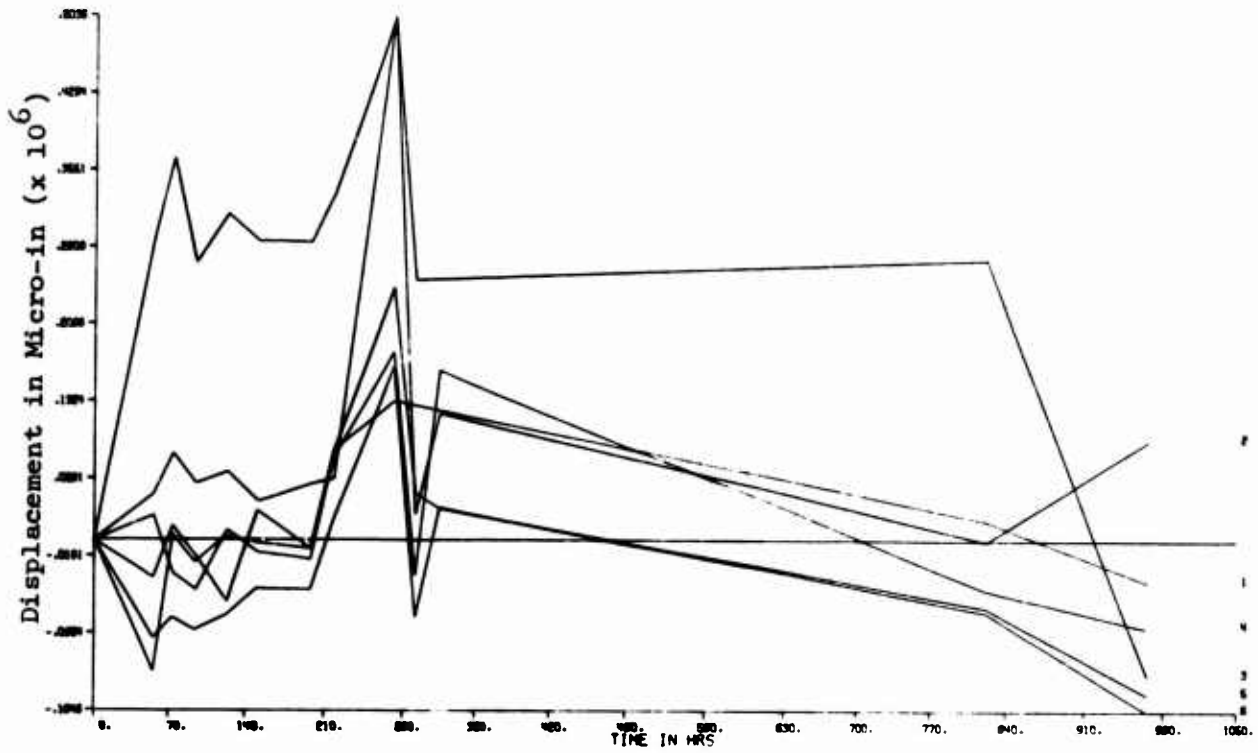
GR-2023 105+54



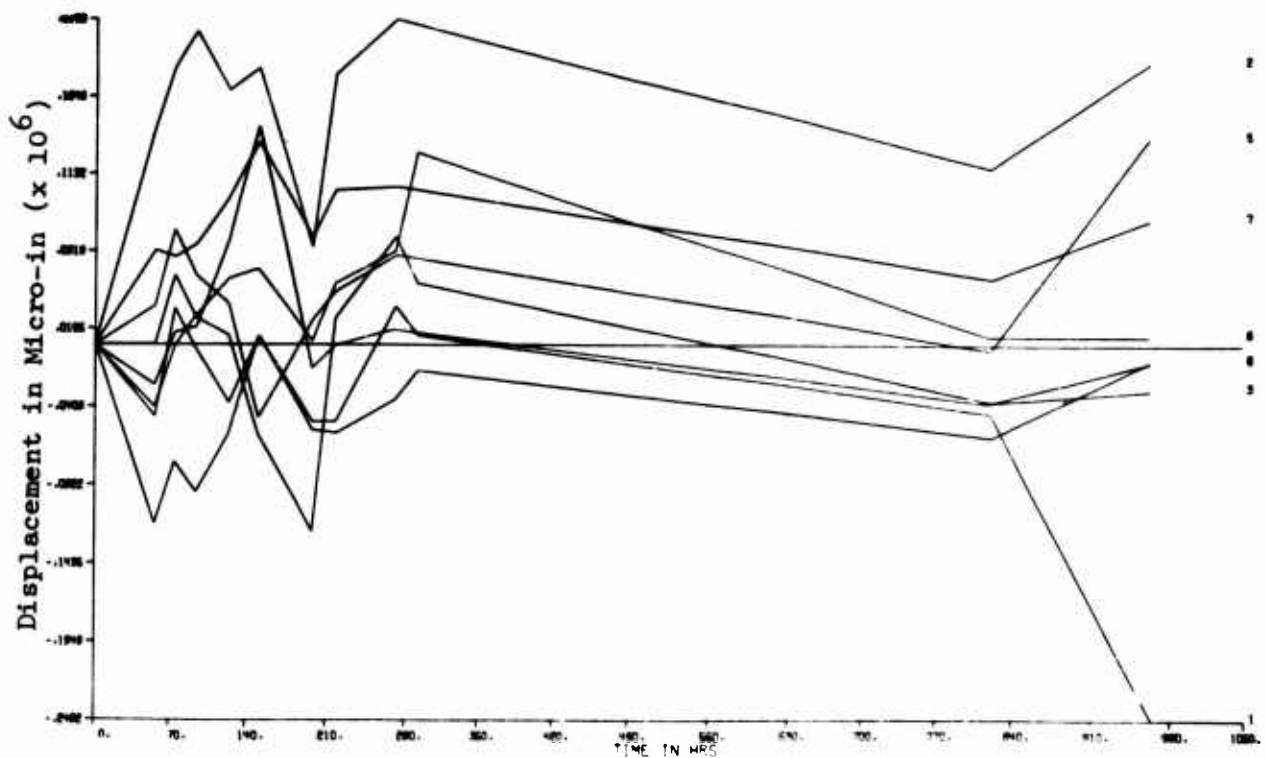
GR-2024 105 + 54



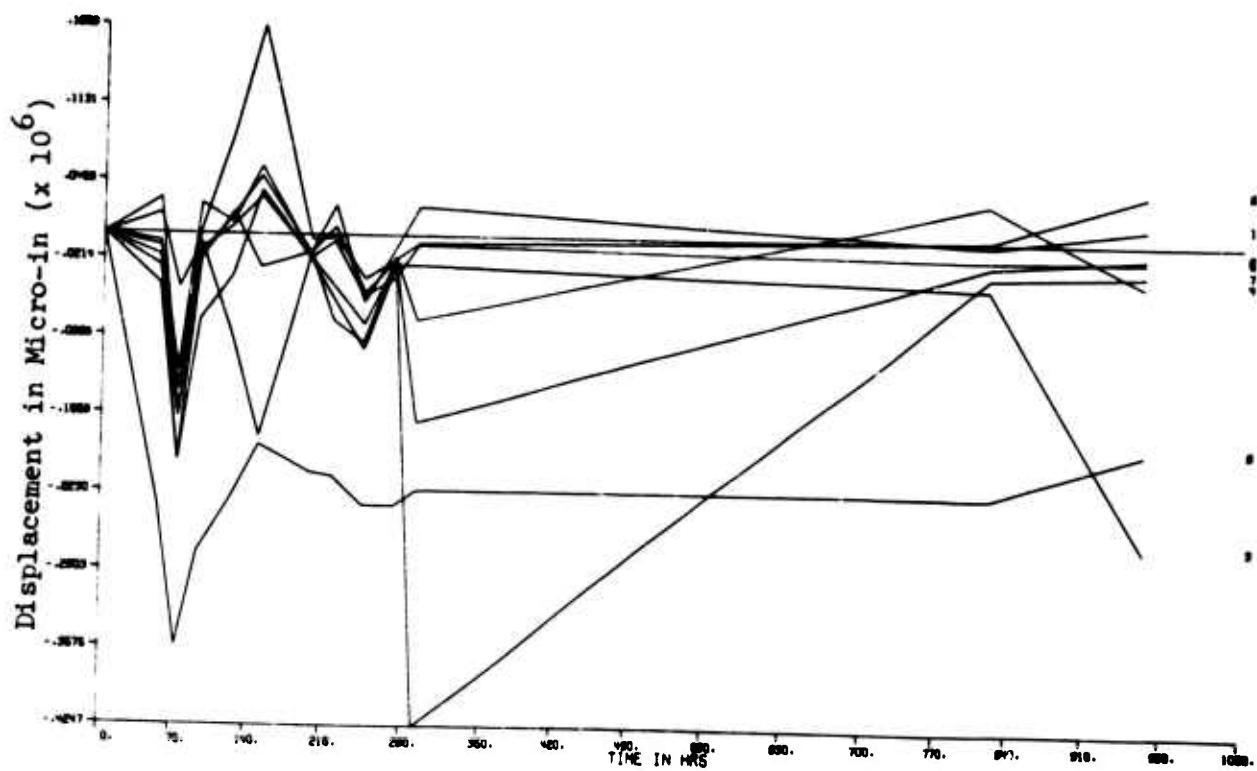
SC-2025 49+27



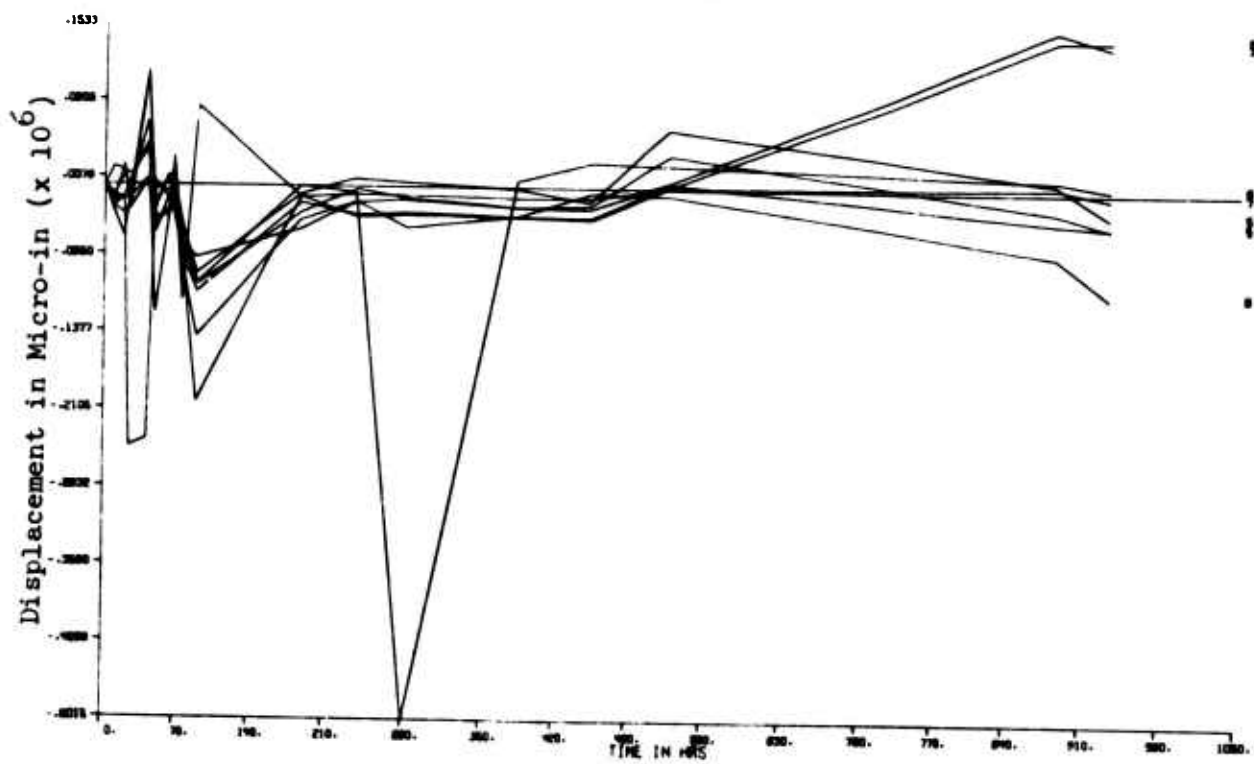
SC-2026 49+27



SC-2027 49+27

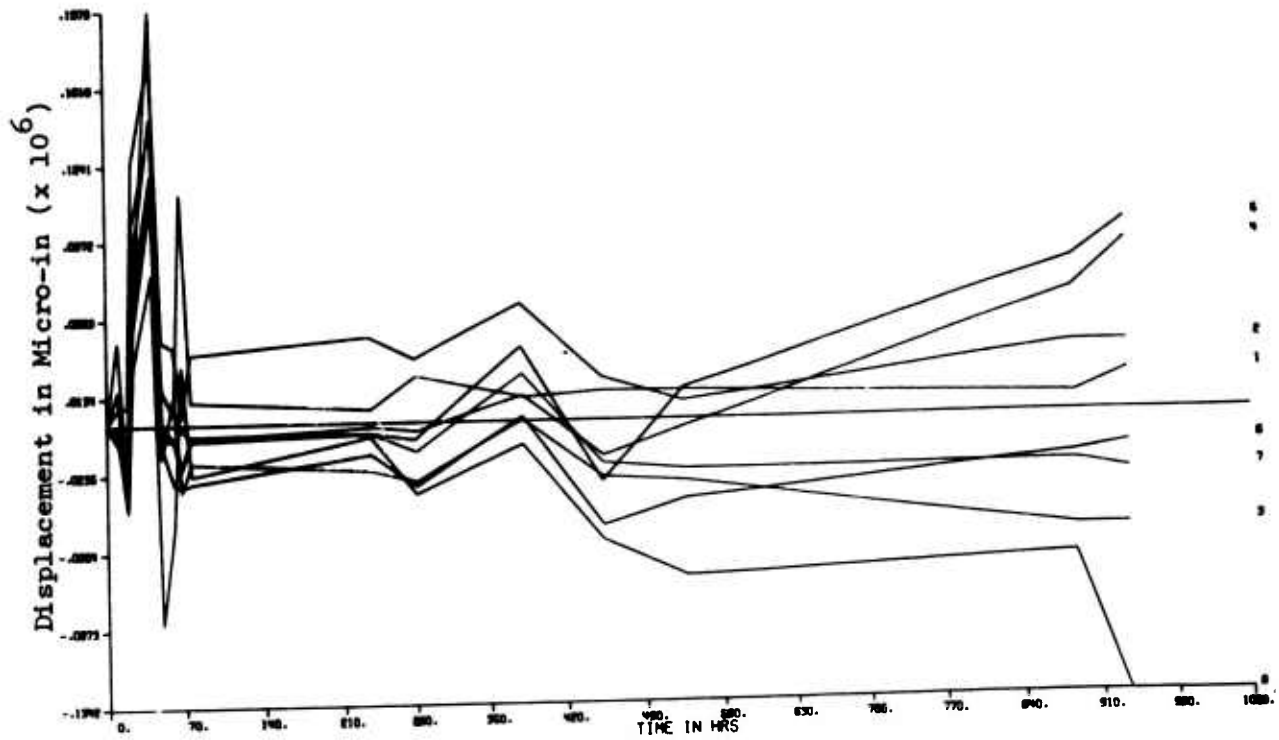


SC-2028 43+85

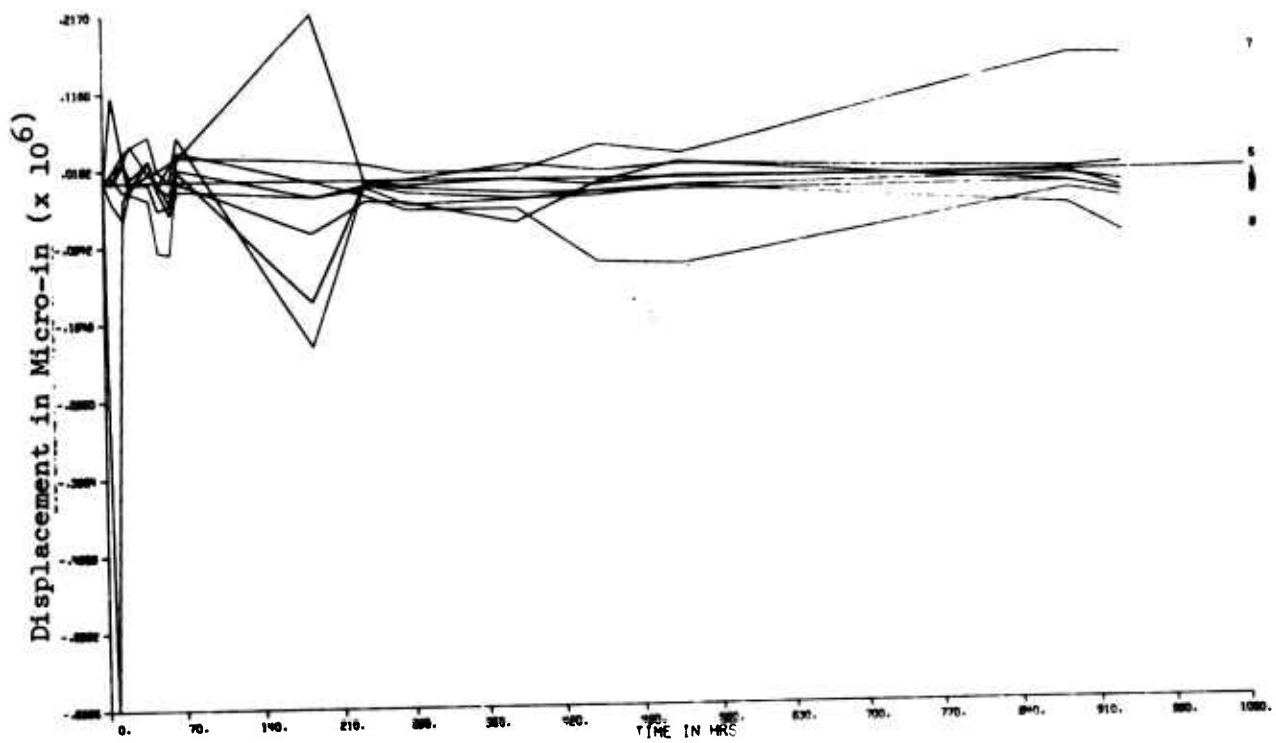


All

SC-2029 43+85

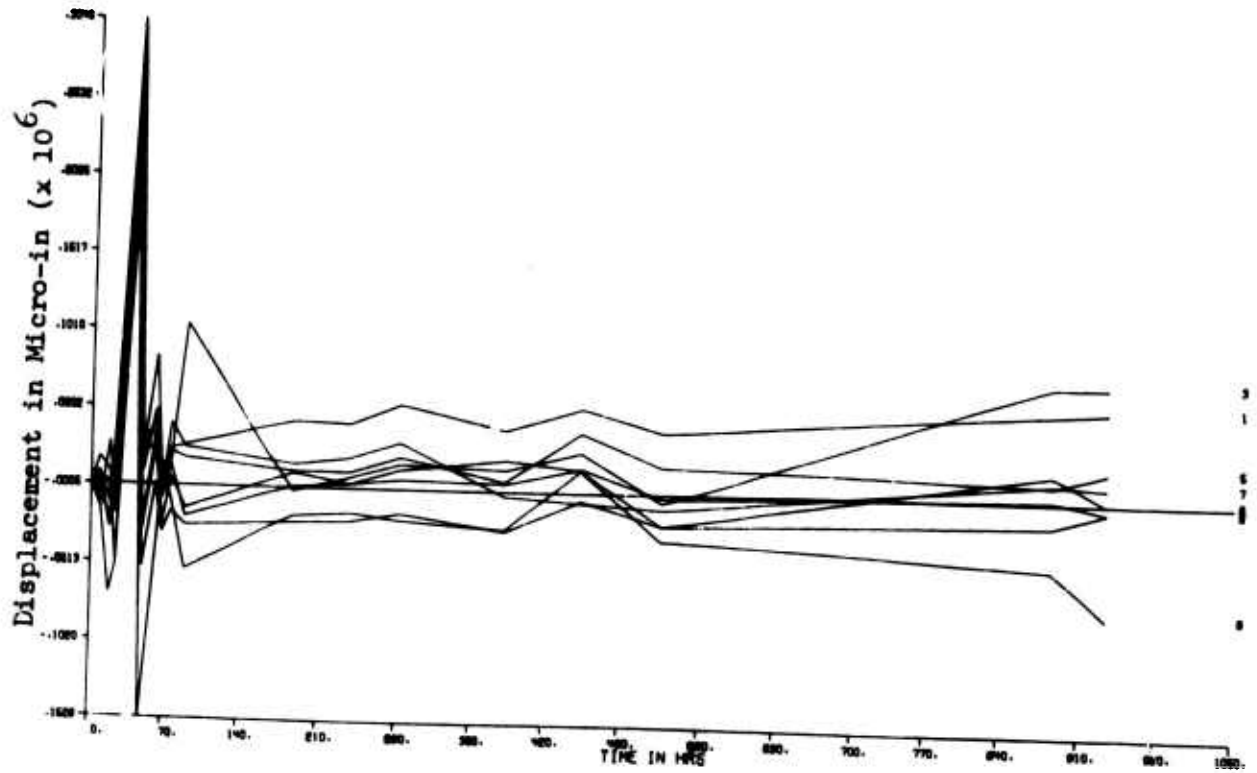


SC-2030 43+85

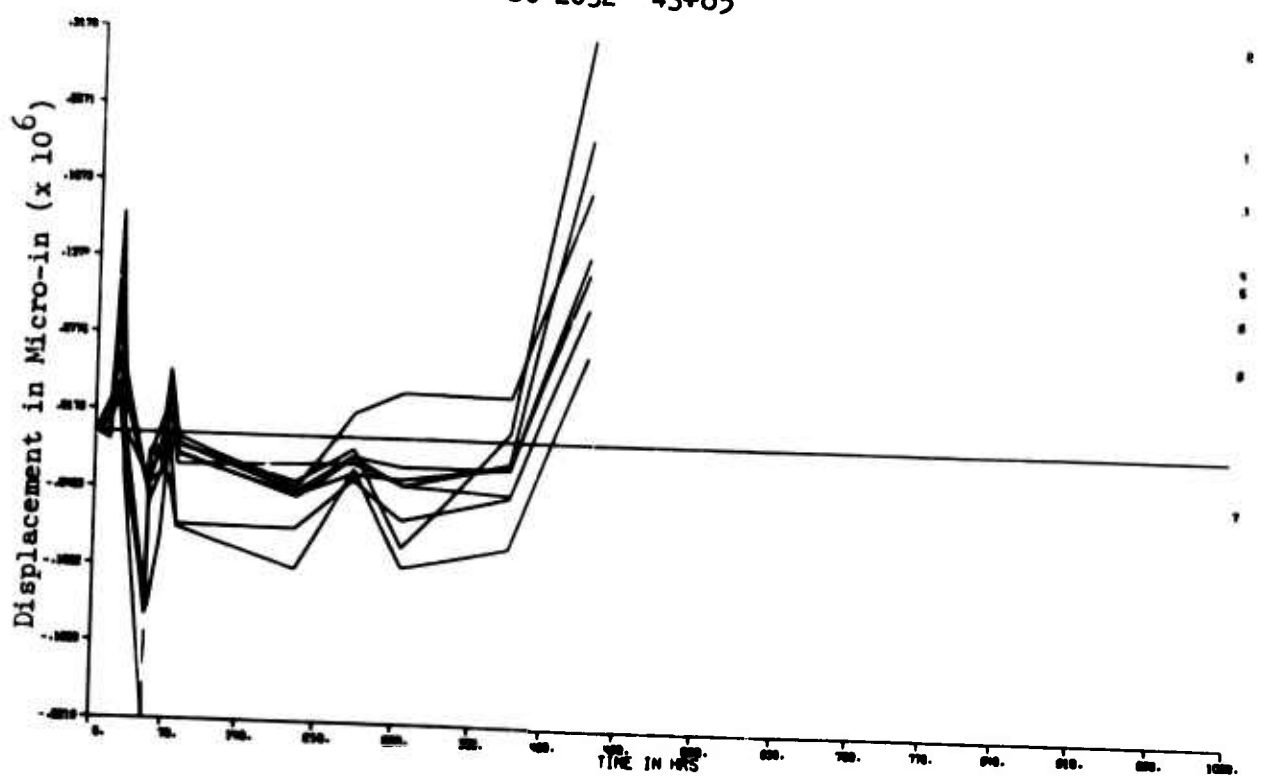




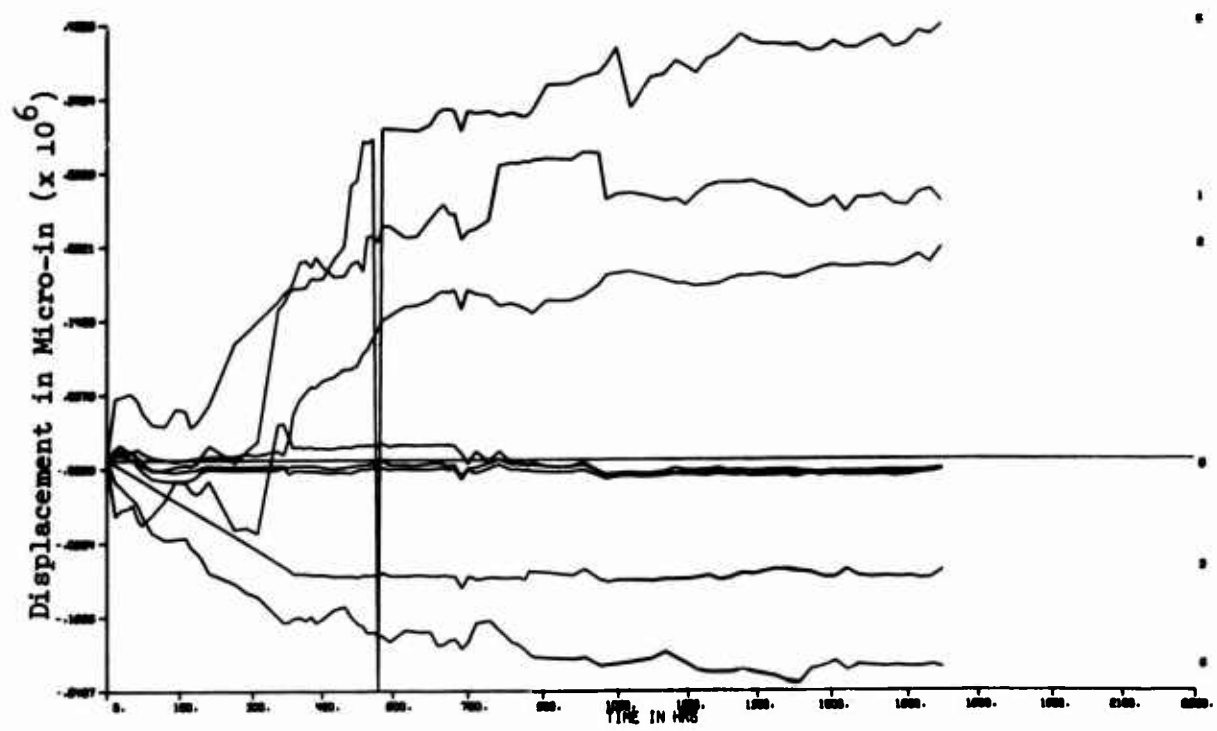
SC-2031 43+85



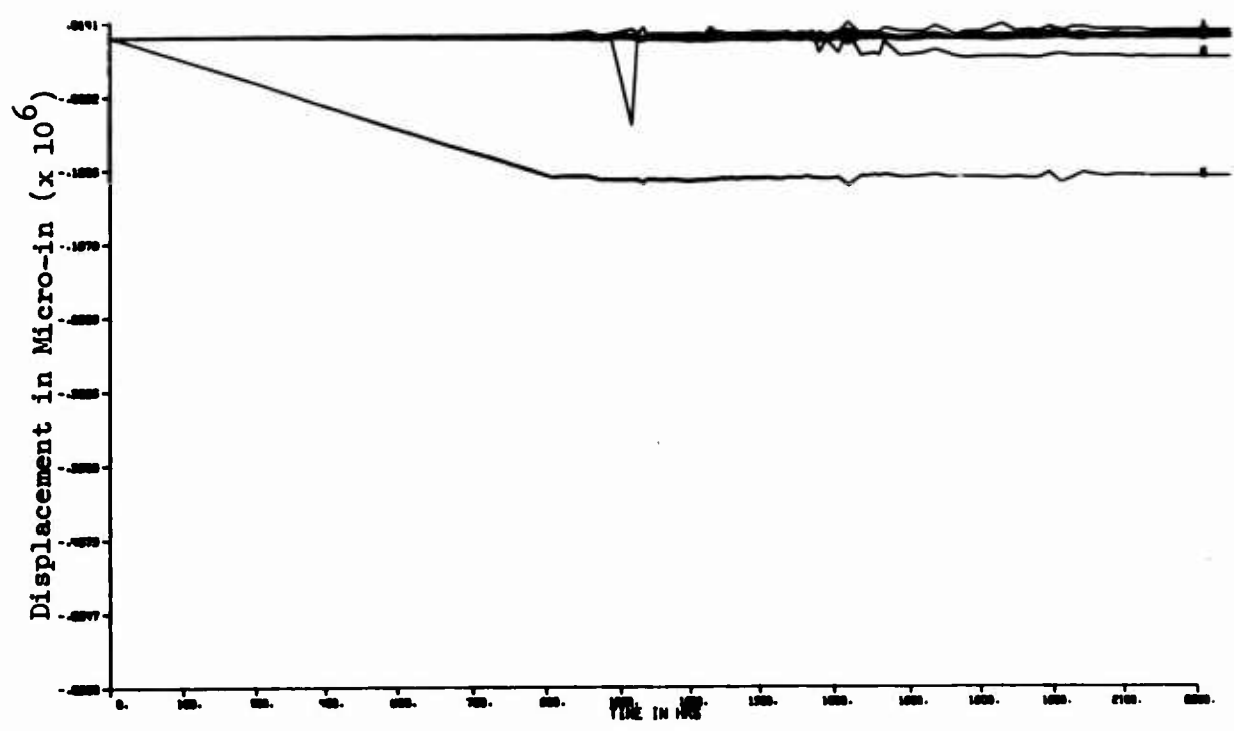
SC-2032 43+85



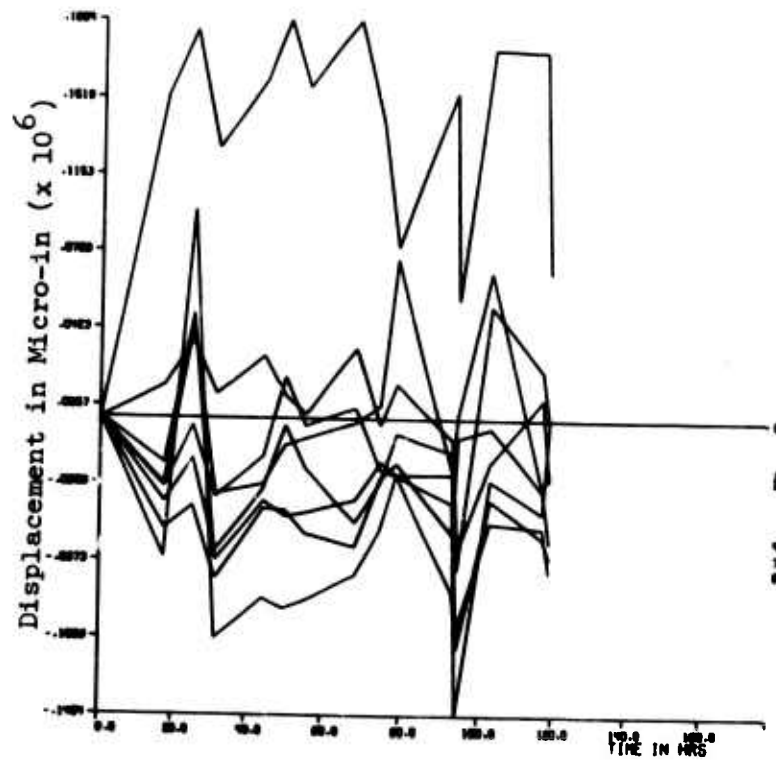
GR-2033 105+05



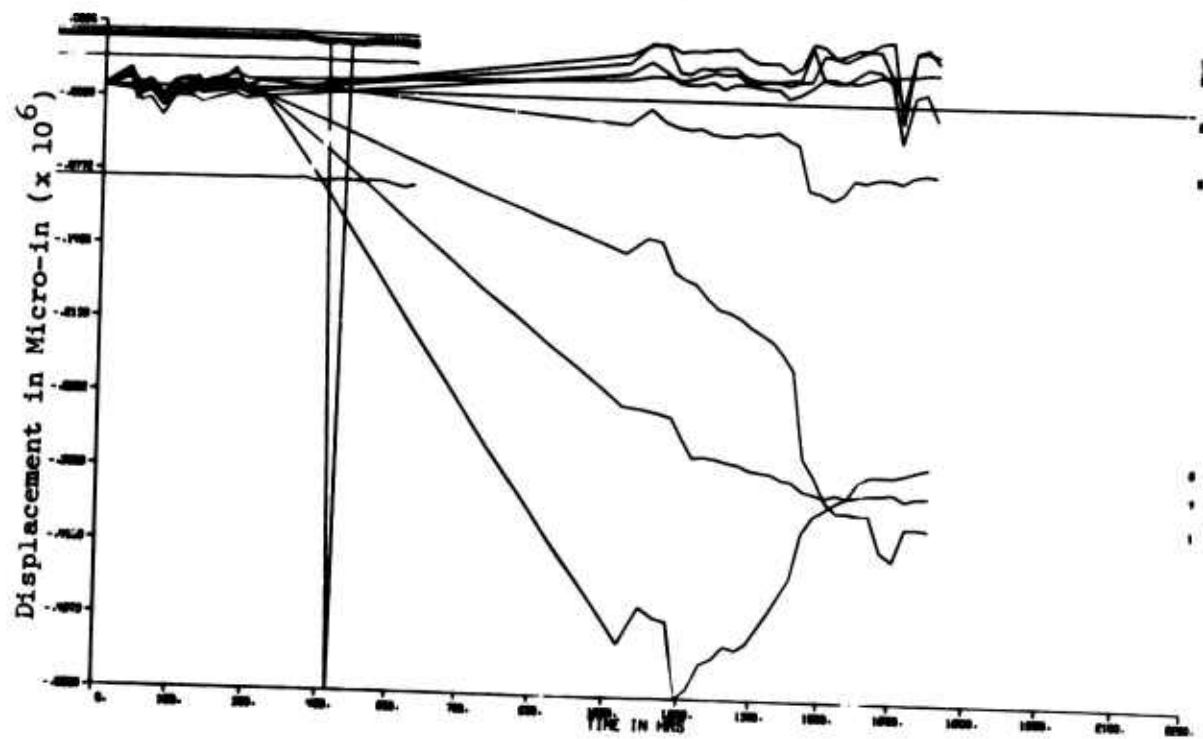
GR-2035 105+05



SC-2099 65+94

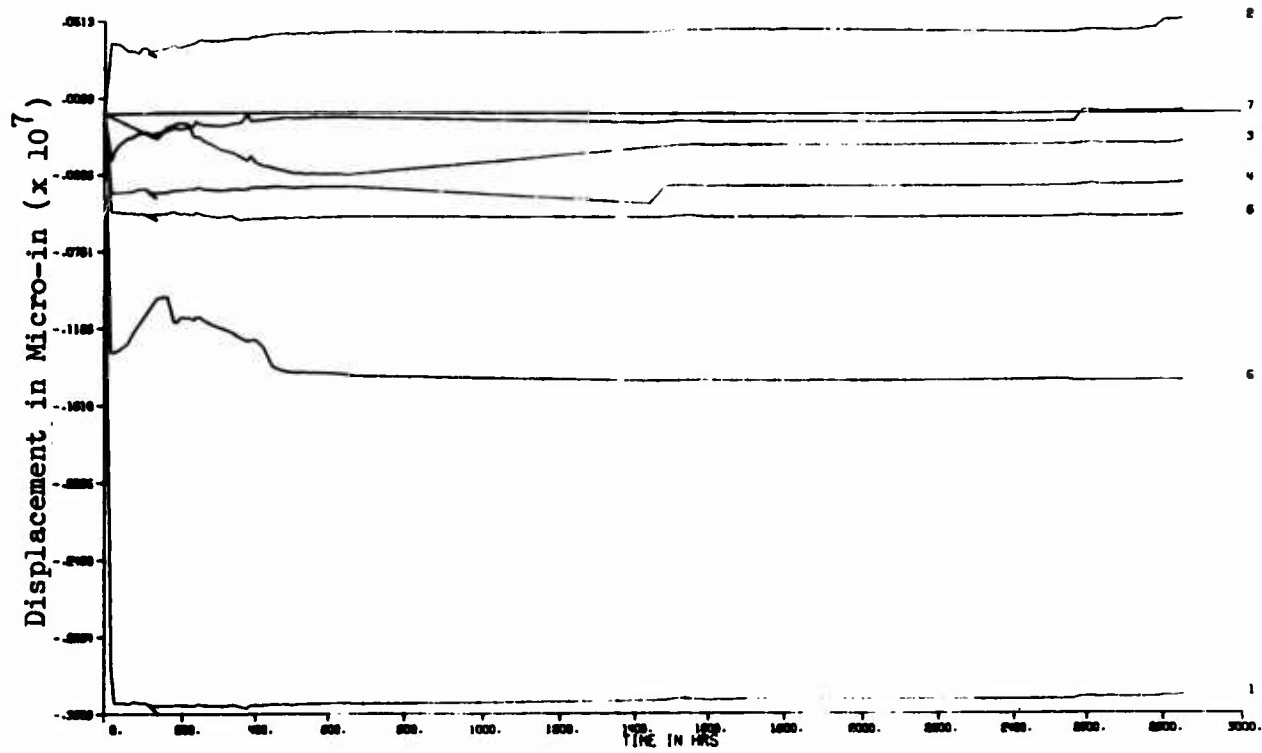


GR-2100 105+05

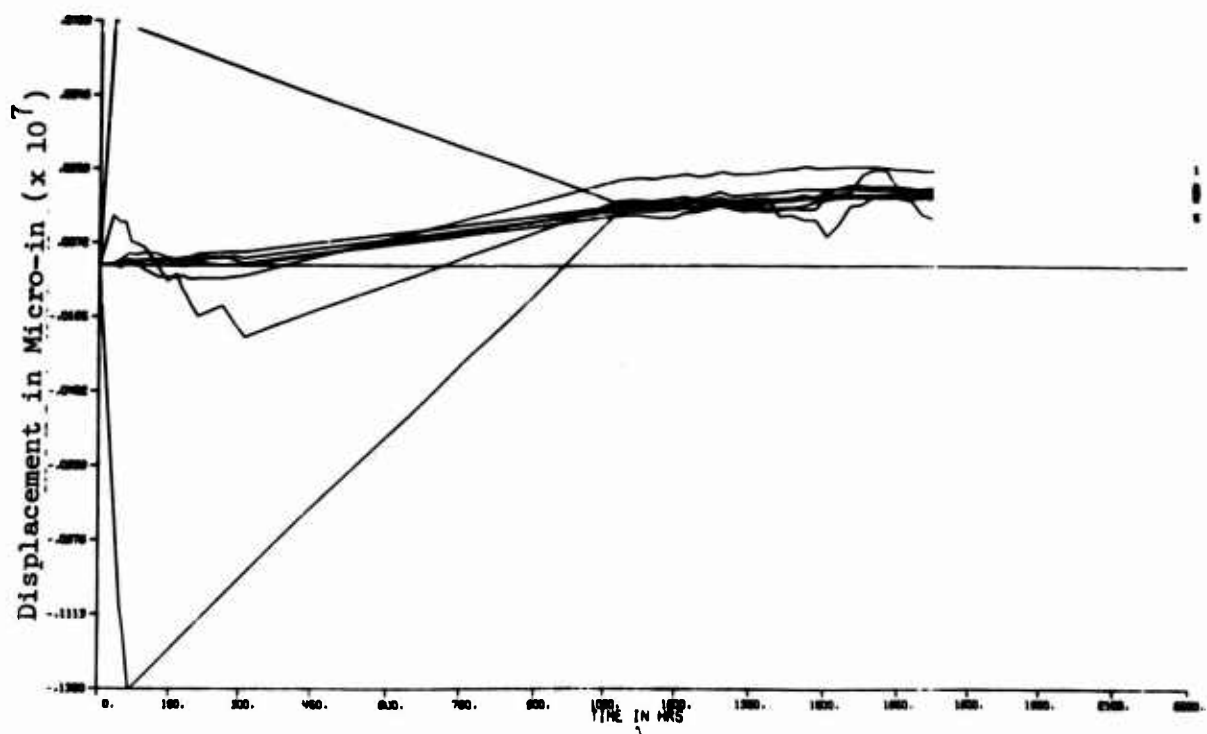


A15

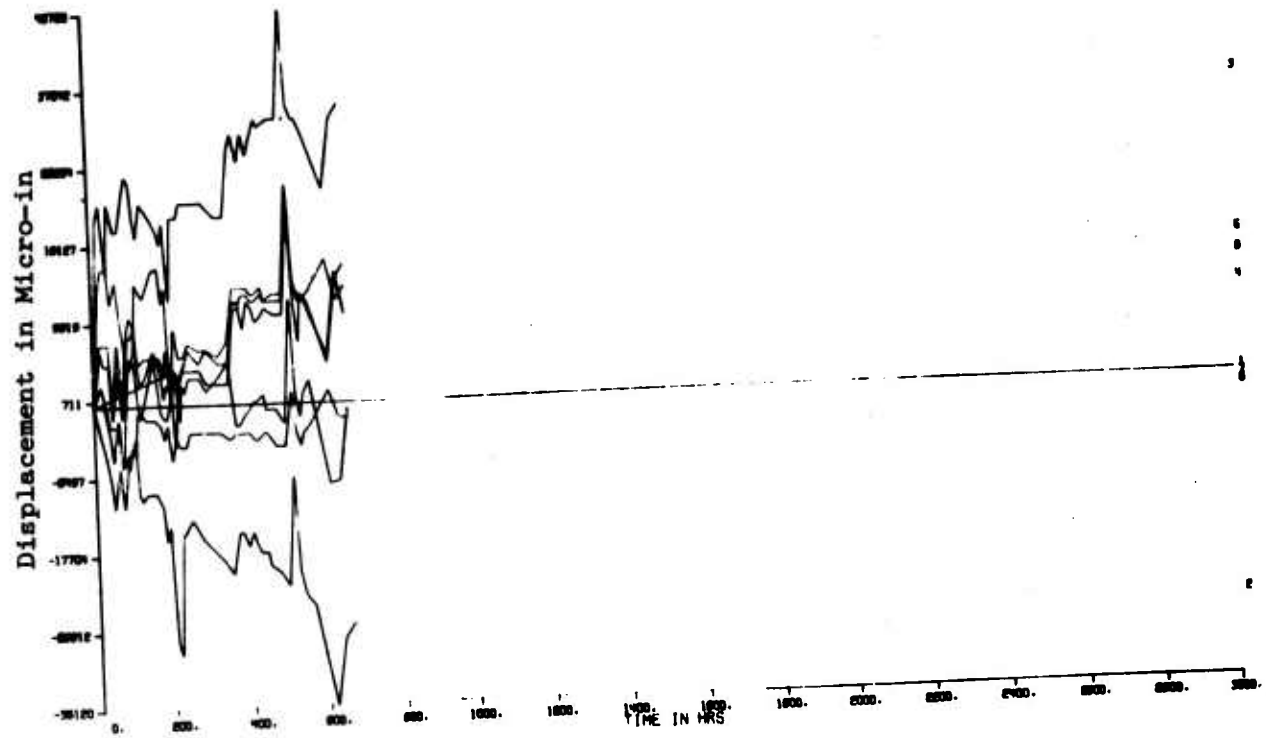
GR-2101 103+51



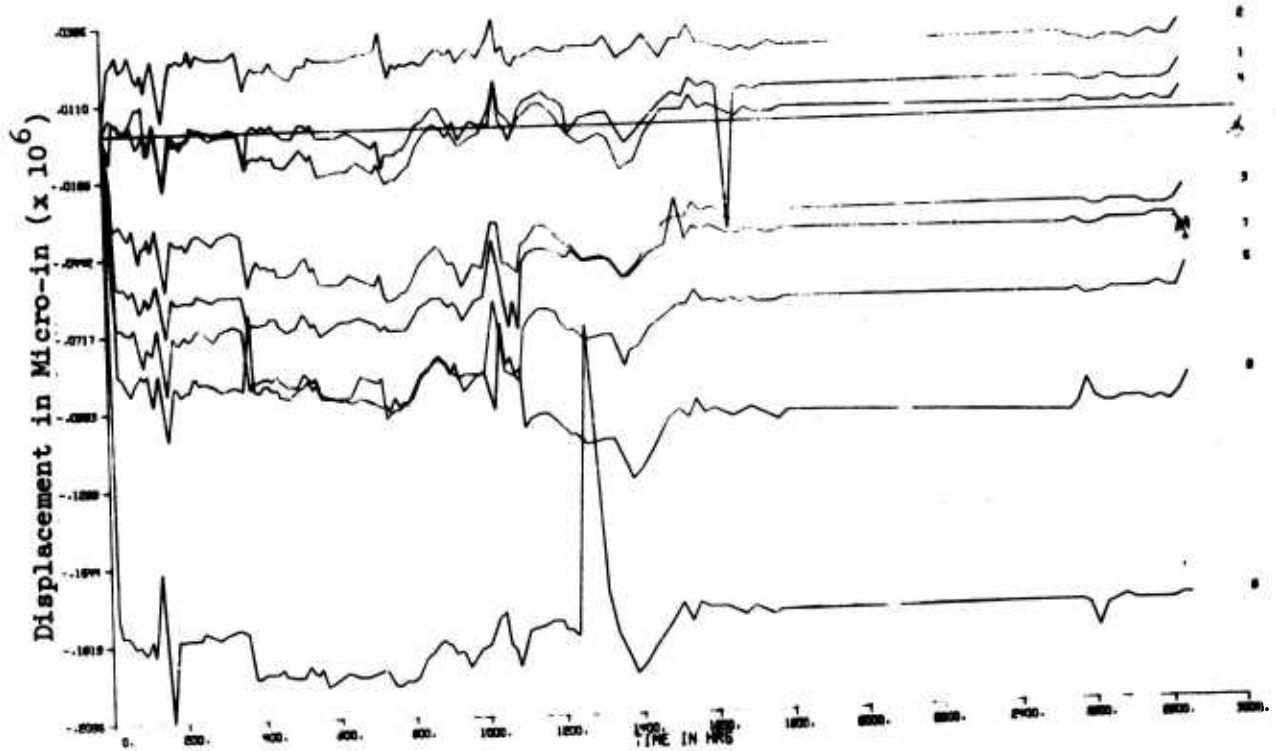
GR-2103 105+5



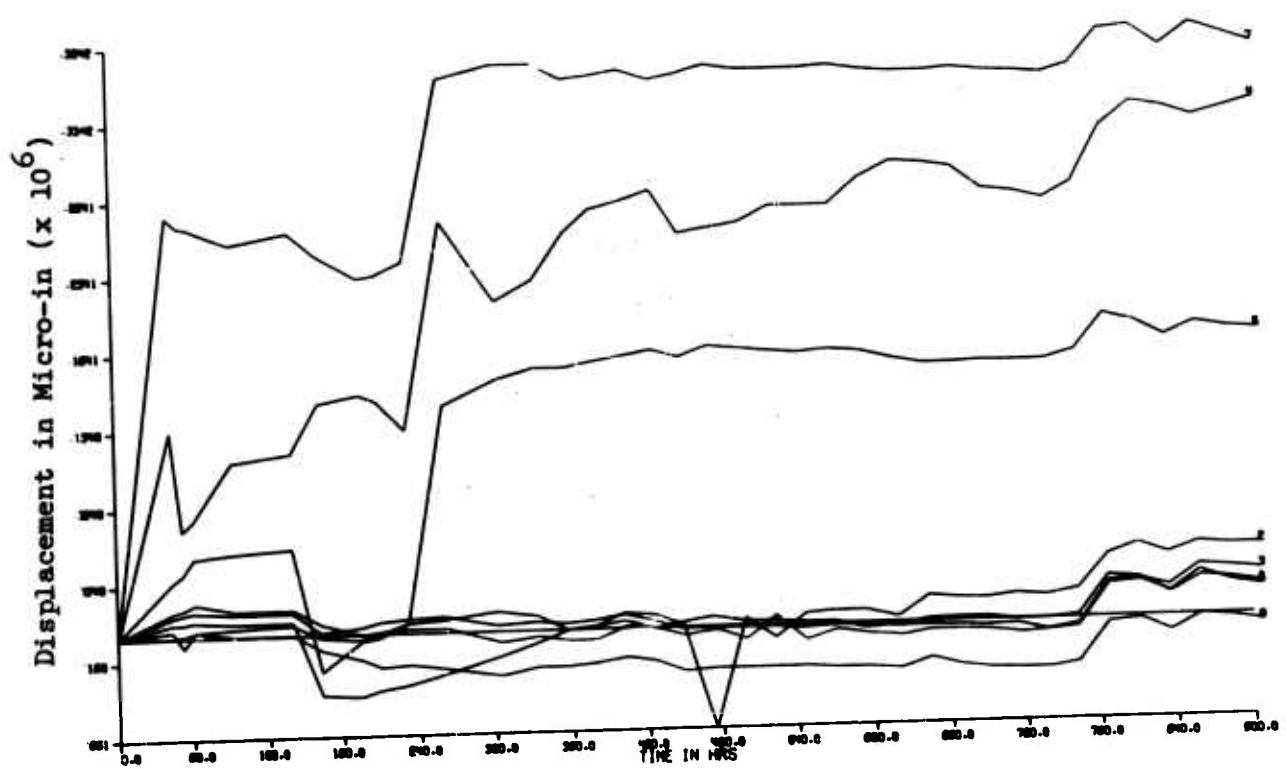
GR-2104 103+51



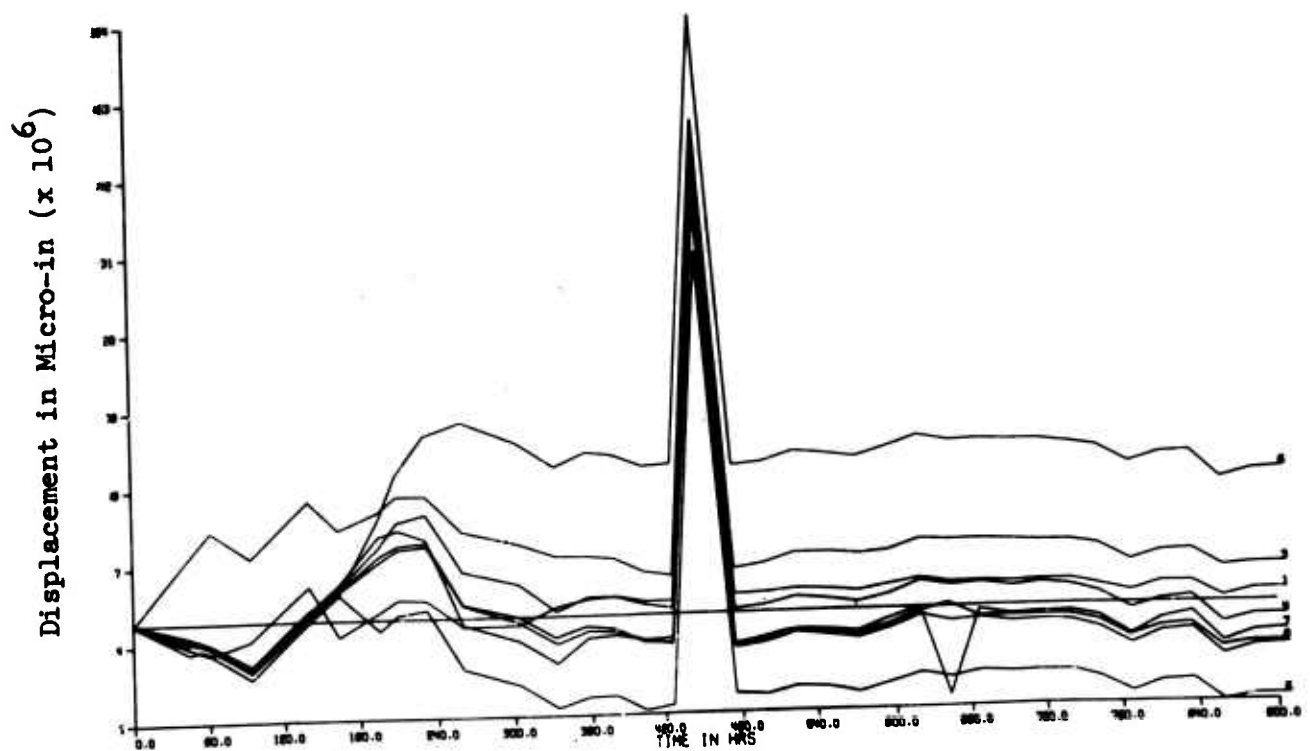
GR-2105 103+51



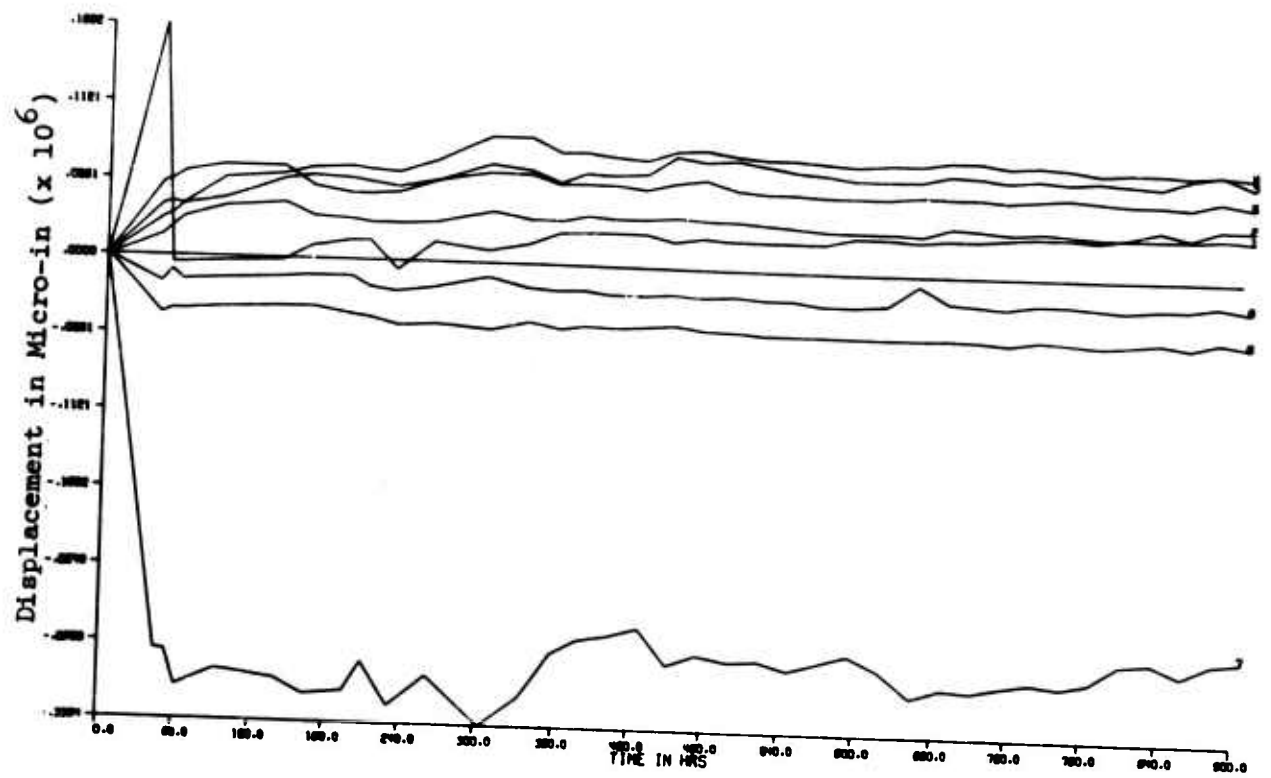
GR-2106 98+35



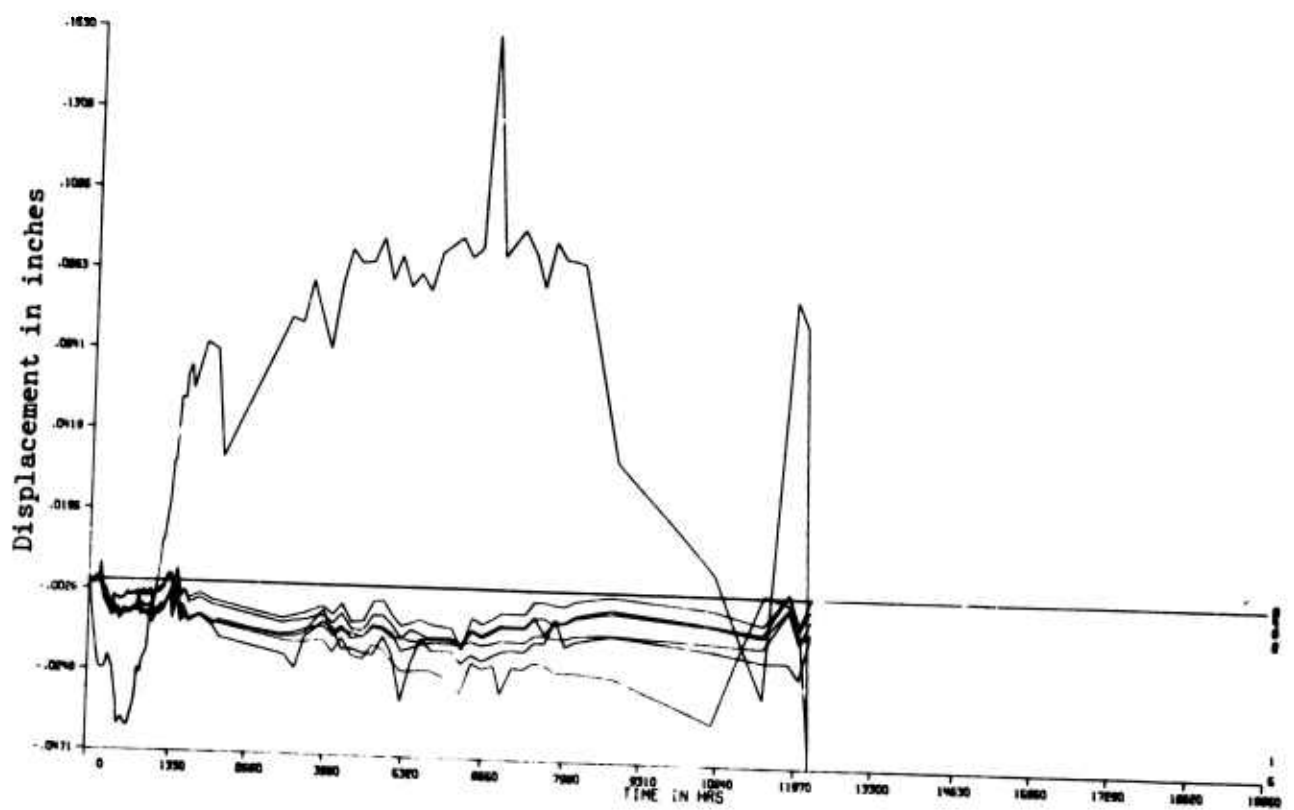
GR-2107 98+35



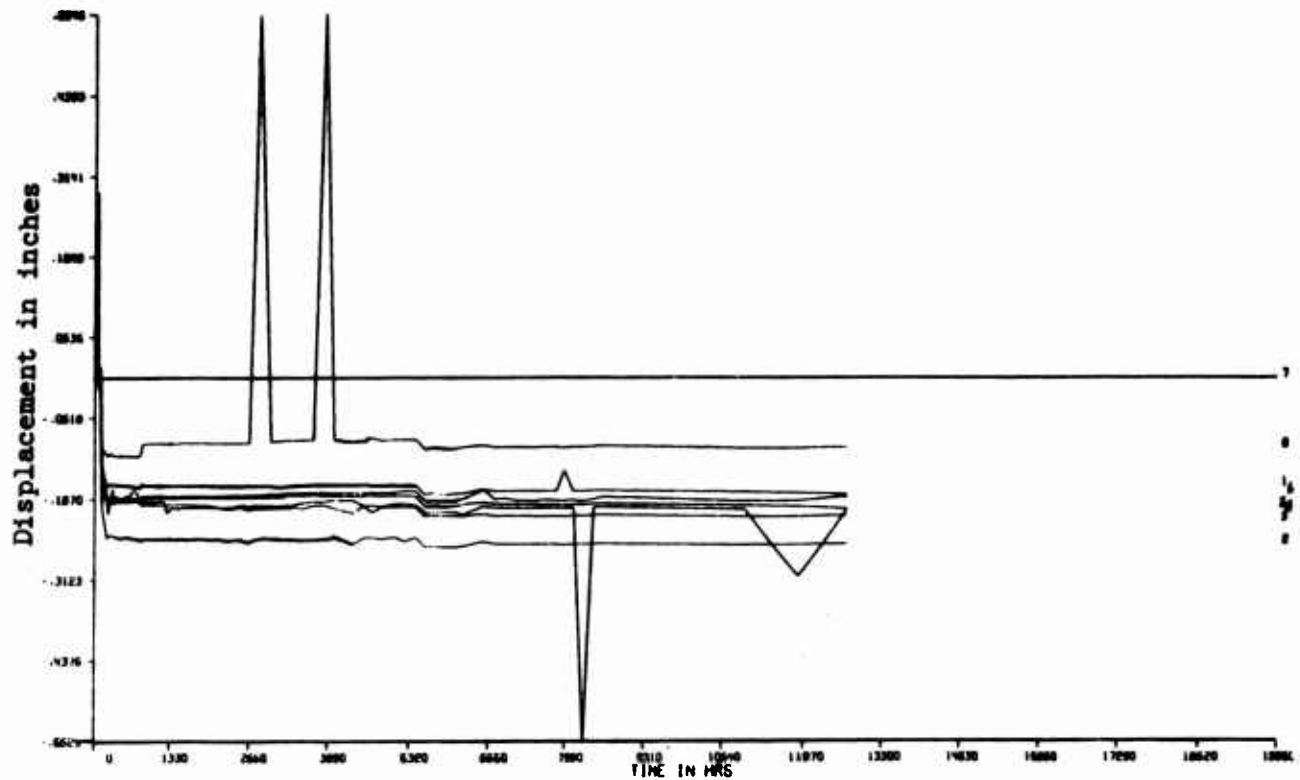
GR-2108 98+35



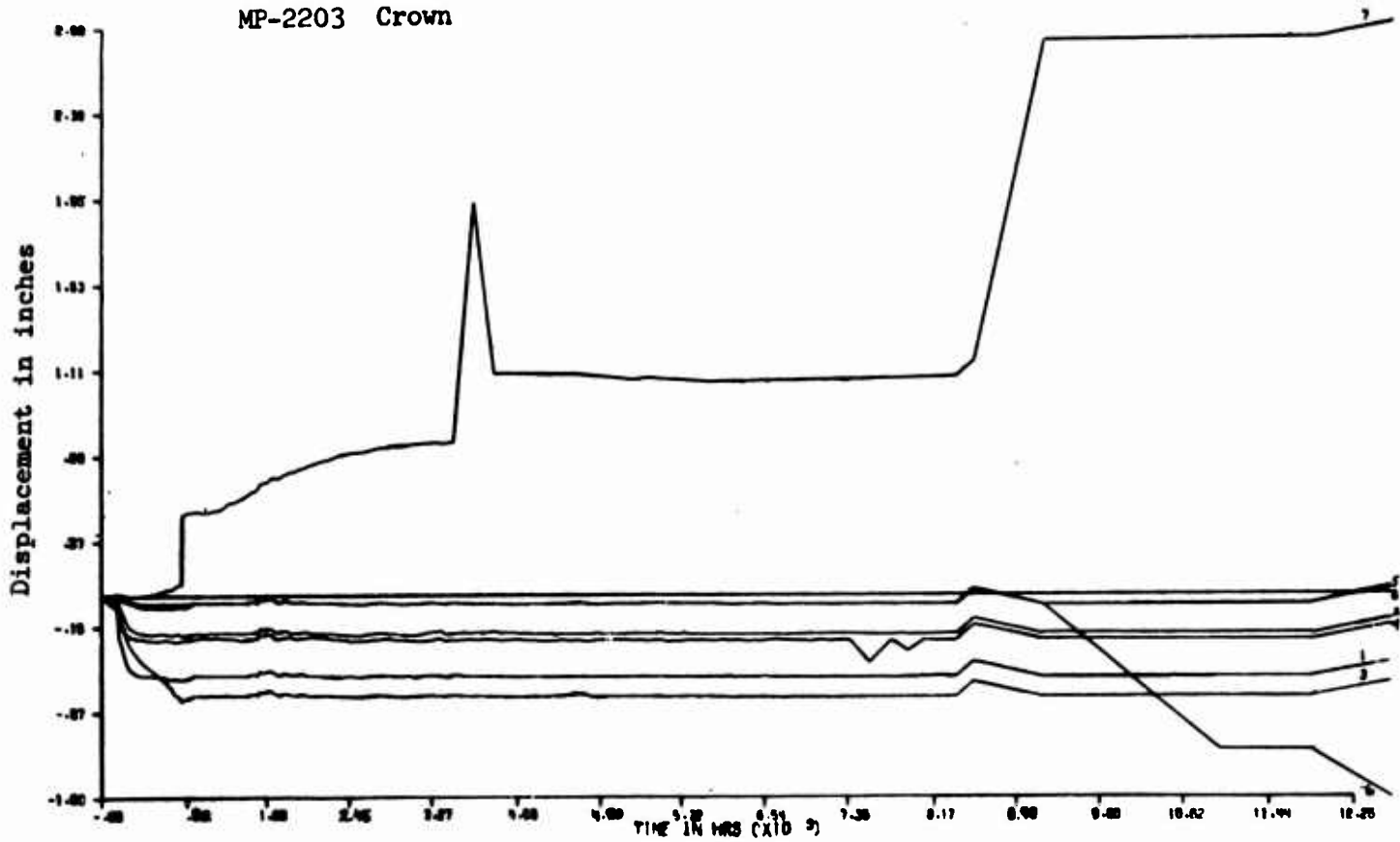
MP-2201 Crown



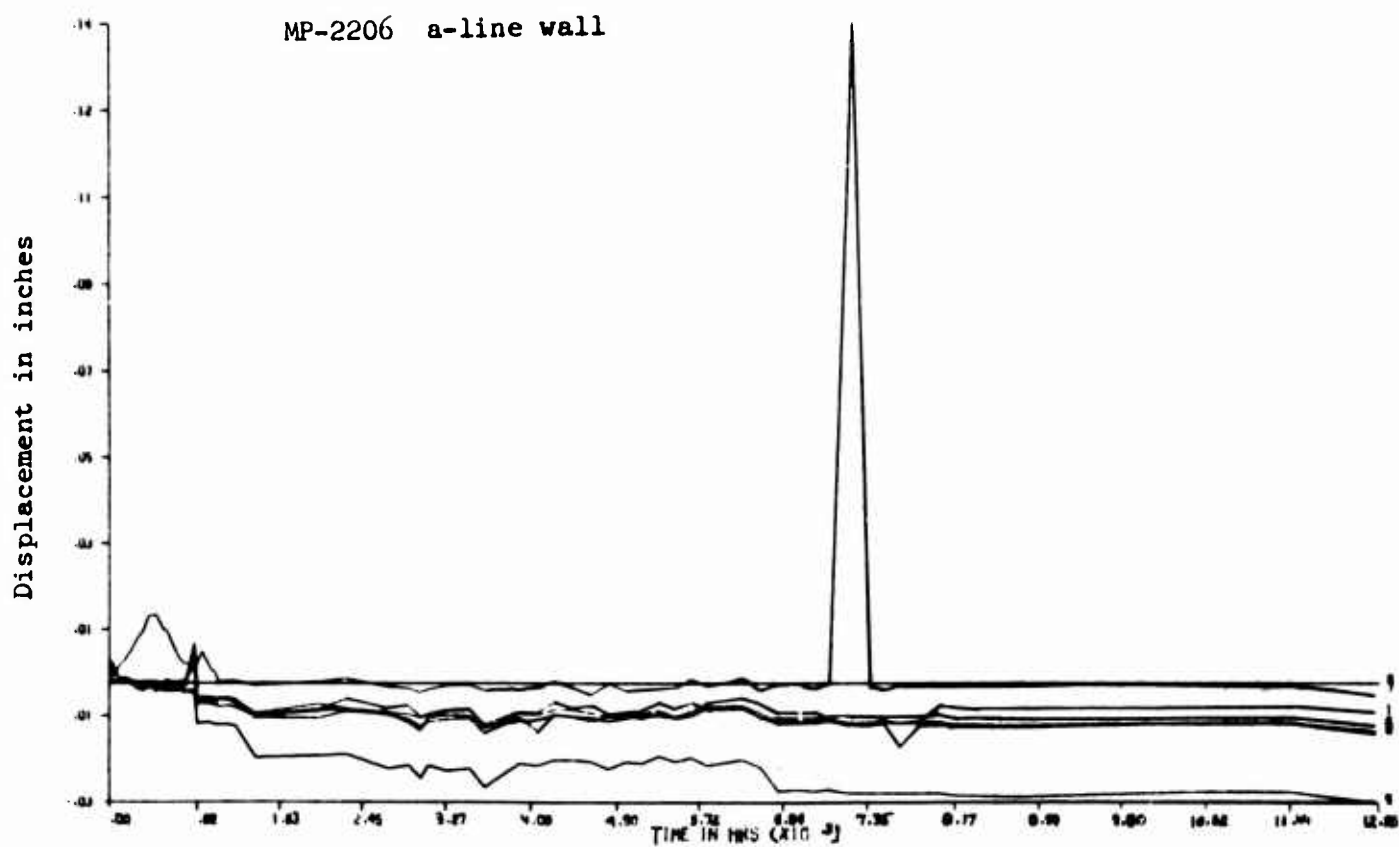
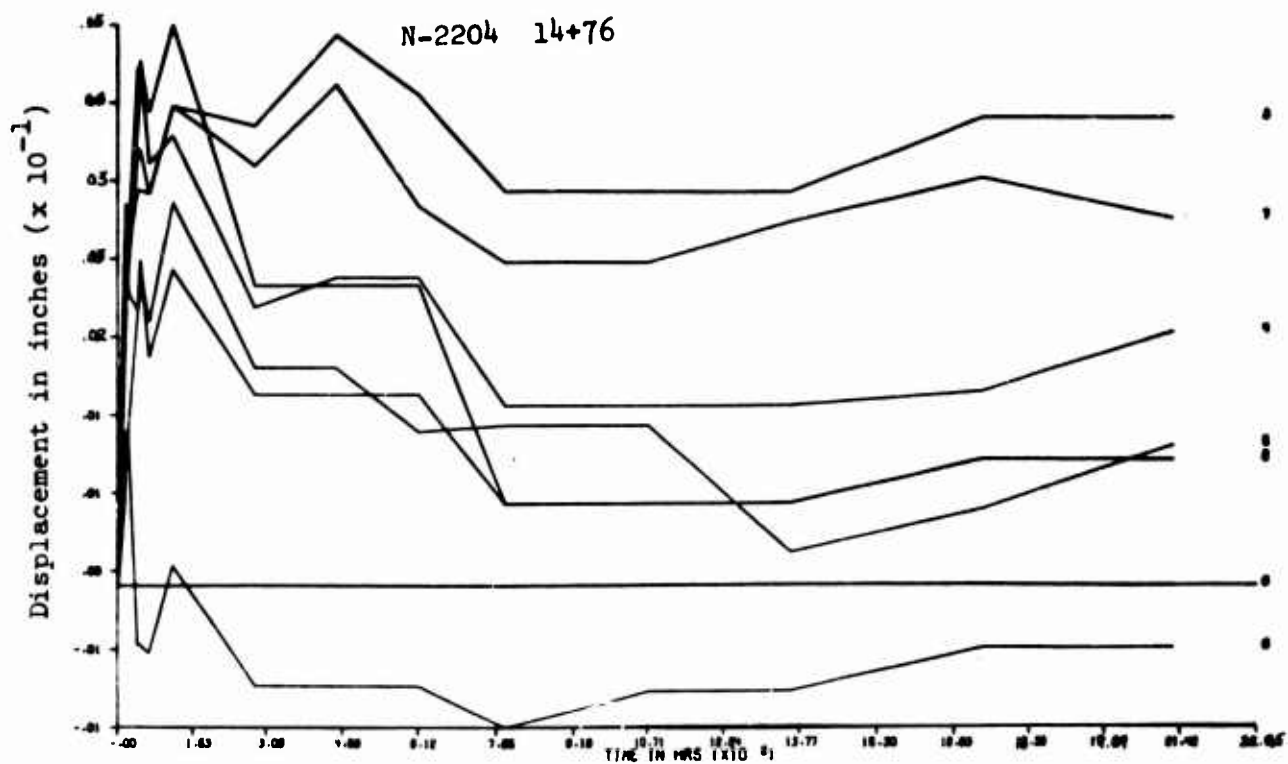
MP-2202 Crown

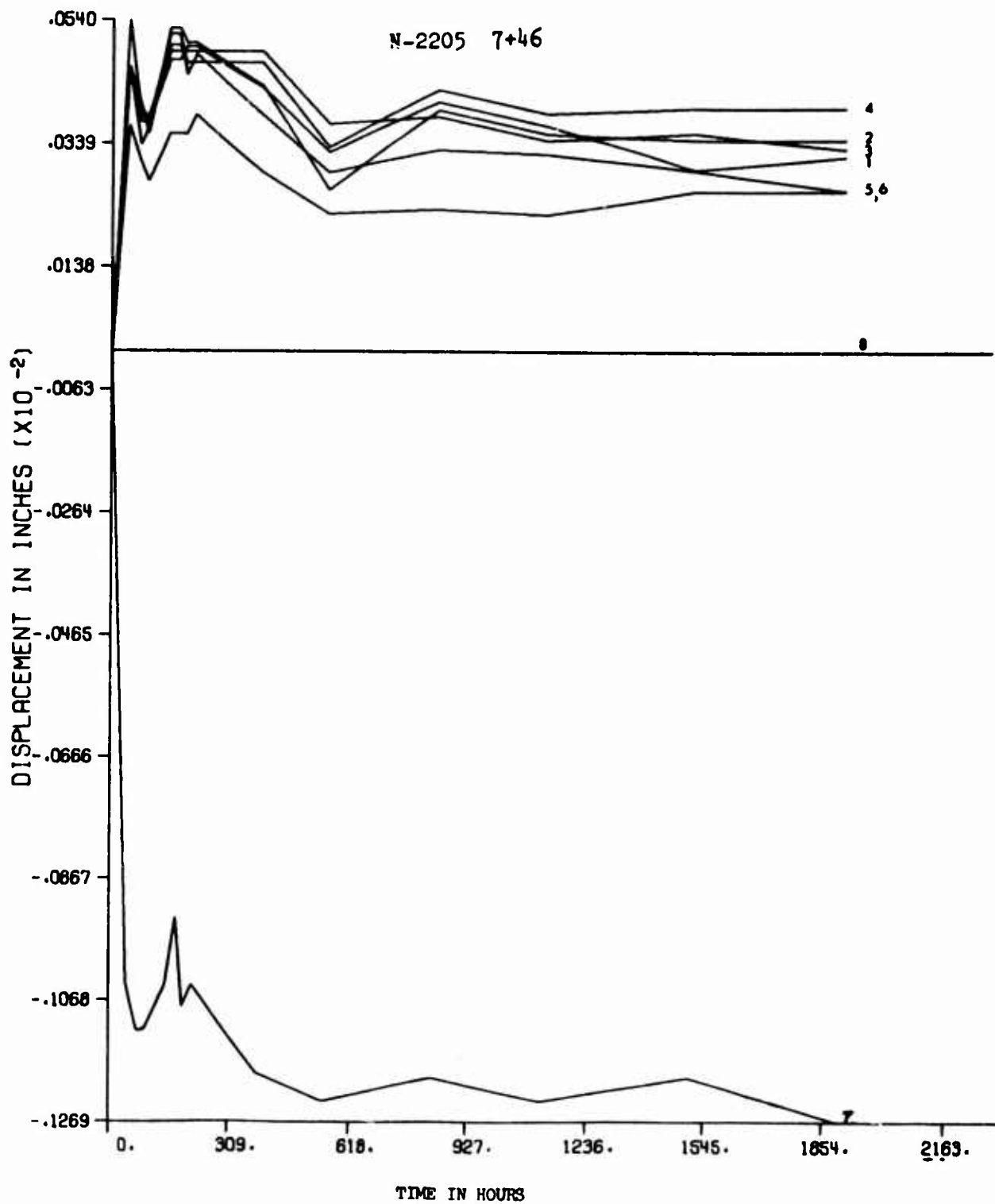


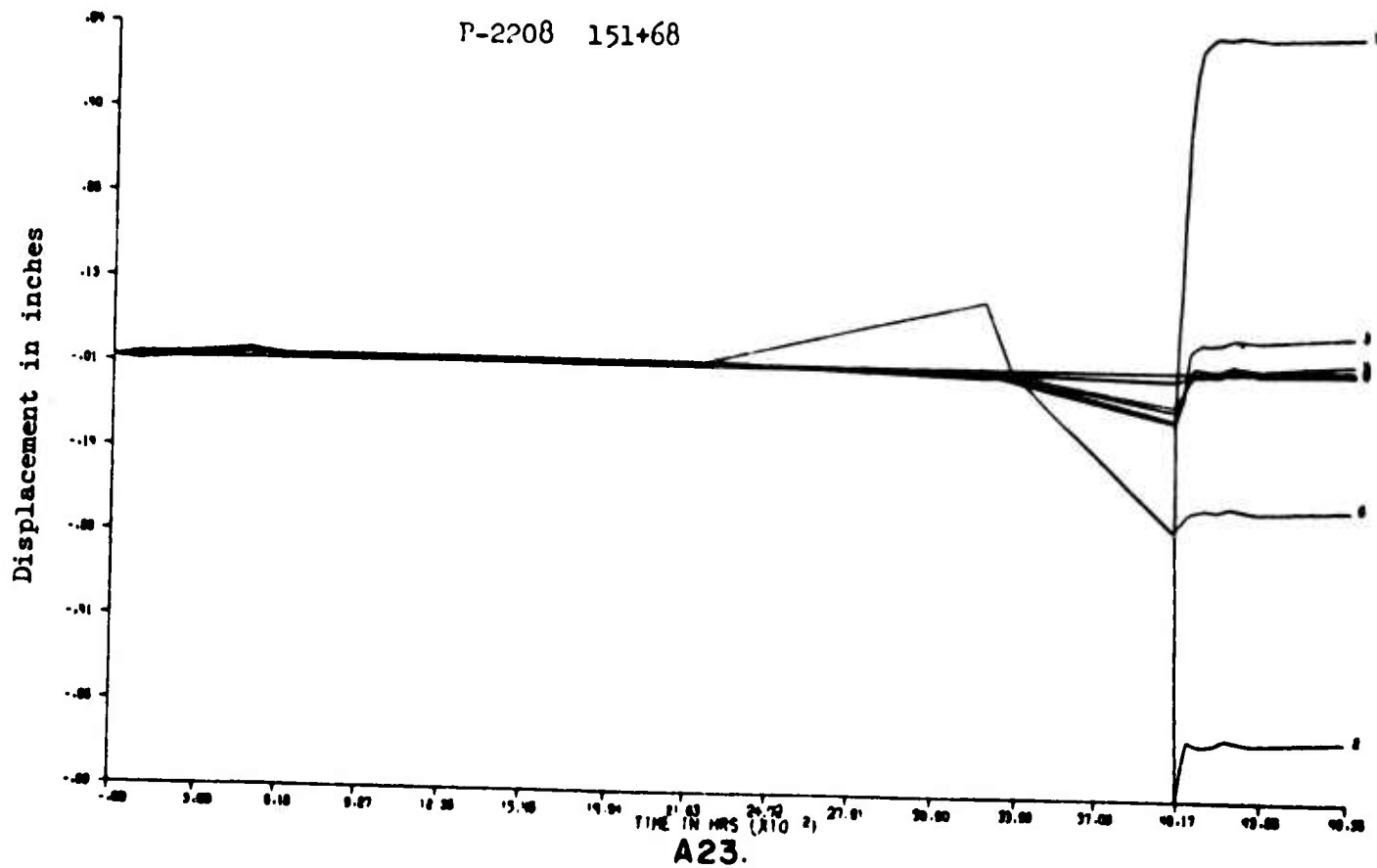
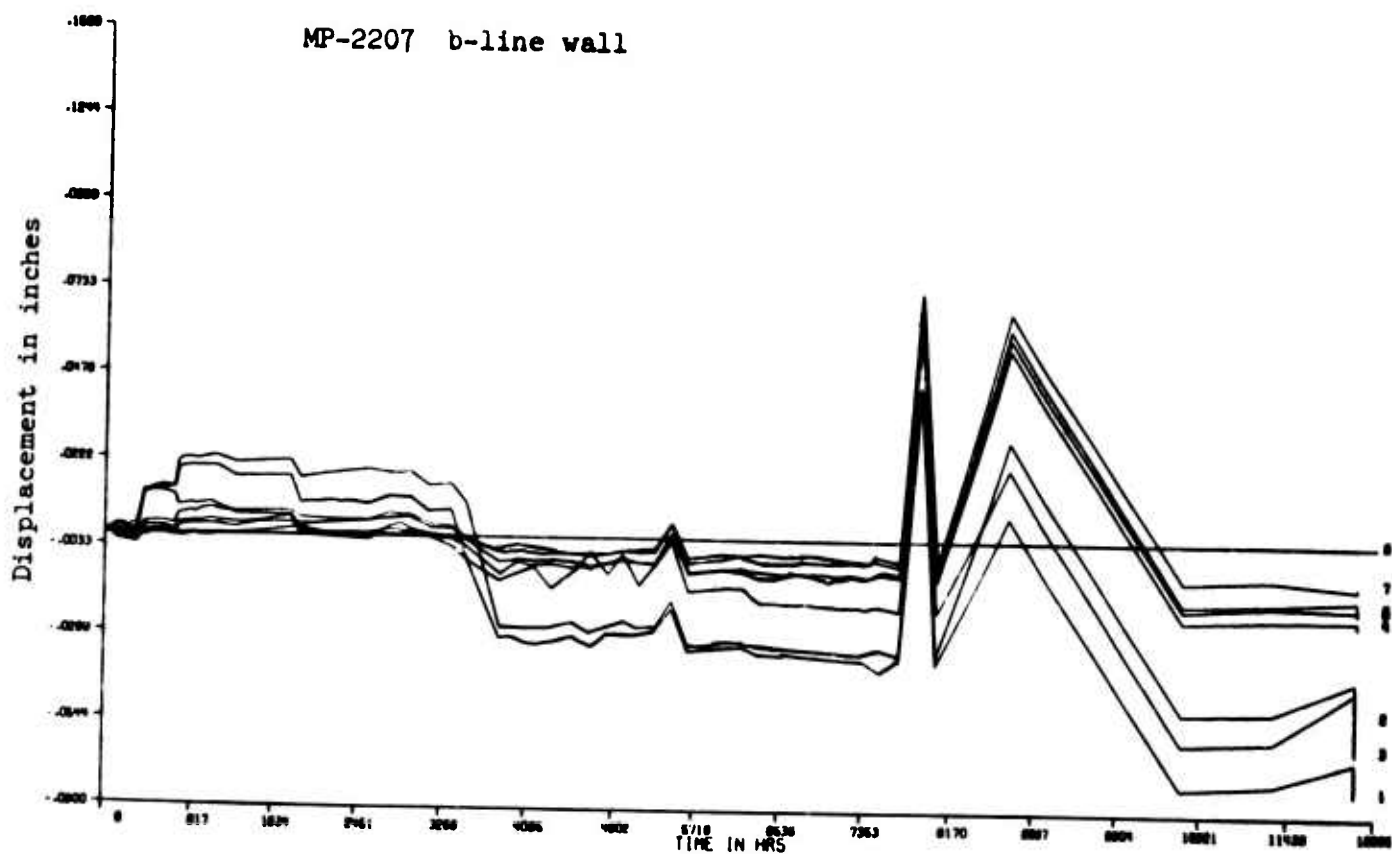
MP-2203 Crown

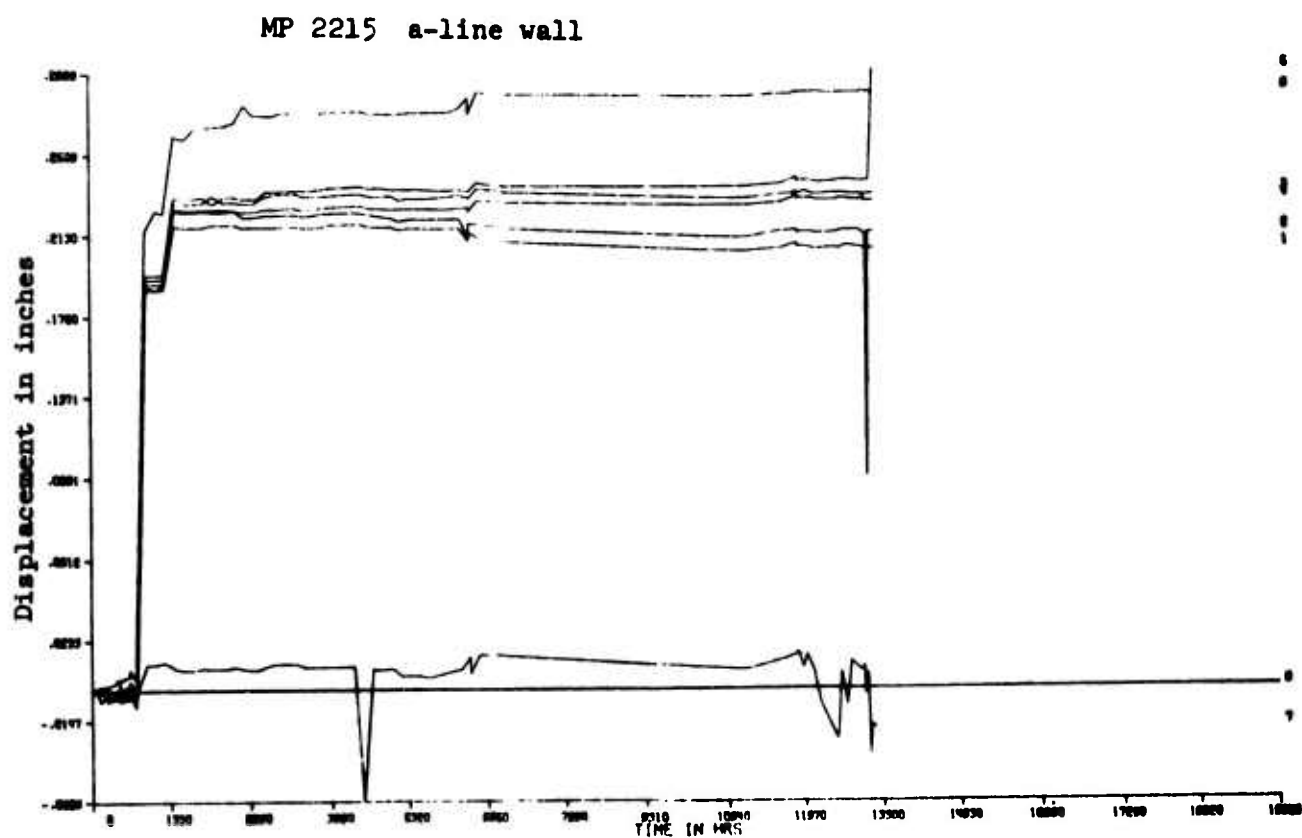
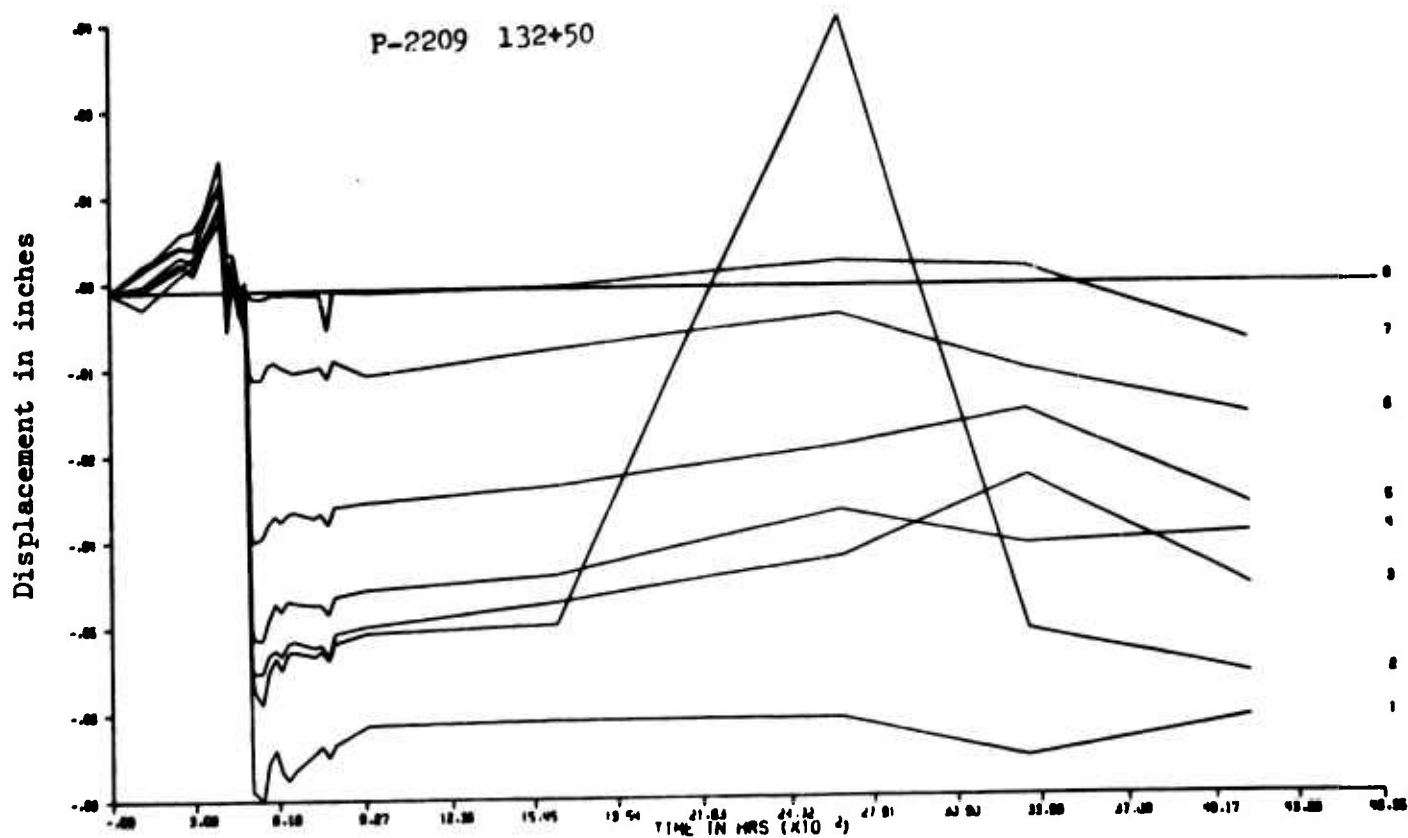




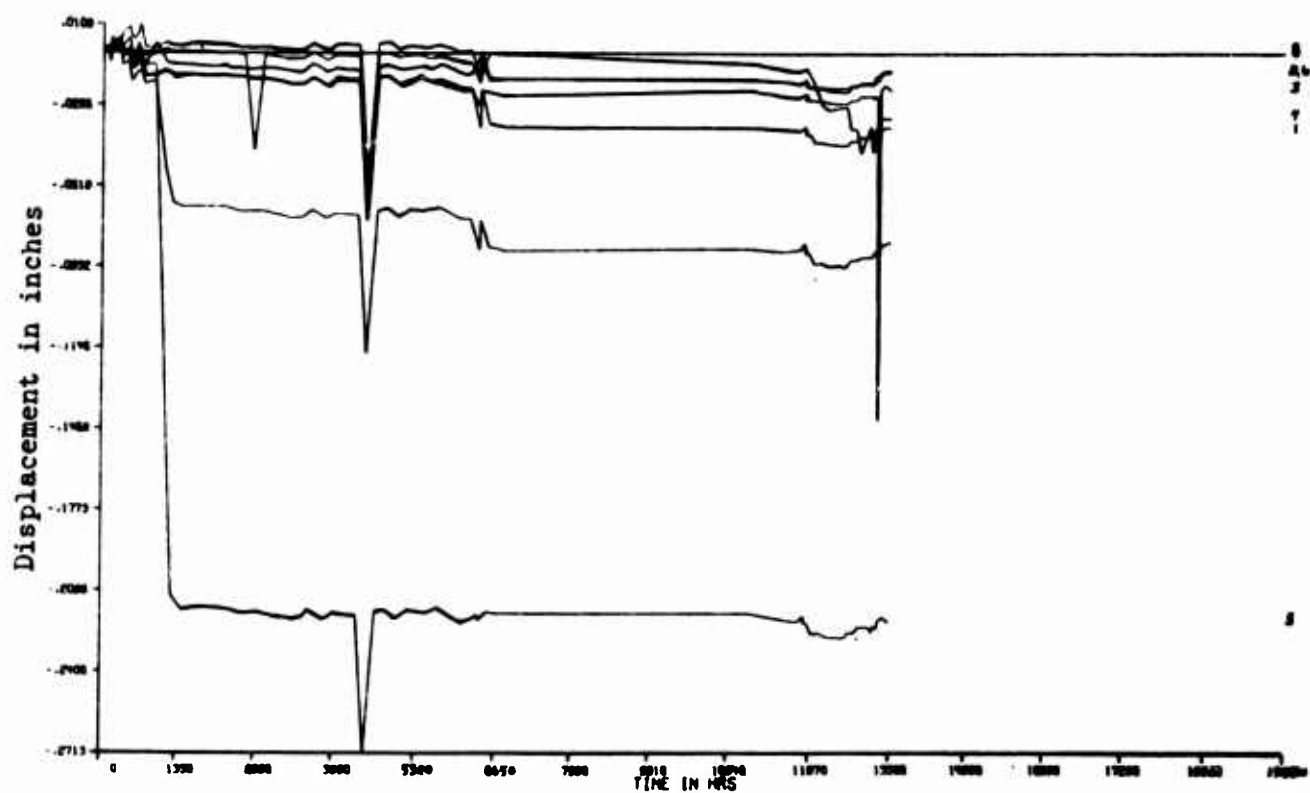








MP 2217 a-line wall



## APPENDIX B

### Computer Programs for Time-Displacement Plots

by

Patricia Nahas

The goal of the computer programming aspect of this research on strain distribution was the production of plots of displacement vs time around each of five underground openings. (See page B-5 for sample printouts of the raw data.) Purdue University's CDC 6500 computer and CALCOMP Plotting System were used for the analyses. The CALCOMP system at Purdue consists of a set of subroutines that produce a file on a disk that is copied onto a plot tape. This tape is then run on a Model 563 CALCOMP Digital Increment Plotter, producing an X-Y plot of digital data. (The user's manual for the CALCOMP Plotter can be obtained upon request.)

The Bureau of Reclamation was the source of the raw data for the Morrow Point, Pacheco, and Navajo Tunnels. It was also the source of Program #1 in the appendix. This program produced output from raw data that included displacements and associated times for each anchor for each station. With slight modifications, this program was run on the CDC computer at Purdue, and in addition the above-mentioned portion of the output was placed on punched cards. (Program #1 in the appendix is the modified version of the program we received from the Bureau of Reclamation.) The data on the resulting set of cards were exactly the points to be plotted from the strain distribution curves; Program #2 in the appendix is the program used to produce the plots.

The initial part of the routine reads in the identification information and stores the times and displacements in arrays. The next section of the program determines the maximum and minimum displacements and this information is used to scale the Y axis. The scale for the X or time axis is predetermined: it can be uniform for all the data or it can be set to reflect the time spread for the particular data in any one set of plots. In any event, it is necessary to know the time span, say in hours, over which the raw readings were collected. The last part of the program consists mainly of calls to the subroutines which produce the plots. These calls provide information regarding the length and labelling of the axes and the points to be plotted. Finally, the program tests the counter variable NOTD against the constant NOT which is set at the start of the program. (Note that NOT could be read in for greater flexibility.) NOT indicates the number of data sets - and hence the number of plots - to be processed on a particular run of the program. If NOTD does not equal NOT, the pen must be repositioned before another plot is begun. Otherwise, the program is finished.

In the case of the data on the Green River and Straight Creek Tunnels, it was necessary to write the routine to compute the times and displacements from the raw data. Programs #3 and #4 in the appendix are the programs used to convert the data from Straight Creek and Green River respectively. These programs also produce the plots for the data being processed. They are

essentially alike, varying only where necessary to accommodate the slightly different formats of the data and the different labellings of the plots.

The initial part of the programs reads in identification information, the calibration factor for each anchor, and the raw data. Taking the time of the first reading as the zero reference time, the program then determines the time in hours of each successive reading. The following section of the program is devoted to the computation of the displacements, with those of the reference anchor necessarily first. It also includes procedures for eliminating bad readings from the raw data; i.e., readings of 00000. or 99999.

In general, the policy with respect to bad readings was as follows. If the bad reading occurred for the reference anchor, it was eliminated and along with it all corresponding readings for the remaining anchors, even if they happened to be good. Hence, referring in the appendix to the raw data for Straight Creek Tunnel (page B- 5), 104 + 83, #2004, note that three readings were eliminated for anchor #8, and correspondingly for the other seven anchors, even though the readings for anchors #2, #3, and #4 were not all bad. In the case where a bad reading occurred for an anchor and the corresponding reading for the reference anchor was good, the reading was eliminated only for the anchor in question. Thus with reference to the same raw data cited above, one counts 24 good readings for the reference anchor, but only 17 for anchor #1, 23 for anchors #2 and #3, 19 for anchor #4, 15 for anchor #5, 20 for anchor #6, and 16 for anchor #7. This procedure for eliminating bad data was selected from among several alternatives. Although it complicates the programming - since one must keep track of the differing number of points to be plotted for each anchor while maintaining the correct time value across all anchors - it enabled us to use as much of the available data as possible.

An important note of information is that the readings for the reference anchor are tested first and if they are bad, they are eliminated along with the corresponding readings for the other anchors. The time array is also altered accordingly and the counter NOR - the variable indicating the total number of readings for the data set in question - is decreased. If the reading is good, the program computes the displacement for the reference anchor as follows:

$$D(K,NA) = [R(K,NA) - R(1,NA)] \cdot CAL(NA)$$

where

$D(K,NA)$  =  $K^{th}$  displacement for the reference anchor

$R(K,NA)$  =  $K^{th}$  reading for the reference anchor

$CAL(NA)$  = calibration factor for the reference anchor

Once the displacements for the reference anchor have been determined, the program proceeds to successively compute those of the remaining anchors. It must take into account the procedure for eliminating bad readings. This involves maintaining a count of the number of good readings for the anchor in question and use of the correct readings for the reference anchor in the computations of the displacement. The general formula for the displacement

$$D(K,J) = [R(K,NA) - R(1,NA)] \cdot CAL(NA) - [R(K,J) - R(1,J)] \cdot CAL(J)$$

where

$D(K,J) = K^{\text{th}}$  displacement for the  $J^{\text{th}}$  anchor

$R(K,J) = K^{\text{th}}$  reading for the  $J^{\text{th}}$  anchor

$CAL(J) =$  calibration factor for the  $J^{\text{th}}$  anchor

$R(K,NA) = K^{\text{th}}$  reading for the reference anchor

$CAL(NA) =$  calibration factor for the reference anchor

and  $D(1,J) = 0$  for every  $J$

However, since the array of raw readings for a particular anchor is corrected before the displacements for that anchor are computed, the  $n^{\text{th}}$  reading for anchor  $J$  may, for example, correspond timewise to the  $m^{\text{th}}$  reading for the reference anchor. In this case, the general formula for computing the displacement must be altered and appears as in statement #40 with the correction variable KOUNT. Reference once more to the case of Straight Creek Tunnel, 104 + 83, #2004 may help clarify the situation. We have

$D(1,8) = 0$   
 $D(2,8) = (10050 - 13535) \cdot (106)$   
 $D(3,8) = (10000 - 13535) \cdot (106)$   
 $D(4,8) = (14570 - 13535) \cdot (106)$   
 $D(5,8) = (10060 - 13535) \cdot (106)$   
 $D(6,8) = (14735 - 13535) \cdot (106)$

and

$D(1,1) = 0$   
 $D(2,1) = D(2,8) - (11920 - 12975) \cdot (112)$   
 $D(3,1) = D(6,8) - (14200 - 12975) \cdot (112)$   
 $\quad = (14735 - 13535) \cdot (106) - (14200 - 12975) \cdot (112)$

where  $D(3,1)$  corresponds to

$D(K,J) = [R(K+KOUNT,NA) - R(1,NA)] \cdot CAL(NA) - [R(K,J) - R(1,J)] \cdot CAL(J)$

with

$K = 3 \quad NA = 8$   
 $J = 1 \quad KOUNT = 3$

The next section of the program determines the maximum and minimum displacements and thus determines a scaling factor for the plots. The times and displacements to be plotted for each anchor are then printed out. These values do not appear explicitly on the plots and a listing of them enables one to know exactly the X-Y coordinates of a particular point on the plot. This listing can also be used to check that the computational portion of the routine is correct.

The latter part of the program is devoted to the plotting. Calls to various subroutines provide the information necessary to draw and label the axes and plots. Since only one line can be plotted at a time but plots for all anchors on one set of axes are desired, the points to be plotted, stored originally in two-dimensional arrays, are transferred to one-dimensional arrays inside the DO-LOOP that actually plots the line. This fact plus the fact that the last two elements of the one-dimensional arrays must provide information on the number of points to be plotted and the scaling factor indicate why such care was taken when the displacements for each anchor were determined.



Lastly, the program checks to verify that all plots for a particular run have been processed and either ends or returns to read the next set of raw data.

The above hopefully will prove helpful to those who wish to repeat these procedures as part of their own research. It is not possible to go into complete detail in describing the data and programs used. Some knowledge of computer techniques is assumed, and it is believed that by reference to the appendix, the reader can reproduce the method used and understand the rationale behind it.

Station Number	MPBX Number								Strain Readings			
	#1	#2	#3	#4	#5	#6	#7	#8	(Anchor Depth) (Calibration Factor)	Rad Data		
104 + 83 022.	18.	10.	02.	2004.	180.	25.0	106.	11450.	12580.		13535.	
104 + 83 02.0	04.0	06.0	09.0	12.0	15.0	20.0	106.	11470.	13090.	10050.		
104 + 83 112.	115.	113.	110.	106.	102.	106.	106.	08650.	09175.	10000.		
023. 18. 00.	12975.	16260.	11300.	13560.	13535.	12100.	12100.	10990.	14005.	14570.		
024. 02. 30.	11920.	16260.	10800.	13535.	13535.	11040.	11040.	10070.	14505.	10060.		
025. 04. 30.	99999.	14240.	08200.	11500.	11500.	09610.	09610.	12190.	14520.	14735.		
025. 11. 00.	99999.	13220.	99999.	99999.	99999.	13050.	13050.	12200.	14550.	14770.		
025. 18. 00.	99999.	10100.	10050.	10035.	10035.	09920.	09920.	12040.	15050.	15180.		
026. 06. 45.	14200.	17800.	12020.	13730.	12280.	12280.	12280.	12270.	14900.	14820.		
026. 17. 00.	14080.	17710.	11940.	14900.	13230.	13230.	13230.	10440.	12740.	12980.		
026. 17. 30.	14160.	17720.	11950.	14945.	13250.	13250.	13250.	12580.	15090.	15140.		
026. 21. 30.	14580.	18200.	12430.	15440.	13730.	13730.	13730.	13680.	16260.	16380.		
027. 02. 15.	14100.	17760.	11955.	14970.	13250.	13250.	13250.	10270.	12850.	12710.		
027. 09. 30.	11220.	14410.	09690.	13340.	11570.	11570.	11570.	12220.	14940.	14815.		
027. 21. 00.	14110.	13040.	12250.	15300.	13510.	13510.	13510.	12220.	11080.	14970.		
028. 04. 00.	13910.	17630.	11920.	16165.	14215.	14215.	14215.	11610.	99999.	15030.		
028. 19. 00.	12980.	16370.	10460.	13190.	11460.	11460.	11460.	11610.	99999.	15100.		
029. 01. 30.	14280.	17780.	11985.	14990.	13325.	13325.	13325.	10300.	99999.	15300.		
035. 03. 35.	14535.	18265.	12045.	15285.	99999.	99999.	99999.	15130.	99999.	18545.		
039. 05. 30.	14200.	18300.	12060.	15180.	99999.	99999.	99999.	99999.	99999.	99999.		
039. 14. 00.	14185.	18200.	12080.	15125.	99999.	99999.	99999.	99999.	99999.	99999.		
042. 02. 00.	14060.	18300.	12030.	15155.	99999.	99999.	99999.	99999.	99999.	99999.		
049. 03. 00.	15940.	16690.	17240.	16400.	99999.	99999.	99999.	99999.	99999.	99999.		
056. 03. 30.	99999.	18280.	12155.	99999.	99999.	99999.	99999.	99999.	99999.	99999.		
061. 06. 15.	99999.	19035.	12690.	15950.	99999.	99999.	99999.	99999.	99999.	99999.		
066. 18. 30.	99999.	19620.	13210.	16880.	99999.	99999.	99999.	99999.	99999.	99999.		
075. 21. 45.	99999.	19370.	12640.	99999.	99999.	99999.	99999.	99999.	99999.	99999.		
082. 11. 30.	99999.	18380.	11550.	99999.	99999.	99999.	99999.	99999.	99999.	99999.		
088. 10. 30.	99999.	21610.	12150.	99999.	99999.	99999.	99999.	99999.	99999.	99999.		
120. 06. 00.	99999.	99999.	15700.	99999.	99999.	99999.	99999.	99999.	99999.	99999.		

Example of how Strain Data from Straight Creek Tunnel

COMPUTER PROGRAM NO. 1

```

PROGRAM EXPRN(INPUT,OUTPUT,TAPE5=INPUT,TAPE6=OUTPUT,PUNCH,TAPE7 =
1PUNCH)
C MPRX DATA REDUCTION PROGRAM NUMERIC AND CARDS FOR X Y PLOT W ORTEL
000002 DIMENSION STRAIN(8,300)
000002 DIMENSION DISPL(8,300),FT(300)
000002 DIMENSION ADEPTH(8),DCANT(8,300),RCANT(8,300),DAY(300),AMONTH(300)
1,YEAR(300),HOUR(300),FEAT(40),DELTA(8,300),DAYMO(12),SUM(8,300),TI
2MF(300),DELTAB(8,300),DIFF(8,300),RELT(8,300),RELTAB(8,300),ADJUS
3T(8,100)
000002 COMMON TIMED(300),RNG(8,10),C1(8,10),C2(8,10),N,NRDG,MCANT
000002 5 READ(5,10) (FEAT(I),I=1,40),STA,PRYM
000014 10 FORMAT(40A1,2A8)
000014 READ(5,8) MCANT
000022 8 FORMAT(I4)
000022 READ(5,20) (ADEPTH(I),I=1,8),C
000032 20 FORMAT(8F5.0,F8.4)
000032 CALL CALRDG
000033 N=1
000034 RLTLST = 0.0
000035 DLTIST = 0.0
000036 25 READ(5,30) (UCANT(I,N),I=1,8),AMONTH(N),DAY(N),YEAR(N),HOUR(N), (RC
1ANT(I,N),I=1,8)
000061 30 FORMAT(8F6.0,1X,3F2.0,F5.2,20X /8F4.0,32X)
000061 IF(DAY(N)+AMONTH(N)) 40,40,35
000064 35 N=N+1
000066 GO TO 25
000066 40 N=N-1
000070 DO 60 I=1,8
000071 K=0
000072 DO 60 J=1,N
000073 IF(DCANT(I,J)) 59,59,53
000074 53 DIFF(I,J)=(UCANT(I,J)-RCANT(I,J))/2.0
000105 IF(K) 55,55,54
000113 54 DAYDIF=DIFF(I,J)-DIFF(I,K)
000114 RELT(I,J)=DAYDIF
000115 II=I
000115 JJ=J
000117 CALL CALNO(DCANT,II,JJ,Y1)
000122 CALL CALNO(DCANT,II,K,Y2)
000132 Y3=ABS(Y1-Y2)
000134 XCANT=ABS(DCANT(I,J)-DCANT(I,K))
000136 IF(XCANT.EQ.0.) GO TO 72
000140 FACT=(Y3/XCANT)
000141 GO TO 75
000142 72 FACT = 0.
000146 75 FNUMB=FACT*(1.0+(C*ADEPTH(I)))
000151 DELTA(I,J)=DAYDIF*FNUMB
000152 GO TO 56
000156 59 DELTA(I,J)=DLTLST
000156 RELT(I,J)=BLTLST
000160 GO TO 60
000164 55 DELTA(I,J)=0.0
000164 RELT(I,J)=0.0
000165 GO TO 57
000174 56 DELTA(I,J)=DELTA(I,J)+DELTA(I,K)
000175 RELT(I,J)=RELT(I,J)+RELT(I,K)
000176 DLTIST=DELTA(I,J)
000177 BLTLST=RELT(I,J)

```

```

00200 57 K=J
00202 60 CONTINUE
00207 601 K=0
00210 504 READ(5,501) K,L,(ADJUST(I,L),I=1,R)
00223 501 FORMAT(2I3,8F8.6)
00223 IF(K) 61,61,502
00225 502 J=L
00227 506 DO 503 I=1,R
00240 DELTA(I,J)=DELTA(I,J)+ADJUST(I,L)
00241 503 CONTINUE
00243 IF(N-J) 504,504,505
00245 505 J=J+1
00247 GO TO 506
00247 61 CONTINUE
00247 DATA (UAYMO(I),I=1,12)/0.0,31.0,28.0,31.0,30.0,31.0,30.0,31.0,31.
10,30.0,31.0,30.0/
00247 DO 60 I=1,N
00251 A=0.0
00251 IF(YEAR(I)-YEAR(1)) 62,65,62
00254 62 A=365.0
00256 65 L=AMONTH(I)
00260 DO 70 J=1,L
00266 A=A+DAYMO(J)
00267 70 CONTINUE
00271 TIME(I)=(A+(DAY(I)-1.0))*24.0+HOUR(I)
00276 TIMED(I)=TIME(I)-TIME(1)
00300 80 CONTINUE
00302 DO 85 I=1,8
00304 DO 85 J=1,N
00315 SUM(I,J)=DCANT(I,J)+RCANT(I,J)
00317 DELTA8(I,J)=DELTA(I,J)-DELTA(MCANT,J)
00320 RELTA8(I,J)=RELTA(I,J)-RELTA(MCANT,J)
00322 85 CONTINUE
00326 M=0
00326 K=1
00330 90 WRITE(6,100) (FFAT(I),I=1,40),STA,PRXM
00342 100 FORMAT(1H1,40X,40HMPBX EXTENSOMETER DATA REDUCTION PROGRAM///,40X,
140A1///,43X,7HSTATION,AR,6X,8HMPBX NO.,AR///,53X,8HDATE ///,53X,1
24HRAW FIELD DATA///,17X,99HCANTLVR 1 CANTLVR 2 CANTLVR 3 CANTLVR 4
3CANTLVR 5 CANTLVR 6 CANTLVR 7 CANTLVR 8 DATE TIME //)
00342 M=M+8
00345 190 IDAY=DAY(K)
00346 MONTH = AMONTH(K)
00350 IYEAR= YEAR(K)
00352 WRITE(6,200) (DCANT(I,K),I=1,8),MONTH,IDAY,IYEAR,HOUR(K),(RCANT(I,
1K),I=1,8),(SUM(I,K),I=1,8)
00377 200 FORMAT(16HDIRECT READINGS,8F10.1,7X,I2,1H/,I2,1H/,I2,F6.2 /,16HRE
1VERSE READINGS,8F10.1/,15HSUM OF READINGS,8F10.1//)
00377 K=K+1
00401 IF(N-K) 250,210,210
00403 210 IF(K-M) 190,90,90
00406 250 WRITE(6,300) (FFAT(I),I=1,40),STA,PRXM,MCANT,MCANT
00424 300 FORMAT(1H1,40X,40HMPBX EXTENSOMETER DATA REDUCTION PROGRAM///,40X,
140A1///,43X,7HSTATION,AR,6X,8HMPBX NO.,AR///,53X,8HDATE ///,53X,1
22HREDUCED DATA///,25X, 59HCANTLVR NO ANCHOR DEPTH DISPL FROM F
3ACE DISPL FROM NO,I2,30HDISPL FROM FACE DISPL FROM NO,I2/,56X,60
4H(IND UNITS) (IND UNITS) (INCHES) (INCHES)/)
100424 M=3

```

```

000425      DO 475 J=1,N
000427      IF(M-J) 471,471,460
000431 471 M=M+3
000433      WRITE(6,300) (FFAT(I),I=1,40),STA,PBXM,MCANT,MCANT
000450 460 CONTINUE
000451      IDAY=DAY(J)
000452      IMONTH=AMONTH(J)
000454      IYEAR=YEAR(J)
000455      ITIME=TIMED(J)
000457      WRITE(6,425) MONTH,IDAY,IYEAR,ITIME
000473 425 FORMAT(2X,4HDATE,I2,1H/,I2,1H/,I2/,2X,16HELAPSED TIME(HR),15/)
000473      DO 475 I=1,8
000475 445 WRITE(6,450) I,ADEPTH(I),BELTA(I,J),BELTAB(I,J),DELTA(I,J),DELTAB(
      I,I,J)
000522 450 FORMAT(29X,I2,12X,F5,1,10X,F7,0,10X,F7,0,8X,F10,6,7X,F10,6)
000522 475 CONTINUE
000527      WRITE(6,500)
000532 500 FORMAT(1H1)
000532      DO 591 I=1,N
000534      FT(I) = TIMED(I)
000536      DO 591 K=1,8
000544      DISPL(K,I) = DELTAB(K,I)
000545 591 CONTINUE
000551      DO 1000 I=1,N
000552      PUNCH 4,FT(I),(DISPL(K,I),K=1,8)
000562 4 FORMAT(1X,F6,0,8F9,6)
000562 1000 CONTINUE
000565      DO 600 I=1,N
000603      STRAIN(1,I)=(-1,0)*DELTA(MCANT,I)-DELTAB(1,I)
000605      STRAIN(1,I)=STRAIN(1,I)/(ADEPTH(1)*12,0)
000606 600 CONTINUE
000607      DO 700 I=2,MCANT
000611      DO 700 J=1,N
000625      I2=I-1
000626      STRAIN(I,J)=(DELTAB(I2,J)-DELTAB(I,J))/((ADEPTH(I)-ADEPTH(I2))*
      112,0)
000633 700 CONTINUE
000641      WRITE(6,500)
000645      DO 800 I=1,N
000647      ITIME=TIMED(I)
000651      WRITE(6,900) I,ITIME,(STRAIN(J,I),J=1,8)
000663 900 FORMAT(15X,15,2X,15,8F10,6)
000663 800 CONTINUE
000666      GO TO 5
000666      FND

```

PROGRAM LENGTH INCLUDING I/O BUFFERS  
070306

UNUSED COMPILER SPACE  
053700

```

SUBROUTINE CALRNG
DIMENSION DEFLT(8,10)
COMMON TIMED(300),RNG(8,10),C1(8,10),C2(8,10),N,NRNG,MCANT
DO 10 I=1,8
  READ(5,5) NRNG
5  FORMAT(I4)
  DO 10 J=1,NRNG
    READ(5,8) DEFLT(I,J),RNG(I,J)
8  FORMAT(2F8.0,64x)
10 CONTINUE
  DO 20 I=1,8
    DO 20 J=2,NRNG
      K=J-1
      C1(I,K)=(DEFLT(I,J)-DEFLT(I,K))/(RNG(I,J)-RNG(I,K))
      C2(I,K)=DEFLT(I,J)-C1(I,K)*RNG(I,J)
20 CONTINUE
  RETURN
END

```

SURPROGRAM LENGTH

000223

UNUSED COMPILER SPACE

057000

```

SUBROUTINE CALN(X,I,J,Y)
DIMENSION X(8,300)
COMMON TIMED(300),RNG(8,10),C1(8,10),C2(8,10),N,NRNG,MCANT
DO 5 K=1,NRNG
  IF(RNG(I,K)-X(I,J)) 6,6,5
6  MAX=K
5  CONTINUE
  Y=C2(I,MAX)+C1(I,MAX)*X(I,J)
  RETURN
END

```

SURPROGRAM LENGTH

000062

UNUSED COMPILER SPACE

057000

# COMPUTER PROGRAM NO. 2

PROGRAM RECL(INPUT,OUTPUT,PLOT,TAPE5=INPUT,TAPE6=OUTPUT,TAPE1=PL01  
1)

```

000002 DIMENSION FEAT(4J),TX(15J),R(8,15J),DSY(15J)
000002 CALL PLOT5
000003 NOT = 0
000004 NOTD = 1
000005 1000 READ(5,1) NOR,NOA
000010 1 FORMAT(2I4)
000015 READ(5,2) MO,IDA,IYR
000027 2 FORMAT(A3,I3,I5)
000027 READ(5,3) (FEAT(I),I=1,40),STA,PBXH
000041 3 FORMAT(4JA1,2A8)
000041 DO 4 K=1,NOR
000043 4 READ(5,5) TX(K),(R(J,K),J=1,NOA)
000057 5 FORMAT(1X,F6.3,8F9.6)
000057 YMAX = R(1,1)
000060 DO 10 J=1,NOA
000062 DO 10 K=2,NOR
000063 IF(R(J,K).GT.YMAX) GO TO 9
000070 GO TO 10
000070 9 YMAX = R(J,K)
000073 10 CONTINUE
000100 YMIN = R(1,1)
000102 DO 15 J=1,NOA
000103 DO 15 K=2,NOR
000104 IF(R(J,K).LT.YMIN) GO TO 14
000110 GO TO 15
000111 14 YMIN = R(J,K)
000114 15 CONTINUE
000121 YSCALE = (YMAX-YMIN)/9.0
000124 CALL SYMBOL(4.,-.4,.2,FEAT,0.0,40)
000130 NN=NOR+1
000132 NNN=NN+1
000133 DO 20 J=1,NOA
000143 R(J,NN) = 0.
000144 20 R(J,NNN)=YSCALE
000146 TX(NN) = 0.
000147 TX(NNN) = 1330.0
000151 CALL SYMBOL(1.0,10.3,.10,8HSTATION-,J.,8)
000155 CALL SYMBOL(2.3,10.3,.10,STA,0.0,9)
000161 CALL SYMBOL(3.8,10.3,.10,9HMBPX NO.,J.,9)
000165 CALL SYMBOL(5.2,10.3,.10,PBXH,0.0,8)
000171 CALL SYMBOL(1.0, 9.9,.10,29HDATE OF FIRST ACTIVE READING-,0.,29)
000175 CALL SYMBOL(5.3, 9.9,.10,MO,0.0,3)
000201 CALL NUMBER(5.8, 9.9,.10,IDA,0.0,2H13)
000205 CALL NUMBER(6.3, 9.9,.10,IYR,0.0,6H1H,,15)
000211 CALL PLOT(0.,((-YMIN/YSCALE)+.46),-3)
000217 CALL AXIS(0.,(YMIN/YSCALE),22HDISPLACEMENT IN INCHES,+22,9.0,90.0,
1YMIN,YSCALE,-1)
000232 CALL AXIS(0.,(YMIN/YSCALE),11HTIME IN HRS,-11,15.0,0.0,TX(NN),TX(NN
1N),-0)
000251 CALL PLOT(0.,J.,+3)
000254 CALL PLOT(15.,0.,+2)
000257 DO 50 J=1,NOA
000261 DO 40 K=1,NNN
000270 40 DSY(K) = R(J,K)
000272 CALL LINE(TX,DSY,NOR,1,0,0)
000276 CALL NUMBER(15.,(DSY(NOR)/DSY(NNN)),.10,J,8.8,2HX2)

```

```

000305      50      CONTINUE
000310      CALL PLOT(17.,((YMIN/YSCALE)-.46),-3)
000315      IF(NOTD.EQ.NOT) GO TO 150
000317      NOTD = NOTD + 1
000320      GO TO 1000
000321      150      CALL SYMBOL(J.,L.,.1,.54      ,90.,.5)
000325      CALL PLOT(0,0,993)
000330      STOP
000332      END

```

PROGRAM LENGTH INCLUDING I/O BUFFERS  
006642

UNUSED COMPILER SPACE  
015600

HF26613. 01/11/71.PURDUE MADE 70/12/00.

```

01.24.23.HF2667 36634,JUDO,CM60000,TP1,T200,P2
01.24.23.U.
01.24.23.MAP(ON)
01.24.24.FUN(S)
01.24.25.CTIME 000.600 SEC. FUN MOD LEVEL 60E
01.24.25.LGO.
01.24.26.CX 2.064 SEC., PX 3.215 SEC.
01.24.26.NL 16200 WORDS
01.24.27.PLOTTING STARTED
01.24.31.PLOTTING SUCCESSFUL
01.24.31.STOP
01.24.31.COPYPLT(PERLOFF,15073,11X 80,2,BLACK)
01.24.31.CX 5.408 SEC., PX 4.131 SEC.
01.24.31.NL 4000 WORDS
02.47.09. MT51 ASSIGNED - CALCOMP
02.47.51.COPYPLT COMPLETED--EXPECT PLOT OUTPUT
02.47.51.PLOT 0.307 HR.
02.48.00.CP 8.792 SEC., PP 42.938 SEC.
02.48.00.LINES 207
02.48.00.CM 0.204 MWD-SEC., FL 4000 WORDS

```



COMPUTER PROGRAM NO. 3

PARTIAL INDEX TO VARIABLE NAMES THAT APPEAR IN PROGRAMS #3 AND #4

SN	Station number for data being processed
NA	Reference anchor number for data being processed
NOR	Number of readings
NOA	Number of anchors
CAL(J)	Calibration factor for J <sup>th</sup> anchor
DAY(K)	Day of K <sup>th</sup> reading
HR(K)	Hour of K <sup>th</sup> reading
TIMIN(K)	Minutes of K <sup>th</sup> reading
R(K,J)	K <sup>th</sup> reading for J <sup>th</sup> anchor
D(K,J)	K <sup>th</sup> displacement for J <sup>th</sup> anchor
T(K,J)	K <sup>th</sup> time in hours for J <sup>th</sup> anchor
NOGR(J)	Number of good readings for J <sup>th</sup> anchor
NOT	Number of sets of data to be processed
NOTD	Counter which keeps track of number of sets of data that have been processed

```

PROGRAM JUDD(INPUT,OUTPUT,PL0T,TAPE5=INPUT,TAPE6=OUTPUT,TAPE1=PL0T
1)
00002  DIMENSION NOGR(8),CAL(8),DAY(140),HR(140),TIMIN(140),R(140,4),T(14
10,8),U(140,8),DSY(140),TX(140)
00002  CALL PLOTS
00003  NOT = 5
00004  NOTD = 1
00005  1000 READ(5,1) NA
00013  1  FORMAT(I2)
00013  READ(5,2) NOR,NOA
00023  2  FORMAT(/I3,I2)
00023  READ(5,3) SN
00031  3  FORMAT(29X,F5.0)
00031  READ(5,4) (CAL(J),J=1,NOA)
00040  4  FORMAT(/8X,8F6.2)
00040  DO 5 K=1,NOR
00042  5  READ(5,6) DAY(K),HR(K),TIMIN(K),(R(K,J),J=1,NOA)
00067  6  FORMAT(3F4.0,8F6.2)
00067  TZERO = 24.*DAY(1) + HR(1) + TIMIN(1)/60.
00074  DO 7 J=1,NOA
00103  7  T(1,J) = 0.0
00105  DO 9 K=2,NOR
00106  DO 8 J=1,NOA
00127  8  T(K,J) = 24.*DAY(K) + HR(K) + TIMIN(K)/60.-TZERO
00131  9  CONTINUE
00133  LL = NA-1
00135  DO 10 J=1,NA
00145  10  D(1,J) = 0.0
00147  DO 16 K=2,NOR
00150  11  IF((R(K,NA).EQ.99999.).OR.(R(K,NA).EQ.00000.)) GO TO 12
00162  D(K,NA) = (R(K,NA)-R(1,NA))*CAL(NA)
00172  GO TO 15
00172  12  IF(K.EQ.NOR) GO TO 14
00174  NOR = NOR-1
00175  DO 13 I=K,NOR
00202  R(I,NA) = R(I+1,NA)
00203  T(I,NA) = T(I+1,NA)
00205  DO 13 L=1,LL
00215  R(I,L) = R(I+1,L)
00216  13  T(I,L) = T(I+1,L)
00223  GO TO 11
00223  14  NOR = NOR-1
00225  15  NOGR(NA) = NOR
00227  16  CONTINUE
00232  DO 17 K=1,LL
00237  17  NOGR(K) = NOGR(NA)
00241  KNOA = NOA-1
00243  DO 50 J=1,KNOA
00245  KOUNT = 0
00245  NNR = NOGR(J)
00247  DO 50 K=2,NNR
00251  KKEEP = K
00252  IF((R(K,J).EQ.99999.).OR.(R(K,J).EQ.00000.)) GO TO 20
00263  IF(KOUNT.GT.0) GO TO 40
00265  D(K,J) = -(R(K,J)-R(1,J))*CAL(J)+D(K,NA)
00300  GO TO 50
00300  20  IF(KKEEP.EQ.NOGR(J)) GO TO 45
00303  25  KOUNT = KOUNT+1

```

```

000306      30      NOGR(J) = NOGR(J)-1
000310      NBR = NOGR(J)
000311      DO 35 KK=KKEEP,NBR
000322      R(KK,J) = R(KK+1,J)
000323      35      T(KK,J) = T(KK+1,J)
000325      IF((R(KKEEP,J).EQ.99999.) .OR. (R(KKEEP,J).EQ.00000.)) GO TO 20
000336      40      D(K,J) = -(R(K,J)-R(1,J))*CAL(J)+(R(K+KOUNT,NA)-R(1,NA))*CAL(NA)
000360      GO TO 50
000361      45      NOGR(J) = NOGR(J)-1
000363      NBR = NOGR(J)
000364      50      CONTINUE
000371      YMAX = D(1,1)
000373      DO 200 J=1,NOA
000374      NBR = NOGR(J)
000376      DO 200 I=2,NBR
000377      IF(D(I,J).GT.YMAX) GO TO 199
000405      GO TO 200
000405      199 YMAX = D(I,J)
000411      200 CONTINUE
000416      YMIN = D(1,1)
000420      DO 202 J=1,NOA
000421      NBR = NOGR(J)
000423      DO 202 I=2,NBR
000424      IF(D(I,J).LT.YMIN) GO TO 201
000431      GO TO 202
000431      201 YMIN = D(I,J)
000435      202 CONTINUE
000442      YSCALE = (YMAX-YMIN)/9.
000445      DO 700 J=1,NOA
000447      WRITE(6,750) J,NOGR(J)
000456      750 FORMAT(1H,4HJ = ,I2,10X,23HNO. OF GOOD READINGS = ,I3)
000456      NBR = NOGR(J)
000460      DO 700 K=1,NBR
000462      WRITE(6,751) R(K,J),T(K,J),D(K,J)
000500      751 FORMAT(1H ,10HREADING = ,F10.2,10X,7HTIME = ,F10.2,10X,15HDISPLAC
1MENT = ,F20.2)
000500      700 CONTINUE
000505      DO 75 J=1,NOA
000521      NN=NOGR(J)+1
000523      NNN=NN+1
000523      D(NN,J) = 0.
000524      D(NNN,J) = YSCALE
000525      T(NN,J) = 0.
000526      75      T(NNN,J) = 170.0
000533      CALL SYMBOL(3.,10.3.,13.9HMPBX NO.,0.,9)
000537      CALL NUMBER(4.3,10.3.,15.5H,0.,4HF5.0)
000543      KN = NOGR(1) +1
000545      KNN = NOGR(1) +2
000547      CALL PLOT(0.,((-YMIN/YSCALE),.46),-3)
000554      CALL AXIS(0.,(YMIN/YSCALE),24HDISPLACEMENT IN MICHO-IN.,24,9.0,90
10,YMIN,YSCALE,-1)
000567      CALL AXIS(0.,(YMIN/YSCALE),11HTIME IN HRS.,-11,15.0,0.0,T(KN,1),T(1
1NN,1),-0)
000606      CALL PLOT(0.,0.,+3)
000611      CALL PLOT(15.,0.,+2)
000614      DO 100 J=1,NOA
000617      MN=NOGR(J)
000620      NOGRJ=NOGR(J)+2

```

```

000622      DO 80 K=1,NOGRJ
000632      DSY(K) = D(K,J)
000633      80   TX(K) = T(K,J)
000635      CALL LINE(TX*DSY,MN,1,0,0)
000641      CALL NUMBER(15.,(DSY(MN)/DSY(MN+2)),.1,J,0.0,2H12)
000650      100  CONTINUE
000653      CALL PLOT(17.,((+YMIN/YSCALE)-.46),-3)
000660      IF(NOTD.EQ.NOT) GO TO 150
000662      NOTD = NOTD+1
000663      GO TO 1000
000664      150  CALL SYMBOL(0.0,0.,.1,5H      ,90.,5)
000670      CALL PLOT(0.0,999)
000673      STOP
000675      END

```

PROGRAM LENGTH INCLUDING I/O BUFFERS  
014200

UNUSED COMPILER SPACE  
014500

MZ36565. 10/29/70.PURDUE MACE 70/10/26.

```

18.45.18.MZ365/ 36634,JUDD,TP1,T60,CM60000,L30
18.45.18.00,P20.
18.45.18.MAP(ON)
18.45.19.FUN(S)
18.45.22.CTIME 001.316 SEC. FUN MOD LEVEL 400
18.45.22.LGO.
18.45.24.CX 2.733 SEC., PX 3.315 SEC.
18.45.24.NL 23500 WORDS
18.45.24.PLOTTING STARTED
18.45.42.PLOTTING SUCCESSFUL
18.45.42.STOP
18.45.43.COPYPLT(JUDD,36634,11X 90,2,BLACK)
18.45.43.CX 12.899 SEC., PX 8.752 SEC.
18.45.43.NL 4000 WORDS
18.59.22. MT51 ASSIGNED - CALCOMP
19.00.25.MT51, WPE RECOVERED.
19.01.35.COPYPLT COMPLETED--EXPECT PLOT OUTPUT
19.01.35.PLOT 0.602 HR.
19.01.45.CP 20.832 SEC., PP 94.186 SEC.
19.01.45.LINES 1204
19.01.45.CM 0.511 MWD-SEC., FL 4000 WORDS

```

COMPUTER PROGRAM NO. 4

```

PROGRAM JUDD(INPUT,OUTPUT,PLOT,TAPE5=INPUT,TAPE6=OUTPUT,TAPE1=PLOT
1)
000002   DIMENSION NOGR(8),CAL(8),DAY(140),HR(140),TIMIN(140),R(140,8),T(14
10,8),D(140,8),DSY(140),TX(140)
000002   CALL PLOTS
000003   NOT = 2
000004   NOTD = 1
000005   1000 READ(5,1) NA
000013     1   FORMAT(I2)
000013     READ(5,2) NOR,NOA
000023     2   FORMAT(/I3,I2)
000023     READ(5,3) DAY(1),HR(1),TIMIN(1),SN
000037     3   FORMAT(7X,3F5.0,7X,F5.0)
000037     READ(5,4) (CAL(J),J=1,NOA),(R(1,J),J=1,NOA)
000056     4   FORMAT(/6X,8F8.0/6X,8F8.0)
000056     DO 5 K=2,NOR
000060     5   READ(5,6) DAY(K),HR(K),TIMIN(K),(R(K,J),J=1,NOA)
000105     6   FORMAT(F4.0,F5.0,F4.0,8F8.2)
000105     TZERO = 24.*DAY(1) + HR(1) + TIMIN(1)/60.
000112     DO 7 J=1,NOA
000121     7   T(1,J) = 0.0
000123     DO 9 K=2,NOR
000124     DO 8 J=1,NOA
000145     8   T(K,J) = 24.*DAY(K) + HR(K) + TIMIN(K)/60.-TZERO
000147     9   CONTINUE
000151     LL = NA-1
000153     DO 10 J=1,NA
000163     10  D(1,J) = 0.0
000165     DO 16 K=2,NOR
000166     11  IF((R(K,NA).EQ.99999.).OR.(R(K,NA).EQ.00000.)) GO TO 12
000200     D(K,NA) = (R(K,NA)-R(1,NA))*CAL(NA)
000210     GO TO 15
000210     12  IF(K.EQ.NOR) GO TO 14
000212     NOR = NOR-1
000213     DO 13 I=K,NOR
000220     R(I,NA) = R(I+1,NA)
000221     T(I,NA) = T(I+1,NA)
000223     DO 13 L=1,LL
000233     R(I,L) = R(I+1,L)
000234     13  T(I,L) = T(I+1,L)
000241     GO TO 11
000241     14  NOR = NOR-1
000243     15  NOGR(NA) = NOR
000245     16  CONTINUE
000250     DO 17 K=1,LL
000255     17  NOGR(K) = NOGR(NA)
000257     KNOA = NOA-1
000261     DO 50 J=1,KNOA
000263     KOUNT = 0
000263     NBR = NOGR(J)
000265     DO 50 K=2,NBR
000267     KKEEP = K
000270     IF((R(K,J).EQ.99999.).OR.(R(K,J).EQ.00000.)) GO TO 20
000301     IF(KOUNT.GT.0) GO TO 40
000303     D(K,J) = -(R(K,J)-R(1,J))*CAL(J)+D(K,NA)
000316     GO TO 50
000316     20  IF(KKEEP.EQ.NOGR(J)) GO TO 45
000321     25  KOUNT = KOUNT+1

```

```

00324 30 NOGR(J) = NOGR(J)-1
00326 NNR = NOGR(J)
00327 DO 35 KK=KKEEP,NNR
00340 R(KK,J) = R(KK+1,J)
00341 35 T(KK,J) = T(KK+1,J)
00343 IF((R(KKEEP,J).EQ.99999.).OR.(R(KKEEP,J).EQ.00000.)) GO TO 20
00354 40 D(K,J) = -(R(K,J)-R(1,J))*CAL(J) + (R(K*KOUNT,NA)-R(1,NA))*CAL(NA)
00376 GO TO 50
00377 45 NOGR(J) = NOGR(J)-1
00401 NNR = NOGR(J)
00402 50 CONTINUE
00407 YMAX = D(1,1)
00411 DO 200 J=1,NOA
00412 NNR = NOGR(J)
00414 DO 200 I=2,NNR
00415 IF(D(I,J).GT.YMAX) GO TO 199
00423 GO TO 200
00423 199 YMAX = D(I,J)
00427 200 CONTINUE
00434 YMIN = D(1,1)
00436 DO 202 J=1,NOA
00437 NNR = NOGR(J)
00441 DO 202 I=2,NNR
00442 IF(D(I,J).LT.YMIN) GO TO 201
00447 GO TO 202
00447 201 YMIN = D(I,J)
00453 202 CONTINUE
00460 YSCALE = (YMAX-YMIN)/9.
00463 DO 700 J=1,NOA
00465 WRITE(6,750) J,NOGR(J)
00474 750 FORMAT(1H1,4HJ = ,I2,10X,23HNO. OF GOOD READINGS = ,I3)
00474 NNR = NOGR(J)
00476 DO 700 K=1,NNR
00500 WRITE(6,751) R(K,J),T(K,J),D(K,J)
00516 751 FORMAT(1H ,10HREADING = ,F10.2,10X,7HTIME = ,F10.2,10X,15HDISPLACE
    1MENT = ,F20.2)
00516 700 CONTINUE
00523 DO 75 J=1,NOA
00537 NN=NOGR(J)+1
00541 NNN=NN+1
00541 D(NN,J) = 0.
00542 D(NNN,J) = YSCALE
00543 T(NN,J) = 0.
00544 75 T(NNN,J) = 170.0
00551 CALL SYMBOL(3.,10.3.,15.9HMPRX NO.,0.,9)
00555 CALL NUMBER(4.3,10.3.,15.5H,0.,4HF5.0)
00561 KN = NOGR(1) +1
00563 KNN = NOGR(1) +2
00565 CALL PLOT(0.,((-YMIN/YSCALE)*.46),-3)
00572 CALL AXIS(0.,(YMIN/YSCALE),24HDISPLACEMENT IN MICRO-IN.,24.9.0.90.
    10,YMIN,YSCALE,-1)
00605 CALL AXIS(0.,(YMIN/YSCALE),11HTIME IN HRS.,-17,15.0.0.0,T(KN,1),T(K
    1NN,1),-0)
00624 CALL PLOT(0.,0.,+3)
00627 CALL PLOT(15.,0.,+2)
00632 DO 100 J=1,NOA
00635 MN=NOGR(J)
00636 NOGRJ=NOGR(J)+2

```

```

000640      DO 80 K=1,NOGRJ
000650      DSY(K) = D(K,J)
000651      80  TX(K) = T(K,J)
000653      CALL LINE(TX*DSY,MN,1,0,0)
000657      CALL NUMBER(15.,(DSY(MN)/DSY(MN+2)),.1,J,0.0,2H12)
000666      100 CONTINUE
000671      CALL PLOT(17.,((+YMIN/YSCALE)-.46),-3)
000676      IF(NOTU.EQ.NOT) GO TO 150
000700      NOTD = NOTD + 1
000701      GO TO 1000
000702      150 CALL SYMBOL(0,0,0.,.1,5H      ,90.,5)
000706      CALL PLOT(0,0,999)
000711      STOP
000713      END

```

PROGRAM LENGTH INCLUDING I/O BUFFERS  
014220

UNUSED COMPILER SPACE  
014400

MU11AAA. 10/27/70.PURDUE MACE 70/10/26.

```

19.09.19.MU11A/ 36634,JUDD,TP1,T60,CM60000,L30
19.09.19.00.P20.
19.09.19.MAP(ON)
19.09.19.FUN(S)
19.09.22.CTIME 001.316 SEC. FUN MOD LEVEL 600
19.09.23.LGO.
19.09.28.CX 2.401 SEC., PX 2.532 SEC.
19.09.28.NL 23500 WORDS
19.09.28.PLOTTING STARTED
19.10.01.PLOTTING SUCCESSFUL
19.10.01.STOP
19.10.02.COPYPLT(JUDD,36634,11x 40,2,BLACK)
19.10.02.CX 14.550 SEC., PX 10.579 SEC.
19.10.02.NL 4000 WORDS
19.19.20. MT52 ASSIGNED - CALCOMP
19.19.25.MT52, WPE RECOVERED.
19.22.24.COPYPLT COMPLETED--EXPECT PLOT OUTPUT
19.22.24.PLOT 0.294 HR.
19.22.38.CP 18.359 SEC., PP 51.414 SEC.
19.22.38.LINES 2107
19.22.38.CM 0.466 MWD-SEC., FL 4000 WORDS

```

## APPENDIX C

This drawing replaces Figure 3.27 in Technical Report No. 1

(Programming error resulted in erroneous displacement values  
being plotted for the measured data on the original figure.)

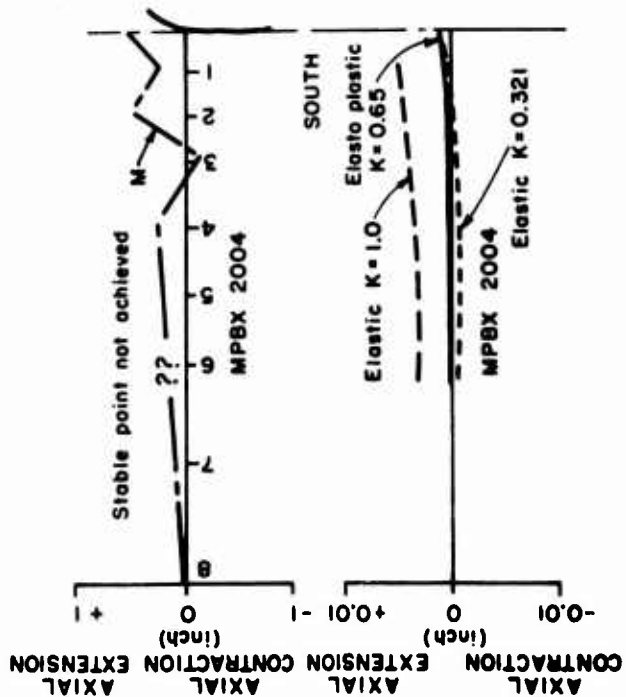
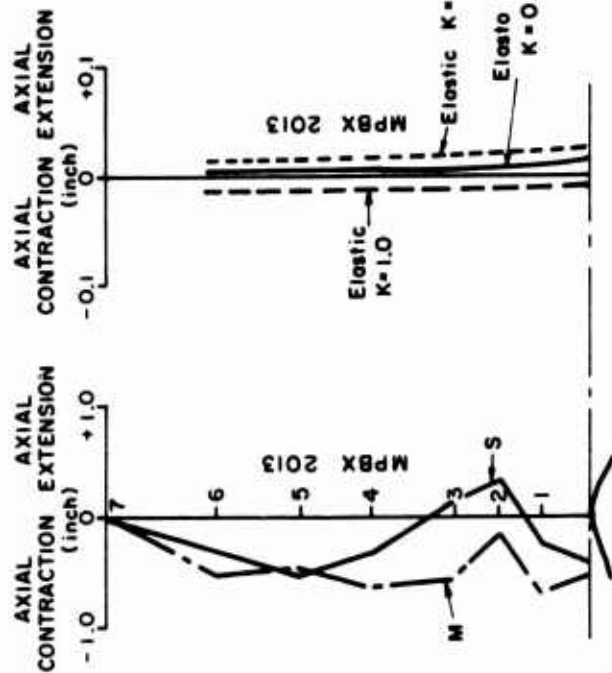


"?" indicates questionable reading

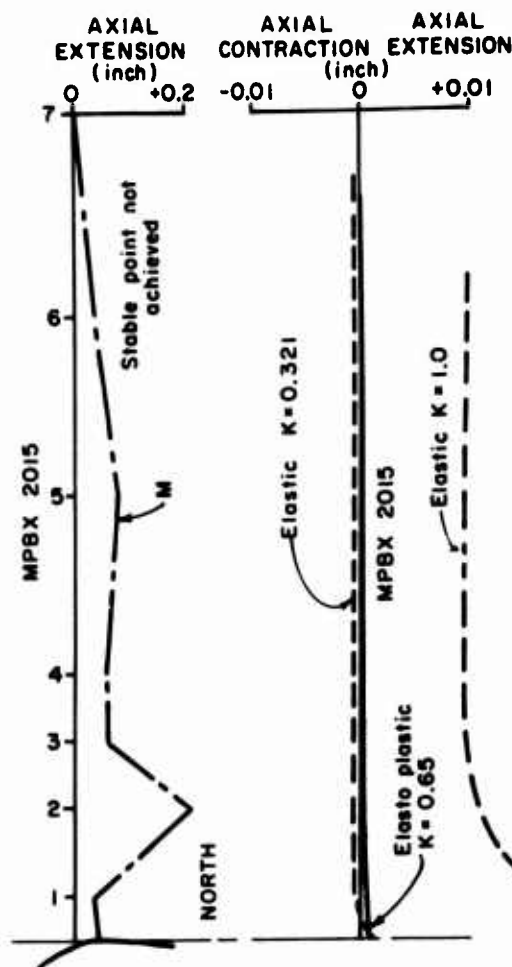
Scale for opening and anchor depths (feet)

0 5 10

a) Vertical MPBX



b) Left Horizontal MPBX



c) Right Horizontal MPBX